Stability Analysis of Jointed Rock Mass Foundation of Concrete Gravity Dam and Slope Stability of Abutment

– a case study of Koysha dam

A thesis submitted to

The school of Earth Sciences

Presented in partial fulfillment of the Requirement for the degree of Masters of Science Geological Engineering (Engineering Geology)

By

Mamo Methe

Advisor: Dr. Bayisa Regassa

December-2023

Addis Ababa University
College of Natural and Computational Sciences
School of Earth Sciences

Stability Analysis of Jointed Rock Mass Foundation of Concrete Gravity Dam and Slope Stability of Abutment

This is to certify that the thesis prepared by Mamo Methe, entitled: Stability Analysis of Jointed Rock Mass Foundation of Concrete Gravity Dam and Slope Stability of Abutment – a case study of Koysha Hydropower Project submitted in partial fulfillment of the degree of Masters of Science in Geological Engineering (Engineering Geology) complies with the regulation of the university and meets the accepted standards with respect to originality and quality.

Signed by Examining committee

Advisor	Signature	Date
Examiner	Signature	Date
Examiner	Signature	Date
Chairman	Signature	Date

DECLARATION

I declare that this thesis, which was completed during the year 2023 as part of my Master of Science Program in Geological Engineering (Engineering Geology) under the guidance of Dr. Baysa Regassa from the school of Earth Sciences at Addis Ababa University, is entirely my original work. Additionally, I confirm that I have not submitted this work to any other University or Institution to obtain any degree or diploma, and I have appropriately acknowledged all the sources of materials used in this thesis.

Mamo Methe

Signature: _____

School of Earth Sciences,

Addis Ababa University

December 2023

AKNOWLEDGEMENT

I would like to express my sincere gratitude to almighty God for granting me the strength, wisdom, and perseverance to complete this research. I am also immensely grateful to my advisor Dr. Baysa Regassa, for his invaluable guidance, unwavering support, and insightful feedback throughout the research.

I extend my heartfelt appreciation to Addis Ababa University College of Natural Science, School of Earth Sciences for providing me with the opportunity to pursue my academic goals and for equipping me with the knowledge and skills necessary to undertake this research. I am also indebted to all my teachers who have contributed to my growth and development as a student.

I would like to acknowledge the site office of Ethiopian Electric Power (EEP) for Koysha Project, the contractor offices, specially Nebil Negash for providing the relevant resources and information.

I would like to acknowledge the support and cooperation of the GIS department in School of Earth Sciences of Addis Ababa University, especially Dr. Biniam Tesfaw for providing me with necessary resources (high-tech computer) and Dr. Haileyesus to carry out the research analysis.

Acknowledgements are also given to all my friends, especially Mesay Tefera, for their unwavering love, encouragement, and support throughout my academic journey. I extend my acknowledgment to all the people who have supported me directly or indirectly in completing this project.

Finally, and most importantly, I thank my families, my sisters, and brothers, especially Berhanu Methe, without whose generous encouragement and help I would have not been able to conduct my research.

ABSTRACT

For high-performance operations and the safety of the dam structures, it is essential to study the rock mass foundation of major dams. Numerical modeling can be used to overcome some of the limitations associated with researching rock mechanics, such as the need for extensive laboratory testing for geotechnical engineering of dam foundations. Numerous researches have employed numerical modeling analysis to identify the failure model and resolve foundational issues pertaining to rock mechanics. The aim of this study is to examine and analyze the stability of the jointed rock mass foundation and abutment slope stability of Koysha RCC dam. The foundation of the concrete dam is affected by complex geology, and two sub-vertical joint sets and one sub-horizontal joint set are dipping sub-parallel to the river direction, frequently infilled with thick, soft compressible clay and decomposed rock remnants. The joints are cutting each other. In this research, a distinct element model (DEM) tool, namely 3DEC 5.20, is used to study and analyze the stability of the foundation. This model enables the building of material and joint models as discontinuous mediums.

Secondary sources have been the main sources of the required material properties. The Mohr Coloumb elastic, completely plastic model served as a representation of the constitutive block model of the rock and soil components. Perfectly elastic joint model properties served as a representation of the joint qualities. In addition to the discontinuum medium, the equivalent continuum concept was used to reduce calculation times and simplify the study.

The results of the central foundation analysis indicated that the jointed rock foundation of the dam was in a state of significant deformation along the infilled J2 joint under all loading conditions. The displacement keeps propagating laterally and vertically following the infill materials along the joint. The result of the abutment analysis revealed displacement of left crest foundation of the dam. From the compressional z-displacement and the pattern of the displacement along the infilled J2 joint set, the research concluded that the infilled material may be responsible for the deformation rather than the joint itself. Generally, the dam body and the whole rock mass foundation of the dam are found to be stable, except for zones of weakly infilled materials along the J2 joint. In order to improve these weak zones along the joint, remedial measures have recommended based on the results of the analysis carried out for improvement by cement grout.

Key words: Stability analysis, Infilled joint, Deformation, Foundation improvement.

TABLE OF CONTENTS

1. DECLARATION ii
2. AKNOWLEDGEMENT ii
3. ABSTRACT ii
4. TABLE OF CONTENTS i
LIST OF TABLES iii
LIST OF FIGURES iv
List of Abbreviations ix
1. CHAPTER 1: INTRODUCTION 1
1.1. GENERAL BACKGROUND 1
1.2. Location of the study area 3
1.3. PROBLEM STATEMENT 4
1.4. OBJECTIVE 7
1.4.1. General Objective 7
1.4.2. Specific Objectives 7
1.5. Research Questions 8
1.6. Significance of the study 8
1.7. Limitations 9
1.8. Thesis outline 9
1. CHAPTER 2: LITERATURE REVIEW 10
2.1. INTRODUCTION 10
2.2. CONCRETE GRAVITY DAM 11
2.3. ROLLER COMPACTED CONCRETE DAMS 12
2.3.1. RCC Dam 12
2.3.2. Design and Construction Considerations of RCC Dam 12
2.4. DESIGN CONSIDERATIONS AND MODE OF FAILURE OF GRAVITY DAM 12
2.4.1. Foundation Considerations 12
2.4.2. Failure Modes 14
2.5. ROCK MASS CLASSIFICATION SYSTEMS 14
2.5.1. Rock Quality Designation (RQD) 15
2.5.2. Geological Strength Index (GSI) 18

2.6. NUMERICAL MODELLING 20
2.7. SUMMARY AND CONCLUSIONS 24
3. CHAPTER 3: STUDY AREA 25
3.1. INTRODUCTION 25
3.2. TOPOGRAPHY AND GEOMORPHOLOGY 27
3.3. DRAINAGE 29
3.4. CLIMATE 30
3.4.1. Rainfall 30
3.4.2. Temperature 31
3.5. REGIONAL GEOLOGY 32
3.5.1. Stratigraphy 32
3.5.2. Structural Set-Up 33
3.6. GEOLOGY OF THE DAM AREA 35
3.6.1. Lithology 35
3.6.2. Geostructural Survey of the dam area 42
4. CHAPTER 4: MATERIALS AND METHODS 42
4.1. INTRODUCTION 42
4.1. RESEARCH METHOD 43
4.2. DATA COLLECTION 45
4.2.1. Secondary Data 46
4.2.2. Primary Data 52
4.3. MATERIALS MODELS 54
4.4. BOUNDARY CONDITIONS 57
4.5. MODELLING APPROACH AND BUILDING THE MODEL 57
5. CHAPTER 5: RESULTS AND DISCUSSION 61
5.1. DISPLACEMENT 64
..... 81
CHAPTER 6: CONCLUSION AND RECOMMENDATIONS 82
6.1. CONCLUSION 82
6.2. RECOMMENDATIONS 84
7. REFERENCES 86
7. APPENDIX 89

LIST OF TABLES

Table 1-1. Correlation between RQD and rock quality (Deere and Deere, 1989) 15

Table 1-2. The input parameters used in RMR_1989 classification system (Palmstrom, 2009) 17

Table 1-3. Adjusting factors for the dam stability (Romana, 2003) 18

Table 3-1. Mean monthly and Annual rainfall surrounding stations (Source: National Meteorological Services Agency) 30

Table 3-2. Rainfall coefficient of the surrounding stations (Source: National Meteorological Services Agency) 31

Table 3-3. Mean monthly temperature data of the site station for the last seven years. 32

Table 3-4. Dam site litostartigraphic units 36

Table 3-5. Summary the major joint sets properties 42

Table 4-1 Material properties of the intact rocks (geological units) 48

Table 4-2. Orientation of the joint sets in the studied regions 49

Table 4-3. Material properties of the rock mass 50

Table 4-4. Results of core samples 53

Table 4-6. Hoek Brown constant for the rock mass 55

Table 4-7. Physical and mechanical values to represent the rock masses in the numerical model 56

Table 5-1. Summary of displacement result of left abutment analysis under different loading conditions 78

Table 5-2. comparison of displacement of central foundation before and after improvement 80

LIST OF FIGURES

Figure 1.1. Geological condition in dam foundation that can result in sliding failure (Wylie, 2003) 2

Figure 1.2. Location map of the project area 4

Figure 1.3. Mapping of the J2 joint on the right abutment section, (Salini-Impregilo, K2 contact characterization, 2017) 6

Figure 1.4. (Left) one of J2 joint dipping into ~ 290 with 24 – 30-degree, filling with thick clay and weathered materials. (Right) insitu sampling of the J2 infilling material for lab test (Salini-Impregilo, K2 contact characterization, 2017) 7

Figure 3.1. Koysha hydropower dam project design 26

Figure 3.2. Topographical map of the study area and surrounding 28

Figure 3.3. Drainage map of the dam area and surroundings 29

Figure 3.4. Mean monthly rainfall of surrounding stations (Source: National Metrological Services Agency) and mean max. and min temperature of the site station. 31

Figure 3.5. Regional structural map of the area (GSE 2018, geological map of Dime map sheet)) 35

Figure 3.6. (Left: Recent deposit of alluvial along river banks, (Right: Columnar basalt on right downstream abutment. (Salini impregilo: basic investigation report, 2016) 37

Figure 3.7. Conglomerate cores 38

Figure 3.8. The spatial coarse conglomerate and a sandy pebble lobe 38

Figure 3.9. the geological units in the area 40

Figure 3.10. Geological map of the study area (a), and vertical cross section of the dam site (not scaled) (b) (modified from Koysha hydroelectric project, investigation report, 2016) 41

Figure 4.1. Detail method flow chart of the research 44

Figure 4.2. General solution procedure for static analysis (Modified from Itasca 2016) 45

Figure 4.3. Stereographic projection of the joints 49

Figure 4.4 Simple mapping of region 1 in the central foundation (4 grids, each 20 x 20 meter gridding) (modified from general geological foundation mapping report, 2017, for modeling purpose) 49

Figure 4.5. Simple mapping of interest region 2 on the right abutment slope, (modified from J2 joint investigation report 2016) 50

Figure 4.6. Hoek Brown Criteria for the Andesite/breccia (a) principal stresses, (b) Hoek brown criteria in Mohr Coulomb plane 51

Figure 4.7. Core samples laboratory tests, weighing tha core sample (left), UCS test of core sample (right) 53

Figure 4.8. (a) Generation of Poly brick block (50m X 50m), the three joint sets, and deformable blocks (meshing) and (b) representation of the discontinuities constitute in the block model..... 59

Figure 4.9. Model geometry, (a) rigid blocks, constitutive model of the geological lithologies (blue - basalt, green - conglomerate, red (lower part) - andesite), joints generation, (b) deformable blocks (meshing) 60

Figure 4.10. constitutive deformable blocks of the dam and section side view..... 60

Figure 4.11. Vertical self-load and horizontal water pressure distributions at central section of the dam . 61

Figure 5.1. Analysis steps and the unbalanced forces for the left abutment trial model..... 63

Figure 5.2. Topographic stresses after initialization of in-situ stress, xx cut plane & yy cut plane at max abutment height..... 64

Figure 5.3. Displacement of foundation for middle level outlet, left: Resultant displacement magnitude, right: the dominant compressional z-displacement..... 65

Figure 5.4. Displacement components, A) X-displacement, B) Y-displacement, and C) Z-displacement... 66

Figure 5.5. Displacement cut plane section at x=19.5, y=-75, z=-14, left: y-y section, right: x-x section... 66

Figure 5.6. bird view plane cut section of foundation at depth of, left: 0.4 m and right: 14 m, displacement follows the joint pattern 67

Figure 5.7. Displacement of the foundation..... 67

Figure 5.8. Z-displacement which is the dominant one 68

Figure 5.9. plane cut section along the dam axis (x=0, y=0 and z=0) 68

Figure 5.10. Plane cut section of the model at, y=-26 (downstream), (A) Resultant displacement, (B) The dominant displacement 69

Figure 5.11. bird view the displacement pattern, that follows the J2 joint set, horizontal plane cut at depth of 5 meters..... 70

Figure 5.12. Displacement components of the maximum displacement at x=-13, y=-26, z=-5 70

Figure 5.13. Plastic deformation in the profile cut through the center of the dam under different loading conditions; at middle level (left), at normal operation level condition (right) 71

Figure 5.14. Displacement of the dam and foundation under middle level outlet (95 masl) and normal operating level (150 masl) conditions 72

Figure 5.15. displacement magnitude at middle level outlet 73

Figure 5.16. displacement of the dam body at middle level outlet 73

Figure 5.17. plane cut section along the dam axis @ y=0 73

Figure 5.18 plane cut at y=-30m d/s from the dam axis 73

Figure 5.19 plane cut @y=-60m from dam axis 73

Figure 5.20 plane cut @y=-90m from dam axis 73

Figure 5.21 plane cut @x=80m from the center to left abutment 74

Figure 5.22 plane cut @x=452m 74

Figure 5.23 plane cut along the flow @x=350m to left 74

Figure 5.24 Displacement magnitude of left abutment 75

Figure 5.25 Z-displacement of the model 75

Figure 5.26 plane cut @y=-60 d/s, from dam axis 75

Figure 5.27 plane cut @y=-90m d/s, from dam axis 75

Figure 5.28 plane cut @y=-30m d/s, from dam axis 75

Figure 5.29 Plane cut along dam axis @y=0m 75

Figure 5.30 plane cut @x=452m from center dam 76

Figure 5.31 plane cut @x=350m from dam center 76

Figure 5.32 plane cut along the flow @x=230m from center 76

Figure 5.33 plane cut @x=315m from the center of dam 76

Figure 5.34. Plastic deformation in the profile cut through the abutment of the dam under different loading conditions; at middle level loading condition (left), at normal opering level condition (right) 77

Figure 5.35. History of displacement components of the left abutment analysis 77

Figure 5.36. Displacement results of left crest under different loading conditions 78

Figure 5.37. Displacement components of left abutment analysis under different loading condition..... 79

Figure 5.38. Displacement magnitude of central foundation after injection of cement grout. 80

Figure 7.1. Displacement of central foundation 89

Figure 7.2. Displacement magnitude of dam body after loading at middle level outlet (95m) 89

Figure 7.3. Displacement of foundation shown on plane cut on the dam axis 90

Figure 7.4. Displacement magnitude of dam body after loading at normal operating level (150m)..... 90

Figure 7.5. Plane cut at 60 meter offset from dam axis ,displacement of central foundation 91

Figure 7.6. plane cut around the toe of the dam body,..... 91

Figure 7.7. Displacement of the left abutment..... 92

Figure 7.8. Plane cut along river flow; maximum displacement observed at 60 meter offset from dam axis 92

Figure 7.9. Displacement of left crest dam body..... 93

Figure 7.10. plane cut along the dam axis 93

Figure 7.11. plane cut in downstream 90 meter from dam axis,..... 94

Figure 7.12. plane cut on the left abutment along the river direction..... 94

Figure 7.13. plane cut on left abutment along the river direction 95

Figure 7.14. Plane cut on left abutment along river direction..... 95

Figure 7.15. Sampling of infilling material from J2 joint set 96

Figure 7.16 Recovery of PVC pipe 96

Figure 7.17. Grading result of one of the infilling material 97

Figure 7.18. Atterberg test result of one of infilling material at site lab 98

Figure 7.19. Soil classification 99

Figure 7.20. direct shear test result at external lab 100

Figure 7.21. J2 joint with thick infilling on the abutment slope 101

List of Abbreviations

C°:	Degree Celsius (temperate unit)
3DEC:	3-Dimensional Numerical Element Modeling Code
AEM:	Applied Element Method
ASTM:	American Society for Testing and Materials
CH:	Fat clay
CL:	Lean clay
CVC:	Conventionally Vibrated Concrete
DEM:	Discrete Element Method
EEP:	Ethiopian Electric Power
Ei:	Younge's modulus of the intact rock
Em:	Equivalent deformation modulus
Erm:	Deformation modulus of the rock mass
ENE:	East north east
E-W:	East West
GSI:	Geological Strength Index
ISRM:	International Society for Rock Mechanics
KHPP:	Koysha Hydropower Project
MPa:	Mega Pascal
kPa	kilo Pascal
NNE:	North North East
NNW:	North North West
NW:	North West
Q:	Tunnel Quality Index
RCC:	Roller Compacted Concrete
RMR:	Rock Mass Rating
RQD:	Rock Designation Index
SNNPR:	Southern Nations Nationality and Peoples Region
UDEC:	Universal Distinct Element Code
UTM:	Universal Transverse Mercator coordinate system

CHAPTER 1: INTRODUCTION

1.1. GENERAL BACKGROUND

Dam is a hydraulic structure of fairly impervious material built across a river to create a reservoir on its upstream side for impounding water for various purposes such as hydropower generation, irrigation purpose, domestic and industrial water supply, flood controlling, ground water recharge, water diversion, fishing and recreation facilities and multipurpose. Hydropower dams are large constructions built to regulate the water flow of rivers and exploit it to create energy. The energy created by the water falling is captured by a generator and passed onto a nearby power grid. Based on the construction materials, dams can be categorized into concrete dam, embankment dam and composite dams. A concrete dam is the strongest type of dam built in modern times and may take several forms. Concrete itself is a building material made from water, cement, sand and gravel, or aggregate. A concrete gravity dam is a structure designed to withstand loads by its own weight and by its resistance to sliding and overturning on its foundation.

Concrete dams can be constructed as both conventional concrete dams and Roller-compacted concrete dams (RCC). The primary modern forms of the concrete dam are conventionally vibrated mass concrete (CVC) gravity, buttress and arch dams, arch dams and roller compacted concrete (RCC) gravity (QHW Shaw, ICOLD 2017). RCC gravity dams are now often assumed to be the most competitive concrete dam type for many sites. RCC is a mix of cement/fly ash, water, sand, aggregate and common additives, but contains much less water and it is placed in a manner similar to paving. RCC can be constructed relatively in lower cost and achievable high speed, in economic benefit as less machinery and minimum skilled man power, and an earlier return on capital investment makes it advantageous than the other dam types. Roller-compacted concrete (RCC) offers a range of economical and safe design alternatives to conventional concrete and embankment dams. The construction of the dam needs relatively competent rock foundation. The stability and safety of RCC constructions are of big concern since a failure is very likely to lead to disastrous consequences.

The geology of the foundation rock affects the stability of the RCC dam. The gravity dam requires a strong rock base, although it may be built on a complexly joined, non-homogeneous rock mass. Due to the jointed rock mass and complicated geology, building a dam on it requires careful

stability evaluation and suitable design considerations. If they are not taken into account, the dam foundation may fail, which would then affect the stability of the dam and cause operating issues. According to Douglas (2002) and the information shown in (Figures 1.1), dams constructed on jointed rock masses are prone to slide failure. The breakdown of the concrete-rock interface's shear strength or failure linked to the discontinuities in the rock mass may cause the dam to slide. Regardless of whether the dam is built with regular concrete or RCC, accurate uplift estimations are crucial. Modern concrete gravity dams contain a gallery inside the structure where grout holes are created to lessen the foundation's rock mass permeability. The uplift forces inside the dam foundation and at the dam foundation contact are decreased by grouting in conjunction with drainage holes.

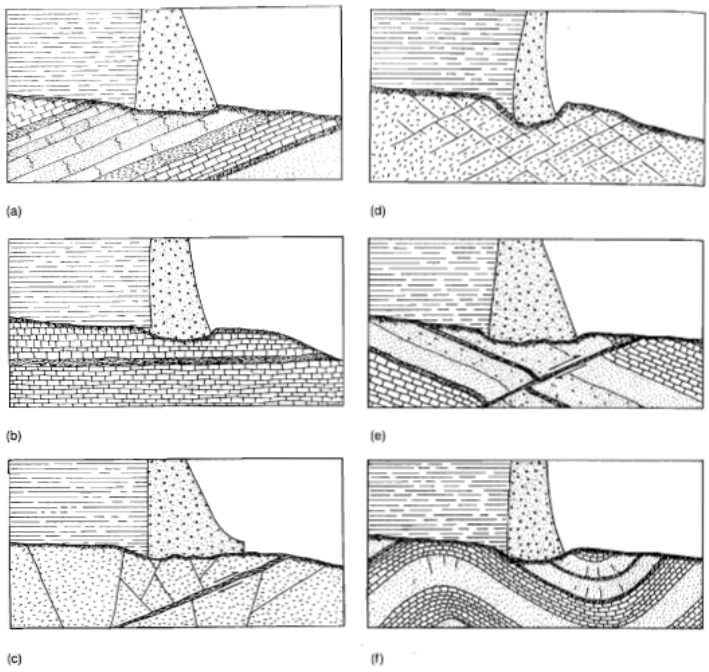

Figure 1.1. Geological condition in dam foundation that can result in sliding failure (Wylie, 2003)

On a base of uniform rock, it is difficult to construct a sizable concrete gravity dam. As a result, careful consideration must be given to the foundation of the dam during design, taking into account the complexity of the geology, the geostructural conditions, and the hydraulic behaviors of the discontinuities. The Koysha dam is intended to be built over complicated geology with several evolutionary histories and a heterogeneous jointed rock mass. A heterogeneous jointed rock mass

may present challenges for the construction of a dam in terms of operating performance and safety (Boyer, 2006; Douglas, 2002). Faults, sheared and fractured zones, seams, and joints are risk factors that might cause a dam to fail. There are several different ways that dams might fail, including overturning, sliding caused by the breakdown of the concrete-rock contact, and sliding owing to discontinuities losing their shear strength.

Numerous computer models have been developed to examine the methods by which the rock foundations of concrete gravity dams fail. The discrete element method (DEM), which comprises discrete elements, DDA, AEM, UDEC, and 3DEC, has been created for modeling discontinuous media (Lemos, 2021). The 3DEC approach, one of the various DEM models, is practical for jointed rock foundations since it offers a strong tool to handle the safety evaluation of structural foundations on rock. It is feasible to describe the in-situ circumstances of rock discontinuities, model development, block and joint deformability, joint water pressure, and the process for safety factor evaluation with the use of DEM (3DEC) (Lemos, 2012).

1.2. Location of the study area

Koysha hydroelectric power project is located on the Omo River, in the South West and South regions of Ethiopia, particularly located in Konta special wereda in South West Region and Mallo Koza werede of Gofa zone in South Nations, Nationality and Peoples Region (SNNPR), approximately 533km southwest of the capital city Addis Ababa accessing through Jima town – Ameya (Konta) and then Koysha, and approximately 584km accessing through Sodo / Arba Minch - Sawla towns and then Koysha site. The proposed dam site is bounded by geographic coordinates of UTM (Adindan, Zone 37N) 227245 - 229581 E and 726355 -730091 N.

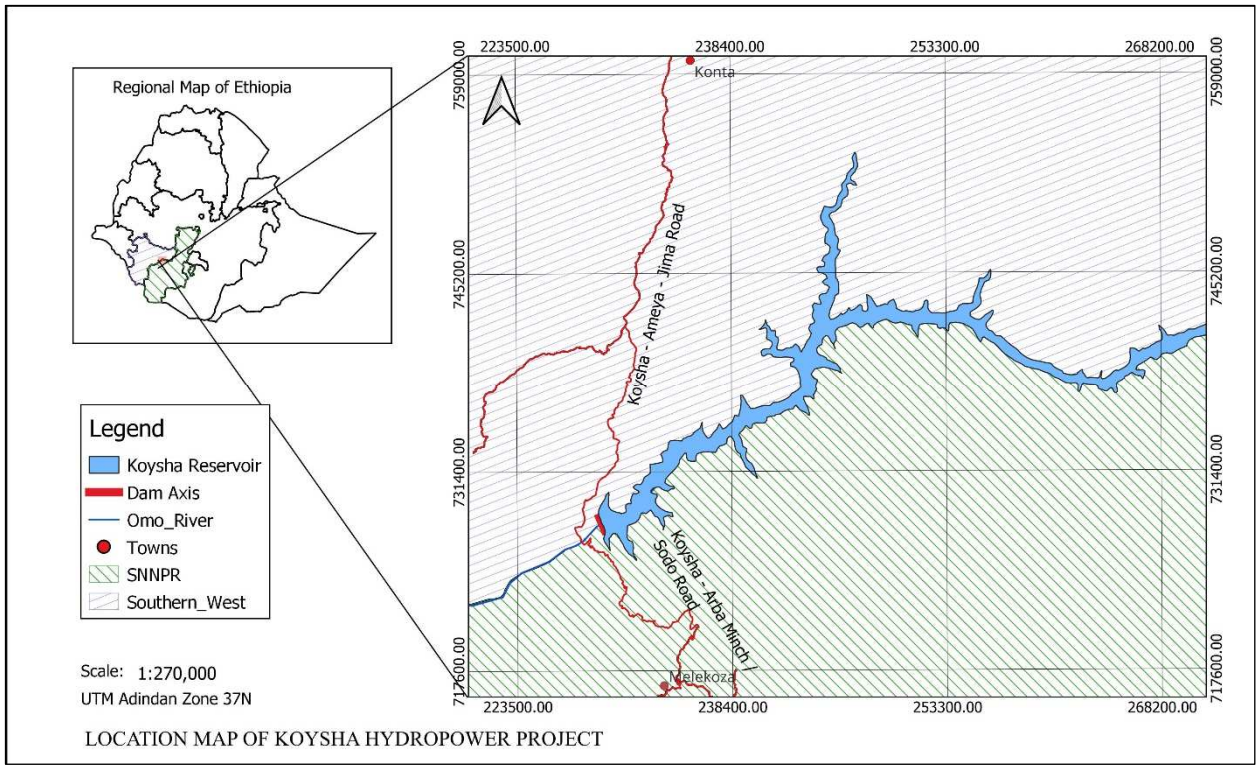

Figure 1.2. Location map of the project area

1.3. PROBLEM STATEMENT

It is crucial to carry out an accurate assessment of the dam's foundation's geological structures, rock foundation strength, and compressibility. The assessment should be used to determine the kinematically viable failure mechanisms. The foundation of the dam has several possible collapse scenarios. The fact that dam engineers only took into account the mechanism of collapse involving shear along the concrete-rock contact is a significant flaw. Typical kinematically feasible failure modes are presented:

1. Shear along concrete-rock contact is an uncommon mode that should have its state monitored, particularly in older dams. It is frequently brought on by shoddy excavation or weak foundations.
2. The development of a non-compression zone, a computed crack, can lead to shear along the concrete-rock contact, even in a good foundation.
3. Shear in rock foundations along or near planar discontinuities, frequent mode, and are prevalent problems.

4. Shear occurs along stepped discontinuities or surfaces between parallel discontinuities in rock foundations, with smaller steps approximating failure surfaces using an inclined plane, while larger steps may require higher analysis.

Shear through highly jointed or weak rock mass, infrequent mode, can be used in moderately jointed rock masses with an adjustment to Hoek-Brown rock mass strength. Generally, Failure modes include shear along planar discontinuities, stepped discontinuities, and shear through jointed or weak rock masses.

According to the geological section of the dam area, the rock masses that outcrop in the project area important to the dam have been divided into three primary litho-stratigraphic groups, ranging in age from the most recent to the oldest: columnar basalt, conglomerate, and andesite/andesite autobreccia.

The complicated geology on which the dam is situated includes thicker lower stratigraphic units which is little weathered to unweathered, strong to very strong known as Andesite flows and andesite autobreccia, which is weak to strong. Columnar basalt flow lithological units form the plateaus on both abutments of the dam site. This basalt flow on the right abutment underneath a strongly welded conglomerate deposit as indicated in the geological section. The abutments and lower components of the foundation are severely affected by variety of geological structures and various joint sets. Among these joint sets, three major dominant joint sets are identified as J1, J2 and J3. The orientations of the three major joints are described below:

Joint set	Mean Dip	Mean Dip direction	Infilling
J1	65	115	-
J2	25	270	Compressible Clay & weathered materials
J3	79	350	-

Some of the J2 joint, (Figure 1.4 & 1.5) infilled with weathered materials and thick compressible soft clay, has a sub-horizontal orientation and dips sub-parallel to river flow. Its shear strength is crucial for dam stability, as infilling thickness increases, the shear strength of infill rock joint decreases, The most obvious effect of the infilling material is to separate the discontinuity walls and thereby reduce rock-rock contact.

According to (Papaliangas (1993), the filling material reduces the shear strength of a discontinuity by means of three basic mechanisms: 1) Reduction of surface textural friction, 2) Change in frictional properties and 3) Change of geometrical component. Shear behavior of filled discontinuities is controlled mainly by: characteristics of filling material, characteristics of joint wall surfaces and ratio between fill thickness (t) and joint wall amplitude (a). when the thickness of the infilling is larger as compared to the waviness (amplitude) of the joint surface (i.e. the ratio t/a large), the joint stiffness and the shear strength will reduce resulting in shear failure. It may happen when the ratio is greater than the crtical limit (t/a >1.2). The shear strength property of infilling or interface between the infilling and rock wall governs the shear strength of the joint, not the rock wall of the joint.

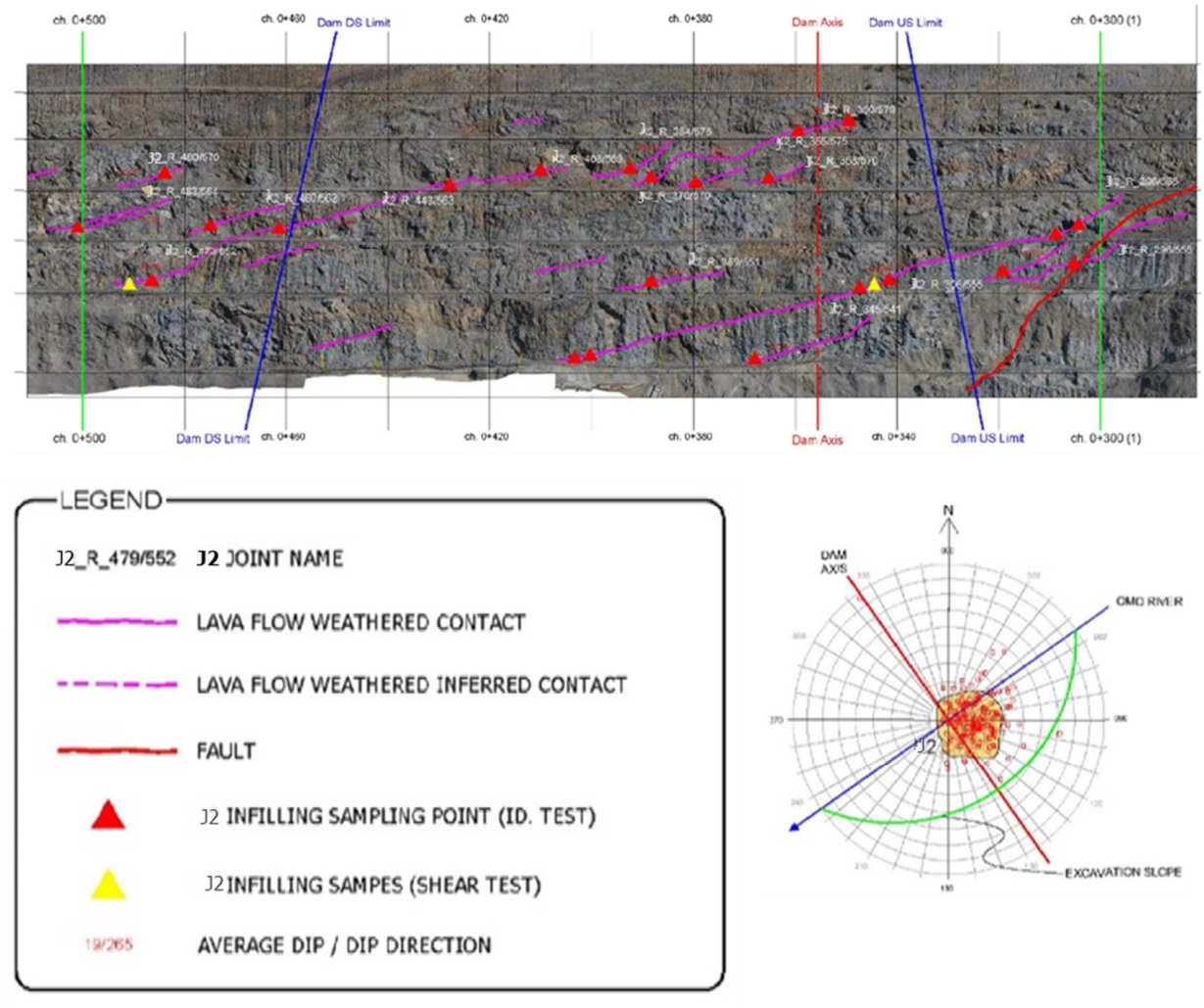

Figure 1.3. Mapping of the J2 joint on the right abutment section, (Salini-Impregilo, K2 contact characterization, 2017)

Figure 1.4. (Left) one of J2 joint dipping into ~ 290 with 24 – 30-degree, filling with thick clay and weathered materials. (Right) insitu sampling of the J2 infilling material for lab test (Salini-Impregilo, K2 contact characterization, 2017)

Shear along the concrete-rock contact and shear along the planar discontinuity are two possible failure mechanisms as a result of this J2 discontinuity. Larger infilling thickness reduces joint stiffness and shear strength, leading to shear failure. Infilling strength governs joint strength. It is important to take into account global failure modes including slide and bearing failures. Therefore, Foundation stability analysis is crucial for safety evaluation of gravity dams, as damage to the foundation can lead to significant loss of life, operational problem and financial harm.

1.4. OBJECTIVE

1.4.1. General Objective

The main objective of the research is to investigate the stability of jointed rock mass foundation of concrete gravity dam and stability of the abutments of Koysha Hydropower dam.

1.4.2. Specific Objectives

The specific objectives of the research are:

- To describe the characteristics of the main discontinuities in the abutments and dam foundation,
- To examine the impact of sub-horizontal infilled joints in the rock mass foundation beneath the gravity dam,

- To create a workable model for the failure process of the dam's jointed rock mass foundation under such challenging geological circumstances,
- Finally, to undertake numerical analysis utilizing the 3D discrete technique (3DEC) in order to simulate the stability of the dam foundation and abutments under standard and various operational conditions.
- To work out the feasible remedial measures for the abutments and the foundation.

1.5. Research Questions

Dam failure has a potential risk for the downstream area if the safety of the dam and the performance of the operation are not proactively determined and monitored under accepted international regulatory requirements. The questions of the research to be answered are:

- What are the critical parameters which may significantly affect the stability of the foundation?
- What are the potential modes of failure in the foundation and abutment slopes?
- What are the sensitive foundation areas (zones), significantly result in failure on the dam structure and performance?
- What are the possible remedial measures for the abutment and the foundation?

1.6. Significance of the study

Dam failure may cause catastrophic hazards in the downstream of the dam. It may cause undesirable loss of life, operational problem, economic damages, destruction of infrastructures, even complete vanish of villages and towns. Generally, dam failure may cause safety problems of the dam. There are different modes of dam failures as result of problems, like seepage and shear, related with foundation, particularly in complex geological structures. Proper geological investigation and evaluation of engineering structures are critical in designing and construction. Besides, the behavior of larger dams necessitates a better understanding of the foundation conditions and a more in-depth analysis of the performance of the dam under various loading conditions. The consequences of the dam failure underscore the importance of the research for stability analysis which may provide a reference for the dam design and engineering reinforcement and remedial of the dam foundation. The results of the research may help to provide insights to the

situation, suggest safe operational guideline and dam safety monitoring mechanisms such as dam instrumentations. The results of the analysis research may save the catastrophes in the downstream.

1.7. Limitations

In the physical world the shapes and roughness of discontinuities in rock mass can significantly impact the stability of dam foundations. In the actual field condition, the shapes of the joints ranges from planar to undulating. The main limitation of the study is assuming the shapes of discontinuities and interface contacts to be planar. Roughness of the joints were not represented. Water pressures in the discontinuities is also one of the significant factors in stability analysis of dam. Fluid flow analysis through the joints and interface contacts is another limitation in this paper. Unavailability of advanced high-tech computer to represent all discontinuities and prolonged time to complete the analysis.

1.8. Thesis outline

The thesis consists of six chapters, as presented below:

Chapter one: introduces the background of the research area. And presents an overview of the research including the research problems, objectives.

Chapter Two: is the general literature review. This presents historical dam failures, and the available rock classification system that can be used to analyze the rock mass behavior for the foundation of dams, an overview of the numerical modeling.

Chapter Three: presents an overview of the study area including: the geomorphological setup, the metrological information and geological lithologies of the study area.

Chapter Four: describes the research methodology. In this chapter the numerical methodology using two numerical, dominantly discontinuum and continuum codes is described.

Chapter Five: this chapter contains the analyses, the effects of sub horizontal infilled joints accompanied by sub vertical joints under different parameters.

Chapter Six: this chapter presents the main conclusions and recommendations.

CHAPTER 2: LITERATURE REVIEW

2.1. INTRODUCTION

Numerous scholarly works have been examined to gather pertinent data concerning the goal, approaches, deficiencies, and additional facets of this investigation. Building massive concrete dams has been a key factor in producing hydroelectric electricity, which is vital for a nation's economy to sustain its growing industrialization initiatives. When compared to the others based on predetermined common factors, roller-compacted concrete dams (RCC) have recently gained preference. They are typically constructed in response to inquiries about construction costs, challenges, and timeliness. Particular consideration must be given to a few parameters during the construction of a concrete gravity dam. One of these factors that needs to be taken into account is the dam's foundation.

For a massive concrete gravity dam to operate safely and to the highest standards feasible, it needs a new, strong rock mass foundation. Because the rock mass may react anisotropically to external forces, discontinuities, faults, seams (infillings), and other geological structures may have an impact on the stability and operating effectiveness of the dam's engineering structures. Comprehending the properties and intricacy of jointed rock masses is essential for the project's design, construction, and post-construction stages. For design purposes, the suitability and stability of the jointed rock foundations have been assessed using a range of techniques and models. These methods include the Rock Mass Classification (RMR), the Geological Strength Index (GSI), and other crucial components that determine the rock's engineering significance.

Modeling of dam stability analysis has been used to determine and predict the failure mode of concrete gravity dam. Various modeling methods have been evolved and developed previously and being under use. 3D discontinuum modeling concept has been developed and found to be suitable for jointed rock mass. One of the 3D modeling of rock mechanics is 3DEC with special features enables to solve problems in rock mechanics industries such as mining, dam constructions. The general relevant literature reviews related to this research are presented in the following paragraphs

2.2. CONCRETE GRAVITY DAM

A concrete gravity dam is a structure designed to withstand loads by its own weight and by its resistance to sliding and overturning on its foundation. The main forces that are acting on the dam and to be considered in the design stability and safety analysis are weight of the dam itself, the pressure of the water retained in the reservoir, uplift pressure, the pressure exerted by the foundation, the dynamic inertial forces of seismic action, and other forces to be considered are the wave forces on the upstream face, pressures of silt and ice. ICOLD registered that concrete gravity dams are in the second-place following earth dam throughout the world. Concrete gravity large dams need sound, competent good quality rock foundation as its weight designed to be placed relatively on small area. They were constructed of stone masonry, masonry of gravity and arch dam, conventionally vibrated concrete (CVC) and roller compacted concrete (RCC). Newer dams of this type are typically composed of unreinforced concrete monoliths with seals at the contraction joints and often mortar bedding at the lifts. The section design of the dam varies for different reasons. It can be essentially and commonly triangular, with its apex at the top and maximum width at the bottom, to ensure stability and to avoid overstressing of the dam or its foundation, or can be slightly curved in plan for aesthetic or other reasons.

The purpose of construction of ancient gravity dams are very limited to water supply and pleasure. The sizes and the heights of the dams were well-researched and documented to be ranges from 4.5 meter for Jawa dam in Jordan around 3000 BC to 46-meter-high Tibi dam in Spain in 1594 succeeding the Roman Subiaco gravity dam of 40 meter high (about AD 54-68). The first modern triangular shaped dams were built in Mexico and French engineers' ingenuity developed and practically illustrated the advantages of the modern triangular shape in 1853 (Schnitter and Nicholas, 1994). With the discovery and technology of use of Portland cement industry, the construction of concrete gravity dam started using Portland cement with controlled water content in order to achieve high strength of the concrete.

Now days the construction of large concrete gravity dam becomes preferred than the others due to various reasons. The advantages are: the least maintenance cost, relatively stronger and more stable as compared to earth dams, high height, does not trial suddenly, it gives enough warning, employment of dam structures is possible such as deep-set sluices and spillway. The development of roller compacted concrete (RCC), with correct construction methodology, significantly reduced

the time taken for construction and the economy needed, compared to large traditional conventionally vibrated concrete gravity dams.

2.3. ROLLER COMPACTED CONCRETE DAMS

2.3.1. RCC Dam

2.3.2. Design and Construction Considerations of RCC Dam

RCC dam stands for Roller Compacted Concrete dam, which is a type of concrete gravity dam that is constructed using a special type of concrete called "roller-compacted concrete" (RCC). The dam made up of a series of vertical panels that are constructed using compacted layers (usually 30-40cm thick) of concrete. Bedding mixes can be used to enhance the bondage between the two hot joints according to the design. Unlike traditional concrete dams that require extensive formwork, RCC dams can be constructed relatively quickly and with much less material. This is because the RCC is compacted in layers using heavy construction equipment such as rollers, which eliminates the need for large amounts of manpower and formwork.

RCC dams are commonly used in areas where traditional concrete dams would be too costly or difficult to build. They are also popular for their superior strength, durability, and low maintenance requirements. There are some considerations for RCC before detailed final designs, including the basic purpose of the dam, the owner's requirements for cost, construction schedule, appearance, watertightness, operation, and maintenance.

Foundations that are suitable for massive internally vibrated concrete dams also are suitable for RCC dams with similar properties. However, because of the low cost, construction techniques, and material properties of RCC, this type of dam can use a wider base and special design details to accommodate foundations that would otherwise be unsuitable (Schrader, 2007).

2.4. DESIGN CONSIDERATIONS AND MODE OF FAILURE OF GRAVITY DAM

2.4.1. Foundation Considerations

Gravity dams are large, massive structures that rely on their own weight and the force of gravity to resist the hydrostatic pressure of water. Therefore, foundation considerations are critical to

ensuring their stability and long-term performance. A robust understanding of the site conditions and careful design must be implemented to deliver safe and reliable infrastructure. Here are some key considerations (Fell 2014):

1. Site Selection: The site selection for a gravity dam is critical as it determines the type of foundation that will be required to support the weight of the dam. The foundation should be strong enough to prevent the dam from sliding or settling.
2. Geology: The geology of the site is an important consideration as it affects the stability of the dam. The rocks and soils at the site should be able to withstand the weight of the dam and the forces generated by water pressure. Assessment of the strength and compressibility of rock masses in the foundations of concrete gravity dams can be done systematically and carefully which may include the assessment of the intact rock and rock mass shear strengths, shear strengths of thick infilled joints and seams, tensile strength, compressibility of jointed rock mass, ultimate bearing capacity of the rock foundation. The bearing capacity is controlled by deformation (Fell, 2014)
3. Structural Design: The structural design of the dam should be carefully considered to ensure that it can withstand the forces generated by water pressure. The dam should be designed to resist uplift forces, overturning forces, and sliding forces.
4. Materials: The materials used in the construction of the dam should be carefully selected to ensure that they are suitable for the site conditions (Schrader, 2007). The concrete used in the dam should have a high compressive strength, be durable and have good workability.
5. Hydraulic Considerations: The hydraulic considerations include ensuring that the dam can handle the expected flow of water, has adequate spillway capacity, and that the crest level of the dam is set at the appropriate height based on the downstream conditions.
6. Environmental Considerations: Environmental considerations must be made during the design and building of the dam to minimize its impact on the surrounding ecosystem. This includes preserving natural habitats, managing water quality, and taking the climate change consequences into account.

2.4.2. Failure Modes

A concrete gravity dam can fail in a number of different ways. Overturning failure, sliding failure, erosion failure, foundation failure, overtopping failure, and structural failure are some of the failure modes. The following is a description of some of the study's failure modes:

1. Sliding failure: Due to a decrease in base resistance, this failure mode occurs when the dam falls over its foundation, causing structural damage and a loss of stability.
2. Foundation failure: This happens as a result of the foundation's insufficient stability or strength leading to the instability of the dam body above. The shear along concrete rock contact failure mode, the formation of a non-compression zone leading to shear, the shear along a planar discontinuity, the shear along a stepped discontinuity, and the shear through a jointed rock mass are examples of this failure mode (Fell, 2014).

2.5. ROCK MASS CLASSIFICATION SYSTEMS

The majority of Mega's civil engineering constructions are based on solid rock. Engineering rock foundations can have a variety of geological formations, lithologies, and geological features. The properties of the rock mass and such geological formations completely determine how well the rock mass foundation materials operate. There are certain foundation flaws that might reduce the integrity of the foundation, including folds, excessively worn (or changed) seams, sheared zones, crushed seams, and joints. Due to these characteristics of the rock mass and the geological structures that have developed through time, the rock mass is heterogeneous and exhibits anisotropic behavior. The existence of discontinuities in the rock mass is mostly to blame for the behavior variance. Mega-civil constructions, like dams, may have stability issues as well as operational and safety issues if they are built on diverse rock foundations. The primary structural failures that might cause issues include sliding, overturning, deformation, and settling. Therefore, it is crucial to take into account the granite mass's strength and deformability properties in their in-situ state for design purposes. Predicting the equivalent strength and deformability characteristics of the rock mass requires both numerical and empirical understanding of the mechanical properties of the intact rock and the rock mass.

The process of gathering and interpreting qualitative and quantitative data that offers indices and descriptive words of the geometrical and mechanical features of a rock mass is known as "rock

mass characterization." Numerous categorization schemes for rock masses have been created throughout the years by various experts. These include the Rock Mass Designation index (RQD) (Deere and Deere, 1989), the Rock Mass Rating (RMR) (Bieniawski and Orr, 1976), the Tunnel Quality Index (Q) (Barton et al., 1974), and the Geological Strength Index (GSI) (Hoek, 1994; Hoek and Brown, 1997; Hoek et al., 1995; Marnos and Hoek, 2001).

2.5.1. Rock Quality Designation (RQD)

The drilling rock core quality is evaluated using the Rock Quality Designation (RQD). The RQD (rock quality index) is a measure of how much the core has fractured. The RQD is determined by adding up the lengths of all the pieces of core in a drill run that are longer than 100mm (4 in.), taking into account drilling-related fractures. The overall length is then calculated as a percentage of the drill run's length by adding these lengths together. The following is how RQD is determined:

$$RQD = \frac{\Sigma(length\ of\ core\ pieces\ with\ lengths>100mm)}{Total\ length\ of\ core\ run} \times 100\% \qquad \text{Equation 1.1}$$

RQD can be estimated at site from volumetric joint count (Jv) using the formula:

$$RQD = 110 + 2.5Jv, \qquad \text{Equation 1.2}$$

Table 1-1. Correlation between RQD and rock quality (Deere and Deere, 1989)

RQD (%)	Rock Mass Quality
<25	Very poor
25 - 50	Poor
50 - 75	Fair
75 - 90	Good
90 - 100	Excellent

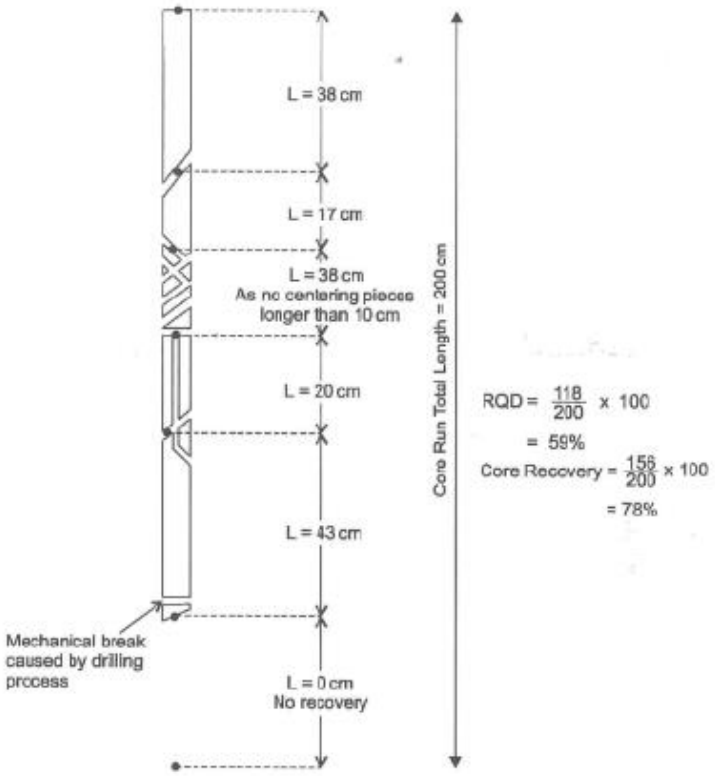

Figure 2.4.1. Computation of rock quality designation RQD
(Deere and Deere, 1989)

Biensiawski (1976) released the initial version of the Rock Mass Rating (RMR) methodology, which has since undergone several iterations and revisions as additional examples have been studied. Therefore, it is crucial to understand which version was applied while calculating the RMR. To categorize a rock mass using the RMR, the technique makes use of the following six parameters:

1. Uniaxial compressive strength of the rock material,
2. Rock Quality Designation (RQD),
3. Spacing of the discontinuities,
4. Condition of the discontinuities,
5. Ground water conditions,
6. Orientation of the discontinuities.

$$RMR = A1 + A2 + A3 + A4 + A5 + B \quad \text{Equation 1.3}$$

where A1 is ratings for the uniaxial compressive strength of the rock material; A2 is ratings for the RQD; A3 = ratings for the spacing of joints; A4 = ratings for the condition of joints; A5 = ratings for the ground water conditions; and B = ratings for the orientation of joints.

Table 1-2. The input parameters used in RMR_1989 classification system (Palmstrom, 2009)

A. Classification parameters and their ratings in the RMR system

PARAMETER			Range of values // RATINGS						
1	Strength of intact rock material	Point-load strength index	> 10 MPa	4 - 10 MPa	2 - 4 MPa	1 - 2 MPa	For this low range, uniaxial compr. strength is preferred		
		Uniaxial compressive strength	> 250 MPa	100 - 250 MPa	50 - 100 MPa	25 - 50 MPa	5 - 25 MPa	1 - 5 MPa	< 1 MPa
	RATING		15	12	7	4	2	1	0
2	Drill core quality RQD		90 - 100%	75 - 90%	50 - 75%	25 - 50%	< 25%		
	RATING		20	17	13	8	3		
3	Spacing of discontinuities		> 2 m	0.6 - 2 m	200 - 600 mm	60 - 200 mm	< 60 mm		
	RATING		20	15	10	8	5		
4	Condition of discontinuities	a. Length, persistence	< 1 m	1 - 3 m	3 - 10 m	10 - 20 m	> 20 m		
		Rating	6	4	2	1	0		
		b. Separation	none	< 0.1 mm	0.1 - 1 mm	1 - 5 mm	> 5 mm		
		Rating	6	5	4	1	0		
		c. Roughness	very rough	rough	slightly rough	smooth	slickensided		
		Rating	6	3	3	1	0		
		d. Infilling (gouge)	none	Hard filling		Soft filling			
			-	< 5 mm	> 5 mm	< 5 mm	> 5 mm		
		Rating	6	4	2	2	0		
		e. Weathering	unweathered	slightly w.	moderately w.	highly w.	decomposed		
		Rating	6	5	3	1	0		
5	Ground water	Inflow per 10 m tunnel length	none	< 10 litres/min	10 - 25 litres/min	25 - 125 litres/min	> 125 litres /min		
		p_w / σ1	0	0 - 0.1	0.1 - 0.2	0.2 - 0.5	> 0.5		
		General conditions	completely dry	damp	wet	dripping	flowing		
	RATING		15	10	7	4	0		

p_w = joint water pressure; σ1 = major principal stress

B. RMR rating adjustment for discontinuity orientations

		Very favourable	Favourable	Fair	Unfavourable	Very unfavourable
RATINGS	Tunnels	0	-2	-5	-10	-12
	Foundations	0	-2	-7	-15	-25
	Slopes	0	-5	-25	-50	-60

C. Rock mass classes determined from total RMR ratings

Rating	100 - 81	80 - 61	60 - 41	40 - 21	< 20
Class No.	I	II	III	IV	V
Description	VERY GOOD	GOOD	FAIR	POOR	VERY POOR

D. Meaning of ground classes

Class No.	I	II	III	IV	V
Average stand-up time	10 years for 15 m span	6 months for 8 m span	1 week for 5 m span	10 hours for 2.5 m span	30 minutes for 1 m span
Cohesion of the rock mass	> 400 kPa	300 - 400 kPa	200 - 300 kPa	100 - 200 kPa	< 100 kPa
Friction angle of the rock mass	< 45°	35 - 45°	25 - 35°	15 - 25°	< 15°

The tunneling and slope work industries are best suited for this categorization scheme. To measure the stability of the dam foundation, Bieniwski and Orr (1976) offered correction factors based on the dip angle of the main joint set. Romana suggested a brand-new set of adjustment variables for the dam stability based on the studies of Snell and Knight (1991).

Table 1-3. Adjusting factors for the dam stability (Romana, 2003)

Type of Dam	VF	F	FA	U	VU
Fill	Others	10-30 DS	0-10 A	-	-
Gravity	10-60 DS	30-60 US 60-90 A	10-30 US	0-10 A	-
Arch	30-60 DS	10-30 DS	30-60 US 60-90 A	10-30 US	0-10 A
R_{STA}	0	-2	-7	-15	-25

Note: DS is Dip Downstream, US is Dip Upstream, and A is any direction.

Where: VF is very favorable, F is favorable, FA is fair, U is unfavorable, VU is very unfavorable.

The deformation modulus (E_{rm}) of rock masses can be obtained by using the following correlation developed by Bieniawski (1978) for RMR greater than 50:

E_{rm}=2 RMR−100 (in GPa) Equation 1.4

The aforementioned equation was created by Serafim and Pereira (1983) to be widely applicable for determining the deformation modulus of rock masses as in the following equation:

E_{rm}=$10^{(RMR-10)/40}$ (in GPa) Equation 1.5

2.5.2. Geological Strength Index (GSI)

GSI is calculated using geological descriptions of the rock mass that take into account two factors: joint or block surface conditions and rock structure, or block size. It is straightforward to use and suitable even for weak rock masses, unlike Bieniwski's grading method. But it requires a close inspection and comprehension of the engineering geological characteristics of the rock bulk. The goal was to calculate the decline in rock mass strength under various geological circumstances. More geological observation than a numerical ranking is required. When things get tough, a different strategy based on the ideas of block volume and joint condition variables is applied. Figure 7 depicts the GSI estimation in the free to use "RocLab" software package from http://www.rocscience.com (Hoek et al., 2002). For generally competent rock masses with GSI > 25, the value of GSI can be related to Rock Mass Rating RMR value as, GSI = RMR – 5. Only the GSI system of rock mass categorization has a direct relationship with engineering factors like the rock mass modulus, Hoek-Brown strength parameters, or Mohr-Coulomb parameters (Cai, 2004). The equivalent deformation modulus (Em) of the rock mass may be computed when the GSI has

been evaluated and the strength parameters for the generalized Hoek Brown criteria have been determined (Hoek et al., 1992).

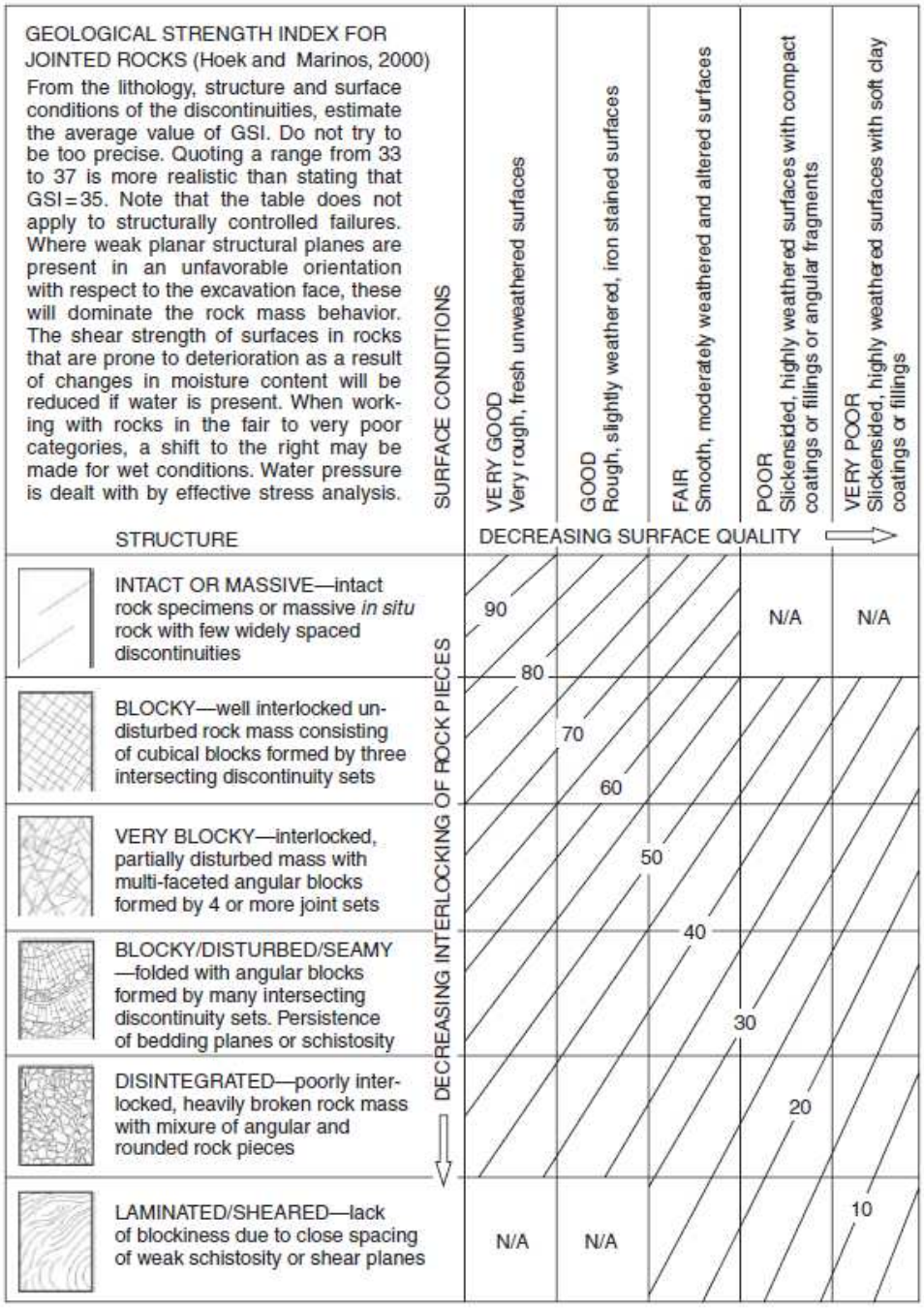

Figure 2.4.2 Estimate of Geological Strength Index (GSI) on the basis of partial interlocking and discontinuity condition

$$E_m = \left(1 - \frac{D}{2}\right)\sqrt{\frac{\sigma_{ci}}{100}}\,10^{((GSI-10)/40)} \quad \text{(units: GPa)}$$

Applied for $\sigma_{ci} \leq 100$ MPa

Equation 1.6

$$E_{rm}(GPa) = \left(1 - \frac{D}{2}\right) \cdot 10^{\frac{(GSI-10)}{40}}$$

Equation 1.7

Where: E_m is equivalent deformation modulus, D is disturbance factor, σ_{ci} uniaxial compressive strength of intact pieces of rock

The Hoek-Brown and Mohr-Coulomb criteria for the rock mass's friction angle and cohesive strength can be met by fitting an average linear relationship to the modified curve produced by the major principal stress for a range of minor principal stress values specified by $\sigma t < \sigma 3 < \sigma 3max$. For a given normal stress, the Mohr-Coulomb shear strength is calculated by substituting these values for c' and ϕ' into the following equation:

$$\tau = c' + \sigma \tan \phi'$$

Equation 1.8

The equivalent plot, in terms of the major and minor principal stresses, is defined by

$$\sigma'_1 = \frac{2c' \cos \phi'}{1 - \sin \phi'} + \frac{1 + \sin \phi'}{1 - \sin \phi'}\sigma'_3$$

Equation 1.9

The software package 'RocLab' has been updated to include both the Hoek-Brown criteria and its corresponding Mohr-Coulomb criterion. The Hoek-Brown parameters, equivalent Mohr-Coulomb parameters, and the GSI value may all be calculated using the charts and tables in this code.

2.6. NUMERICAL MODELLING

Previously, several researches have been done related to stability of concrete gravity dam on jointed rock mass. It has been important to analyze of potential failure mode of dam foundation defined by the rock mass discontinuities. There are various numerical modelling methods to make analysis of such failures, including the Finite Element method (FEM), the Discrete Element Method (DEM) represents the rock mass as an assembly of blocks in interaction along the

discontinuities (Lemos, 2012). There are different DEM techniques for modelling discontinuous media includes Discrete elements, DDA, AEM, UDEC, 3DEC, etc (Lemos, 2021).

Research has been conducted to investigate the foundation failure mechanisms of a rock dam foundation by means of a numerical method, ie., Universal Discrete Element Code (UDEC) and the geomechanical model method (Donghui Chen, 2020). The result of the research indicated that the failure mechanism of the foundation rock masses, as characterized by gentle through-going and steep structural discontinuities, is not a conventional type of shear failure mechanism but a buckling one. The researcher suggested that the use of 3D approach with technological advancement will improve the accuracy of the results.

A numerical model for the hydromechanical analysis of masonry dams based on the discrete element method is presented (Bretas et. al., 2012). A numerical model for analysis of masonry gravity dams based on the Discrete Element Method is presented (Bretas et. al., 2014). This approach, however, has several limitations and fails to reproduce the buckling mechanism observed in underground hard rock mines. The failure mechanism of the foundation of Baxio dam has been investigated using the DEM (3DEC) method. The application of DEM involves in the model generation, such as representation of the rock discontinuities, model generation, block and joint deformability, joint water pressure and the procedure for safety factor evaluation (Lemos, 2012). The researcher concluded that using this numerical model provide a powerful tool to address the safety assessment of structural foundations on rock and requires continued investigation on a range of issues (Lemos, 2021). Practical joint generation techniques specifically intended for stability analysis; a consistent and dependable treatment of rock bridge or dam-rock interface fracture; estimation of joint water pressure distributions providing a reasonable envelope for specific in situ conditions are central in dam foundation failure studies among the range of issues.

3DEC (Distinct Element Code) is a numerical modelling software used for analyzing rock mechanics, mechanical behavior of soils, joints, geotechnical engineering, and related field of study with complex geometries such as tunnel, excavations, hydropower and slopes. The software uses a combination of continuum mechanics, fracture mechanics, and contact mechanics to analyze the response of these materials to different loading conditions, including seismic events and underground blasting. The software uses programming to create numerical models of

discontinuous media such as jointed rock masses, concrete structures, or soil. It utilizes programming languages such as FISH (FLAC/3DEC Internal Scripting Language) or Python. Through these programming, the software allows users to automate simulations, perform parameter sweeps, and post-process simulation results. 3DEC allows users to simulate the behavior of materials that undergo complex deformation or failure modes, such as those undergoing extensive shear or fragmentation since it has ability to model the interactions between individual particles or grains within a material.

3DEC numerical modelling software specifically designed for analyzing rock mechanics, which enables users to create and manipulate complex 3D models of geological and geotechnical structures, including the generation and manipulation of meshes. The software offers various options for mesh generation, including blocky, polyhedral, tetrahedral, and Voronoi, allowing users to choose the most appropriate type of mesh for their specific modeling needs. It is capable of simulating fractures following existing joints. It takes into account the orientation and location of pre-existing discontinuities in the rock mass to simulate the initiation and propagation of fractures through these (https://docs.itascacg.com). This allows for more accurate and realistic modeling of rock mass behavior and helps engineers in designing and assessing rock structures.

3DEC, UDEC, and Plaxis are computer programs for simulating the behavior of rocks and soil materials. Here are some of the advantages of 3DEC over UDEC and Plaxis: (1) 3DEC uses a Discrete Element Method (DEM) to model rock behavior. This method allows the software to represent discontinuities and fractures in the rock, which makes for a more realistic simulation (Lemos, 2021). (2) 3DEC offers a wider range of customization options than UDEC and Plaxis. Users can define their own boundary conditions and input parameters, which makes it easier to model complex real-world problems. (3) 3DEC has a more advanced graphics engine than UDEC and Plaxis. This makes it easier to interpret results and identify potential issues in a model. (4) 3DEC includes integrated fluid-flow capabilities, which means that users can model the behavior of water and other fluids through porous media (Lemos, 2021). This feature is not available in UDEC and is only available in a limited capacity in Plaxis. Additionally, there are some preferable features over the other geotechnical softwares such as: With 3DEC, simulations can be performed on a three-dimensional scale, which is beneficial when analyzing underground rock systems that have complex geometries, The software has various built-in material models for different rock

classes like brittle and ductile rocks, jointed rocks, and more, The code is capable of simulating multi-physics phenomenon and can handle several boundary conditions at the same time.

These features make 3DEC a powerful tool for investigating complex rock mechanics problems in various industries like mining, hydropower, civil engineering, etc. Generally, 3DEC is a powerful tool for simulating geological processes and predicting the behavior of rock masses and soil structures. Its accuracy and versatility make it an indispensable tool for researchers and professionals in the field of geomechanics.

In 3DEC, there are various types of constitutive model to represent material and discontinuity (Itasca manual, 2016). Some of material models are described below:

1. Null (EXCAVTE command): is assigned to represent material which is removed from the model,
2. Linear elastic model: is valid for homogeneous, isotropic, continuous materials which exhibit linear stress-strain behavior. Used to describe uni-axial, triaxial compression, and extension tests. This model requires material properties of density, bulk modulus, shear modulus, cohesion, and internal friction angle of the rock.
3. Elastic, anisotropic: is appropriate for elastic materials that exhibit a well-defined elastic anisotropy,
4. Mohr-Coulomb plasticity: utilized to define the strength of a rock mass using Mohr-Coulomb criteria and applied for materials that give when subjected to shear loading. This model requires material properties such as density, bulk modulus shear modulus, cohesion, internal friction angle, tensile strength, dilation angle of the rock.

The application of the material model uses actual data and/or requires generation of input data from primary or secondary geotechnical laboratory tests and/or valid and reliable site data of the rock / rock mass using proposed empirical equations. The Young's modulus of the intact rock can be obtained from laboratory direct shear test results.

To determine the deformation modulus of the rock mass, the following equation may be used (Yan Xing, P. H. S. W. Kulatilake, L. A. Sandbak, 2017):

$$E_{rm} = E_i\left(0.02 + \frac{1 - D/2}{1 + e^{((60+15D-GSI)/11)}}\right)$$ *Equation 1.10*

Where: Erm is Young's modulus of the rock mass; Ei is the Young's modulus of the intact rock; D is disturbance factor; GSI is geological strength index.

To determine the Mohr-Coulomb parameters, internal friction angle (ø) and cohesion (c), the following equations can be used:

$$\emptyset = \sin^{-1}\left[\frac{6am_b\left(s+m_b\sigma_{3n}\right)^{a-1}}{2(1+a)(2+a)+6am_b\left(s+m_b\sigma_{3n}\right)^{a-1}}\right] \quad \text{Equation 11}$$

$$c = \frac{\sigma_{ci}\left[(1+2a)s+(1-a)m_b\sigma_{3n}\right]\left(s+m_b\sigma_{3n}\right)^{a-1}}{(1+a)(1+2a)\sqrt{1+\left(6am_b\left(s+m_b\sigma_{3n}\right)^{a-1}\right)/(1+a)(1+2a)}} \quad \text{Equation 12}$$

Where: mb, s, a are rock mass constants,

There are two built-in models available to represent the material behavior of discontinuities:

1. Joint area contact — Coulomb slip (elastic-perfectly plastic): this model used to represent the failure in the deformable rock mass. It requires material properties of normal and shear stiffness, internal friction angle, cohesion, tensile strength and dilation angle of the joint. The Itasca manual proposed an empirical equation to generate input data for joint stiffness in the rock mass. Direct laboratory test results may be used for the rest of joint properties otherwise scaling down of the joint properties in the rock mass may be used in the case of equivalent continuum concept (Yan Xing, P. H. S. W. Kulatilake, L. A. Sandbak, 2017).
2. continuously yielding

2.7. SUMMARY AND CONCLUSIONS

Most of historical dam failure studies identifies two failure modes: that are sliding failure, which occurs when a dam falls over its foundation, and foundation failure, which occurs due to insufficient stability or strength of the foundation, and shear along concrete rock contact failure mode. The insufficient stability of the foundation is a result of the geological structures in the rock foundation which is controlled by the presence of discontinuities, properties of infillings materials, seams, gauges, and hydraulic behaviors of discontinuities.

Understanding the properties of jointed rock masses is crucial for design, construction, and post-construction stages. Techniques like RMR and GSI assess the foundation's suitability and stability, determining its engineering significance. However, From the literature review, these methods were

not enough to understand the behavior of complex rock mass foundation and responses of the rock mass foundation under various loading conditions.

Previously, research on the stability of concrete gravity dams on jointed rock masses has been conducted using various numerical modelling methods. From the literature review, 3DEC modeling was found to be reasonably practical to simulate jointed rock mass foundation. This numerical model provides a powerful tool for addressing safety assessment of structural foundations on rock and requires further investigation on various issues. 3DEC is a numerical modeling software used for analyzing rock mechanics, mechanical behavior of soils, joints, geotechnical engineering, and related fields with complex geometries. It allows users to create and manipulate complex 3D models of geological and geotechnical structures, including the generation and manipulation of meshes. However, 3DEC requires constitutive material model properties and joint model properties to be represented in the model. Hence, secondary data of laboratory tests are required in order to obtain representative input parameters for the numerical models.

CHAPTER 3: STUDY AREA

3.1. INTRODUCTION

Ethiopia has an abundance of rivers that provide the country with the potential for large sustainable energy resources in the form of hydropower. Several power planning studies have estimated that Ethiopia's hydroelectric potential is in the order of 45,000 MW, a potential greatly in excess of foreseeable domestic demand. Currently only less than 25 percent of the available total quantity is being harnessed for generating hydroelectric power. Preliminary investigations have indicated that the most promising sites could be developed at lower costs than other power generation options. The long-term plan realized that exporting electric power to a domestic demand and increase exports of electricity and make the sector a major foreign currency earner for the country.

Koysha (KHPP) (under construction) is the fourth hydropower plant of Omo/Gibe River cascade in Ethiopia, see Appendix, comprising Gilgel Gibe I (185 MW), Gibe II (420 MW) and Gibe III (1'870 MW), all currently in operation. Koysha is a step forward in the development of the entire

hydropower potential of the Omo River and represents a realization of the large-scale vision started more than 25 years ago with the design of Gilgel Gibe hydroelectric power plant.

The Koysha hydroelectric power project comprises a 180m-high, roller-compacted concrete (RCC) gravity dam, and a 250m-long, 41m-wide, and 60m-high surface powerhouse equipped with eight Francis turbine units of 270MW rated capacity each and total capacity of 2'160 MW. The RCC gravity dam with a crest length of 990m will create a reservoir capacity of nine billion cubic meters (bcm). The project also features a 330m-long and 42m-high cofferdam. The main dam will have six spillway gates, 20m-wide and 17m-high, with a discharge capacity of 13,100m3/s. The project also involves the construction of a diversion canal and two 6m-diameter middle-level outlets embedded in the dam body to control the reservoir level. The power station will utilize three 650m-long steel penstocks. The other electrical component of the power station includes a total of 24 transformers, including three single-phase 400kV transformers and a switchyard.

Figure 3.1. Koysha hydropower dam project design

An EPC/Turnkey contract agreement was signed between Ethiopian Electric Power (EEP) and Slini Impregilo (Webuild group) S.p.A. whose offices are located in Via dei Missaglia 97, 20142 Milan Italy, to execute the work for the sum of 2,455,035,197 Euro excluding Value Added Tax in 2015. The dam work and related other works are designed by Studio Petrangeli consulting engineer, Rome, Italy.

3.2. TOPOGRAPHY AND GEOMORPHOLOGY

The Koysha project site is situated in a mountainous region with elevations ranging from 520 to 2700 meters above sea level. The project area is dominated by highlands, which are generally steep and broken, and some areas are covered with dense vegetation. There are several rivers that flow through the project region, including the Omo River, which is the main source of water for the hydropower project. The Koysha hydropower project is being built on the Omo River, which flows through a deep valley with steep slopes.

he topography around the project site is steep, rugged, and characterized by highlands, deep valleys, and dense vegetation. These topographic features are mainly the result of the geological structures and geological phenomenon such as volcanism, rifting process associated with Main Ethiopian Rift System and erosions and depositions. Despite the challenges posed by the difficult terrain, it presents an excellent location for hydroelectric power generation. The topographical map of the study area and surrounding is presented in figure 3.2. below.

The main Omo river, its tributaries, and channels, in addition to primarily geological structures, have been responsible for long-term erosions and depositions of earth elements that have formed the V-shaped river valley at the dam site. The rivers and channels eroded and transported earth elements from high terrain and steep slopes due to the rapid rate of stream flow, where they were later dumped along the river banks, on the hill sides, and at the place of confluence as delta. The majority of the recent materials are found along the river banks and consist of alluvial deposits of various materials brought in from far and near. These alluvial deposits contain cobbles, stones, gravel, sand, silt, and clay. The size and depth of the alluvium vary from one location to another. Quaternary columnar basalts, which are distinguished by fine-grained, dark-gray, extremely strong, fresh rock, are found on the upper plateaus of both the right and left abutments of the dam region. The thin top layer broke down into reddish clay soil, which was then covered by plants and long grass. Additionally, the basalt units are mapped on top of other hills on the dam abutments' right side, downstream from the right plateau, and upstream and downstream from the left plateau. The slopes of the dam's abutment are covered in thick accumulations of colluvium materials, which are primarily made of columnar basalts, silt, and clay matrix. On the upstream side of the left abutment and steep slope, there are thick deposits of colluvium.

On the abutment slope, with the exception of the gentle slopes to the left, the colluvium materials entirely cover the underlying conglomerate lithological unit. The right abutment of the dam, which extends from upstream to downstream of the plateau, is the only place where this conglomerate block is visible. On the upstream and downstream sides, tributary streams have formed gentle slopes that the conglomerate outcrops on. Gravels, pebbles, sandstone, and siltstone make up the

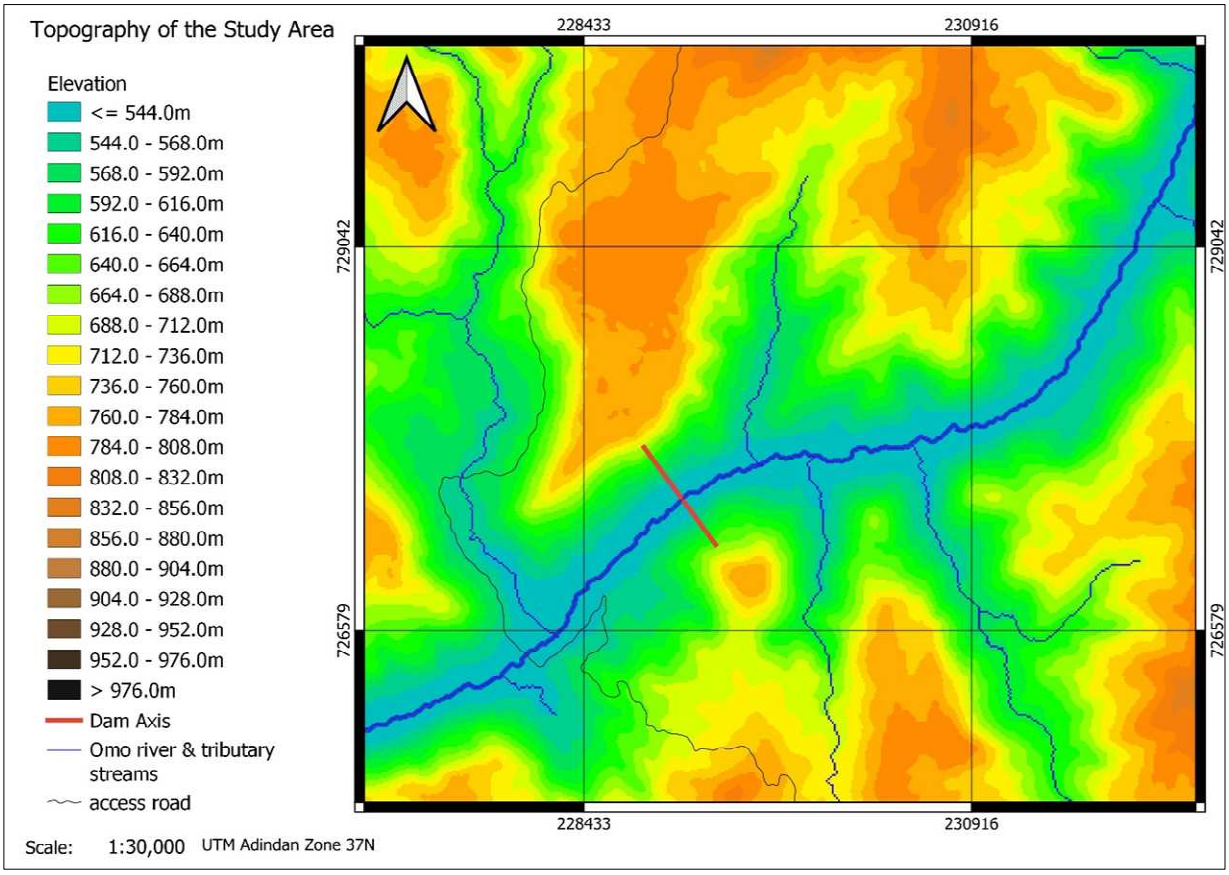

Figure 3.2. Topographical map of the study area and surrounding

majority of the conglomerate unit. One of the site's joint sets (J2) is consistent with the orientation of the thin siltstone and sandstone layer toward the west (24/270). The joint's orientation might match that of an older lava flow beneath it made of an Andesite/Andesite autobreccia. This rock formation forms the base of the riverbed where the dam and other civil facilities will be built. During the excavation phase, many Petrified woods were discovered on the conglomerate's excavation slope.

3.3. DRAINAGE

All seasonal and intermittent streams flow from the northern catchments of the Gibe/Omo river towards the south direction and reaches the drainages of study area. The northern part of omo river catchment has a number of tributaries from the NE, the largest ones being the Walga and the Wabi River. These drain largely cultivated land, much of it with rather impeded drainage. The Tunjo and Gilgel Gibe Rivers are important tributaries, also draining mainly cultivated lands from the SW. These have a higher proportion of more permeable soils than the Walga and Wabi catchments. In the valley bottom the land is mainly classified hydrologically as rangeland. Going downstream another important tributary is found from the west, the Gojeb River. The Gibe River is known as the Omo River in its lower reaches, south-western from the confluence with the Gojeb River.

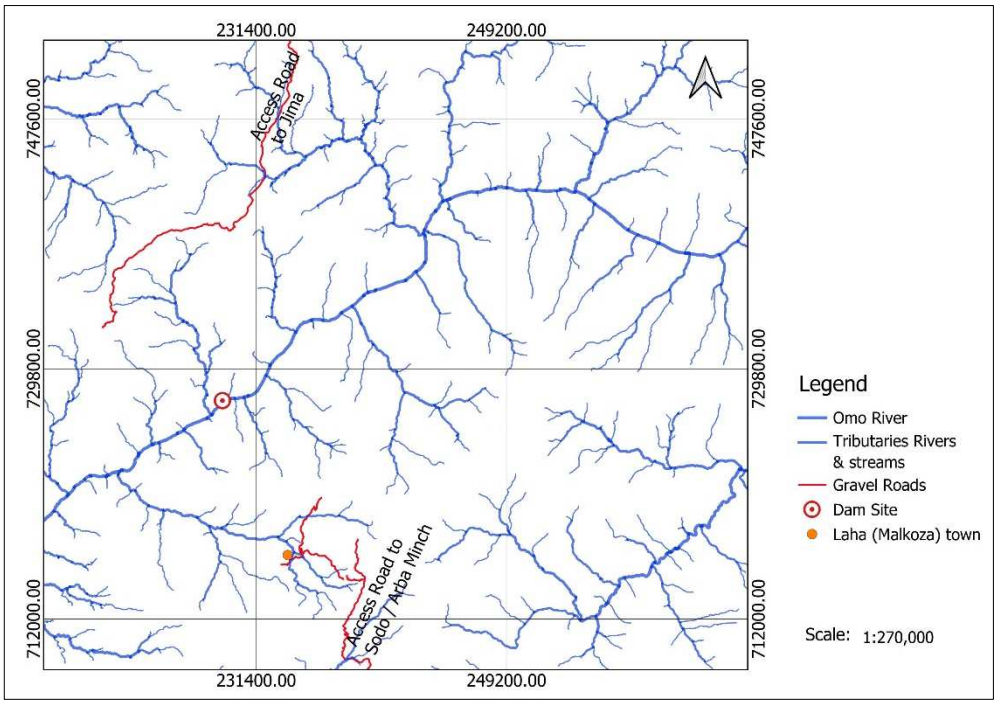

Figure 3.3. Drainage map of the dam area and surroundings

In the dam site the Omo river flows to the southwest. Streams and rivers in the Omo drainage basin in the study area drain from northwest to southeast, north to south, south to north and southeast to northwest towards the Omo river. As it is known by being wet region, most of the streams that in Omo basin in the study area are classified as intermittent and dominantly perineal, and the drainage patterns of most streams and rivers are sub parallel and dendritic pattern. In the study area the

major perineal tributaries of the Omo drainage basin include Zirgina, Chebera and mensto rivers which drain to the south to join the Omo river and Yirgino and Maze river catchment in Gofa drains to the north to join the Omo drainage basin. They drain uplands that have been less intensively used for agriculture. The prevailing vegetations of all the large tributaries headwaters is wooded shrubland.

3.4. CLIMATE

3.4.1. Rainfall

The project found in wet zone of the country where prolonged period of rainfall is reported annually. The rain starts on mid of March and continue with little variation without interruption with maximum rain in April, May, August and September.

Rainfall data record from 2004 to 2022 for the area are used from three surrounding station located in Sawla (1380 masl), Chida (1700 masl) and Bonga (1750 masl) towns. These data are summarized as a mean on the monthly and annually bases in the following table 3.1. below.
As presented in Table 3.1 below the precipitation occurs throughout the year except November to February. The monthly mean records of rain fall shown for each station indicates that the mean annual rain fall at Chida, Bonga and Sawla stations were 1507 mm, 1737 mm and 1480 mm, respectively. Thus, the study area receives mean annual rain fall of about 1575 mm. As it is indicated in the summary table, in all stations surrounding the study area the heaviest rainfall occurs in April and May whereas the minimum or dry season are from December to February.

Table 3-1. Mean monthly and Annual rainfall surrounding stations (Source: National Meteorological Services Agency)

Stations	Mean Rainfall, °C												Mean mm/year
	Jan	Feb	Mar	Apr	May	Jun	Jul	Aug	Sep	Oct	Nov	Dec	
Chida	54.8	79.6	146.8	155.1	195.6	134.0	161.6	170.1	150.3	144.4	67.0	42.9	1507
Bonga	46.9	69.3	125.2	190.1	211.5	201.3	204.2	209.2	197.1	146.2	71.2	59.8	1737
Sawla	48.2	49.6	119.2	220.4	178.9	127.0	153.0	129.1	145.3	156.4	108.5	44.4	1480

"Rainy months "and" dry months "of any year is distinguished by calculating rain fall coefficient (RC). It is the ratio between the mean monthly rain fall and one twelfth of the annual mean (Tamiru

Alemayehu et al, 2006). Rainy months have rain fall coefficient (RC) of above 0.6 where as those of dry months have less than 0.6 (Tamiru Alemayehu etal, 2006).

The rain fall coefficient is shown in Table 3.2. From Table 3.2 it is observed that the rainy months of study area are from March to October and the dry months are from November to February.

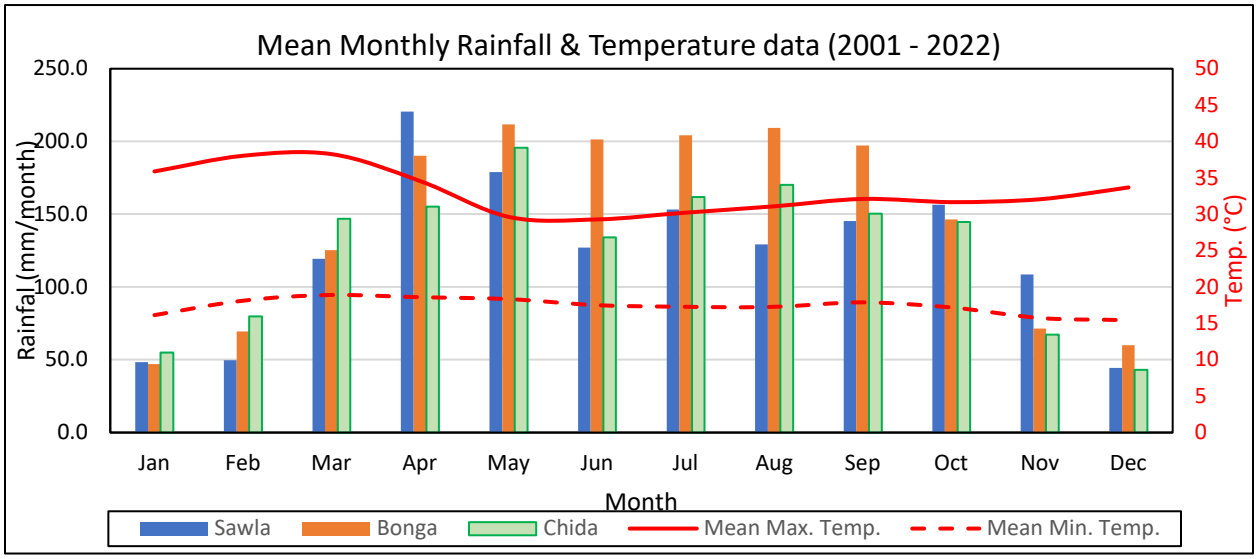

Figure 3.4. Mean monthly rainfall of surrounding stations (Source: National Metrological Services Agency) and mean max. and min temperature of the site station.

Table 3-2. Rainfall coefficient of the surrounding stations (Source: National Meteorological Services Agency)

Stations	Jan	Feb	Mar	Apr	May	Jun	Jul	Aug	Sep	Oct	Nov	Dec
Chida	0.4	0.6	1.2	1.2	1.6	1.1	1.3	1.4	1.2	1.2	0.5	0.3
Bonga	0.3	0.5	0.9	1.3	1.5	1.4	1.4	1.4	1.4	1.0	0.5	0.4
Sawla	0.4	0.4	1.0	1.8	1.5	1.0	1.2	1.0	1.2	1.3	0.9	0.4

3.4.2. Temperature

The study area is known by its rugged topography which is a result of the geological phenomenon. Altitude is one of the factors which controls the temperature variations in the study area. Air temperature decreases with increasing altitude at a mean rate of 0.7°C for every 100 meter (Fetter, 1994). Based on Ethiopian climatic zoning, the dam site area lies under Hot zone (Kolla), which comprises area below 1500-meter altitude. For the Altitude reasons, the temperature data from the

three aforementioned stations are not utilized here to analyzes the temperature of the study area. The seven years mean monthly temperature data of the project site station is summarized and presented in the table 3.3. below.

As it is presented in the table below, the hottest months are January, February and March which has a mean maximum temperature of 37.4°C and the coldest seasons in the year are May, June, July and August which has a mean maximum temperature of 30.1°C and mean minimum temperature of 17.6°C. The mean maximum annual temperature recorded in the project site is 38.3°C. The mean maximum and mean minimum temperature of the study area are presented graphically in the figure 3.2.

Table 3-3. Mean monthly temperature data of the site station for the last seven years.

	Jan	Feb	Mar	Apr	May	Jun	Jul	Aug	Sep	Oct	Nov	Dec
Mean Max. Temp. °C	35.9	38.0	38.3	34.6	29.6	29.3	30.2	31.1	32.1	31.7	32.1	33.7
Mean Min. Temp. °C	16.1	18.1	18.9	18.6	18.3	17.5	17.3	17.3	17.9	17.2	15.7	15.4

3.5. REGIONAL GEOLOGY

3.5.1. Stratigraphy

The first geological map covering the project area is mapped at 1:250000 published by the Geological Survey of Ethiopia (geological map of Dime map sheet in 2018) after the project has been commenced, before that, all the geological information is based on either the photointerpretation of aerial photographs without field evidences (Merla et al., 1973, Tefera et al. 1996), or by reconstructing detailed model (Davidson 1983).

The regional geology of the project area consists of the Precambrian crystalline basement rocks, the Paleozoic and Tertiary sediments, the Tertiary volcanics and fluvial and lacustrine sediments of Pliocene-Pleistocene ages. The oldest crystalline basement rocks of the southwestern Ethiopia outcrop in two main parts: in Illubabor and southwest of Kafa and in Gamo Gofa southwest of Sidama (Davidson et al. 1973; Davidson, 1983). These basement rocks were divided into three main domains: (1) Hammar domain: included a complex of older gneiss and granulite of Konso, Alghe, Awata, Yabello and Baro Group. (2) Akobo domain: made up of a variety of supra-crustal schists and gneisses that are metamorphosed from green schist to middle amphibolites facies; commonly intruded by plutons having gabbroic to granitic composition. (3) Surma domain:

consisted of foliated and ortho gneisses; and mylonite. The Paleozoic sediments consists of terrestrial sediments, consolidated, non-metamorphosed sedimentary rocks, mainly sandstone with conglomerate and intercalated siltstone (Davidson, 1983), which were classified as the Gilo, Kari and Meti sandstones, and occurred above unconformity between the crystalline basement and its Tertiary volcanics. The volcanic rocks were consisting of the Eocene oldest Akobo basalts (49.4-46.0 Ma), (Davidson and Rex, 1980), the Omo basalt (40-25Ma), the Jima volcanics (37-10 Ma) and the Wollega basalts (15-7 Ma). Merla et al. (1979). The Tertiary volcanics unconformably overlain the crystalline basement rocks.

The Omo basalt were commonly fine grained columnarly jointed. The effusive flows of the lower and upper units of Jima volcanics were mainly composed of massive, white to pinkish and gray rhyolites, comendites, and pantellerites in thick flows alternating with tuffs and subordinate basalts. The Wollega basalt resting on the basement and on the tilted Omo basalts and Jima volcanites, predominant columnar alkaline basalt flows inter layered, particularly in the upper portion, with acidic tuff and loose fluvial lacustrine deposits.

The Tertiary volcanic rock of Southwestern Ethiopia also categorized in to Pre-rift volcanic rocks of main sequence (bimodal basalt and rhyolite) (49-35 Ma) and post-rift youngest volcanic rocks (32-21 Ma) Davidson and Rex (1980). The post-rift sequence (19 Ma to present) comprised the mid Miocene flood basalts, which lied unconformably on the tilted pre-rift flows, overlying silicic lavas and pyroclastic rocks, phonolite and alkali trachyte flows, small intrusions, and the Quaternary volcanics.

3.5.2. Structural Set-Up

Regional Geological Structures

Geology and structures associated with the geological activities play significant role on the stability of the dam foundation and safe operation of the dam structures. The presence of geological structures such as faults/shear zones, discontinuities, unfavorable weak layers, folds, lineaments may cause structural and operational failure if they are not taken into account in the design and constructions. It is rare finding homogeneous foundation; hence, it makes impossible construction of large dams on homogeneous rock foundation. Koysha dam is designed to be constructed on jointed rock mass and complex geology with special attention in identifying the geological

structures in the investigation, design and construction phases. It is very important to observe and understand the geological structures at the dam site with regional geological structures.

The dam project situated in the regional geological structures where early deformation (ductile structures) and later deformational phases (brittle structures) exhibited on the exposed rocks. The ductile structures found as regional level include folds and foliations. Brittle deformations resulted faults, dikes, veins and joints, the brittle structures affected both crystalline basement and volcanic rocks.

1. Foliation, it occurs as planar fabric in the basement rocks consisting of gneissic banding. They are generally oriented toward NE strike. The gneissic foliation was defined by the preferred alignment of mineral grains such as mica, pyroxene and hornblende, and elongated quartz and feldspar, contained within each metamorphic layering.

2. Lineations, occur as non-penetrative linear structure that is mainly defined by parallel alignment of mineral grains or stretched mineral aggregates defined by felsic and minor mafic minerals. It occurs sporadically in migmatitic gneisses defined by quartz, feldspat and biotite.

3. Folds, in the map area were formed by compressional deformation found in high-grade gneisses. Folds such as similar fold, recumbent fold, drag fold (parasitic fold), ptygmatic fold and plunging fold are encountered in the regional area.

4. Normal fault and graben system (Cenozic structures), most of the area displays Sub-parallel half-grabens constitute from west to east, the North Omo, Berso, Sawla, Beto and Mati-Dancha basins. The North Omo graben is bounded by normal faults trending in NNE direction. The Berso basin includes 30 to 38 km long and 5 to 10km wide tilted blocks that generally trend NNE parallel to normal faults bounding the North Omo basin. In the NE-SW trending Sawla basin, the border fault becomes steep, and the trap series observed dipping ~20° toward the west. The Beto basin, situated between the Sawla and Mati-Dancha basins in the southeastern part of the map sheet, trends NE. The master fault bounding the Beto basin tilted the trap series for about 20° and locally up to ~40° to the west. 5. NW fault (Cenozic Structures), NW to NNW trending faults are the most prominent set of faults in the south-central and southeast corners of the map sheet. The NNW fault which passes through the Omo River gorge extends up to the northern extreme of the map area where it is cut by the E-W faults. Another major NW trending fault system occurs in the central

part of the area. At its southern end this fault exhibits reddish brown, strongly crushed basaltic/rhyolitic breccias.

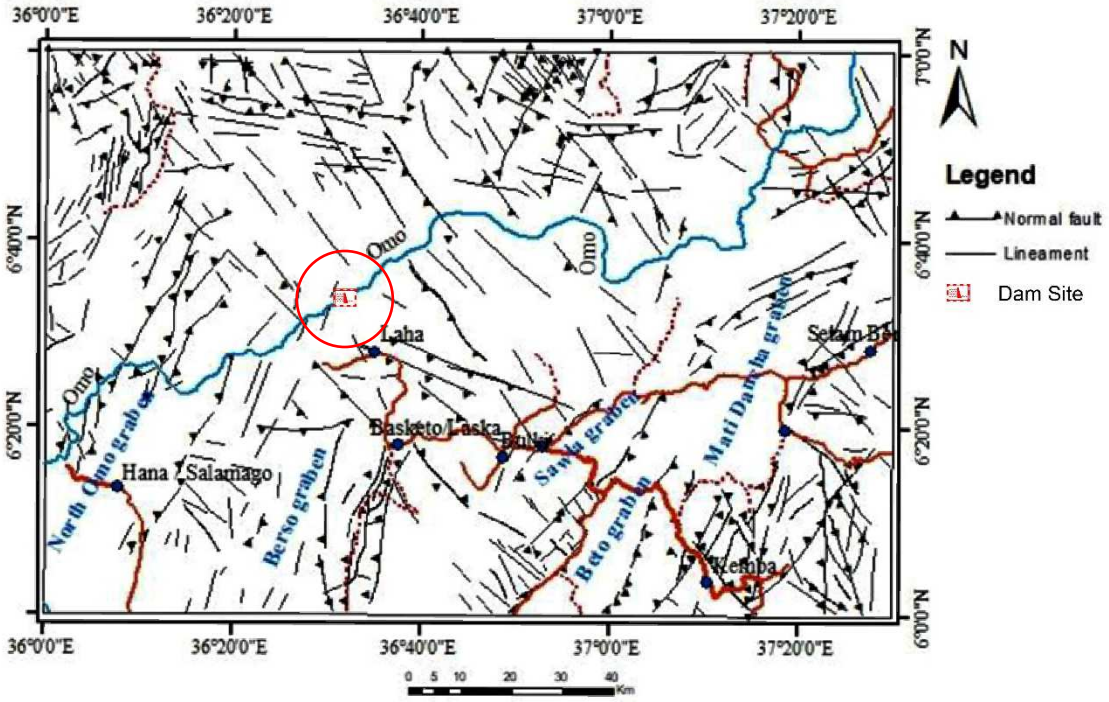

Figure 3.5. Regional structural map of the area (GSE 2018, geological map of Dime map sheet))

6. Joints, are widely observed in tertiary basalts with defined pattern of joint sets and random joints. Most of the joints are filled by secondary material such as calcite, iron oxide, silica & feldspar, clay and weathered materials.

The structural set up of the region is presented in the figure below as reported by the geological survey of Ethiopia in February 2018.

3.6. GEOLOGY OF THE DAM AREA

3.6.1. Lithology

The rock masses outcropping in the dam site have been classified into five main lithostratigraphic units, resumed in the following table, where the formations are listed from to the most recent up to the oldest, Fig. 3.6. shows the geological map of the dam area.

(A) – Recent Deposits

It consists of silty sand fluvial deposits. The thickness is low being in the range of few meters in both the banks. A greater thickness has to be expected in right bank at the confluence with the tributary creek, located approximately 500 m upstream the dam center line. In both sides of the valley a thick accumulation of coarse rock debris is present.

Table 3-4. Dam site litostartigraphic units (Koysha project, Salini-Impregilo, General geological report, 2016)

A0	Recent Deposits	Recent alluvium deposits
Bc	Upper Basalt Formation	Unweathered Columnar basalt lava flows
Cc	Conglomerate Formation	Slightly weathered gravel and pebble clast-supported conglomerate. Siltstone and sandstone occur as intercalated beds.
A2	Andesite / Basalt Formation	Aphanitic olive gray fine-grained very strong andesite. Thin secondary and late calcite veins are present. It represents the massive interior of the lava flow.
A1	Andesite / Basalt Formation	Autobrrecia: composed of angular cemented clasts of centimetric dimension due to fragmentation on outer surfaces of lava flows. Displacement between blocks is limited, with calcite or zeolites filling millimetric to centimetric cracks.

(Bc) – Upper Basalt Formation

This formation outcrops starting from elevation about 690 m a.s.l. and hence does not stratigraphically concern the dam foundation. It morphologically forms the plateau on both the abutments. It consists of columnar basalt lava flows. The rock mass is unweathered composed by black, fine grained and very strong basalt, locally vesicular. The flow interior is dense with little fracturing. The thickness reaches about:

- Right Bank: approximately 115 m in borehole R01;
- Left Bank: about 80 m in borehole L04.

Figure 3.6. (Left: Recent deposit of alluvial along river banks, (Right: Columnar basalt on right downstream abutment. (Salini impregilo: basic investigation report, 2016)

(C) – Conglomerate Formation

This Formation is composed by two members:

- Conglomerate (Co) that covers almost the totality of the formation. It is composed by slightly weathered gravel and pebble clast-supported conglomerates mainly formed by basalt and rhyolite-trachyte rounded elements. It occurs as cemented, strong to moderately strong rock (grade R3-R4 25-100 MPa). The matrix is sandy. Locally the conglomerate is interbedded by decimetric plastic clayey levels.
- Siltstone and Sandstone (Cs) that occur in the right abutment as intercalated lobes of few meters thick (Bh_R02). They appear as brown, lithified, fine grained and moderately strong siltstone. Rock cores have generally a high RQD (mean 70%) and an estimated medium strong strength (25-50 MPa) (ISRM, 1978, [8]). In the left abutment (Bh_L02) loose clayey sand level about 20 meters thick was drilled just below 29 m of colluvium approximately between elevation 668 and 648 m a.s.l..

The conglomerates outcrop in the right abutment from about el. 610 up to approximately 665 m a.s.l. along the incisions created by the creeks. Stratigraphically the deposit overlies the A2/A1 formations and is capped by the Bc formation.

As far as the left abutment is concerned, no conglomerate outcrops were observed during the geological survey. Some isolated pebble elements, that attest the occurrence of the conglomerates formation, were found only in a narrow area at 610 m a.s.l.. According to the structural setting, the conglomerate formation is expected to be found underlying the Andesite/Autobreccia unit A2/A1. The borehole L02 has shown the presence of about 20 meters of clayey sand between el. 668-648 m a.s.l. beneath the colluvium. This level shows sedimentary structures and could belong to a distal part of a fan system or to an alluvial plain. At present the ongoing drilling of the borehole L04, located in the left plateau, encountered the brecciated basalt concerning to the A1 formation without interbedded conglomerate formation below the columnar basalt (Bc). This evidence suggests a wedge geometry for the C formation also in the left abutment.

In mountainous areas the streams usually download debris at the mouth of the valleys forming fans. The grain size normally decreases starting from the proximal areas located at the outlet of the valley toward the distal part (Fig 3.6). The conglomerate formation in sedimentary environment is fluvial and likely related to alluvial fans.

Figure 3.8. The spatial coarse conglomerate and a sandy pebble lobe

Figure 3.7. Conglomerate cores

(A2) – Andesite Formation

This formation is formed by aphanitic olive gray fine-grained basalt. It is emplaced as swarms of

dykes intruded into the A1 Formation (Hypabyssal intrusions). The dykes have the following characteristics:

- their medium thickness is approximately 2.5 m and ranges between 1 and 10 meters;
- they form sheet-like bodies inclined 25° ENE;
- on the riverbed they extensively outcrop on both the banks;
- along the hillsides they outcrop sporadically because of the debris cover;
- their presence is encountered also in the cores of the drilled boreholes;
- they are controlled by regional stress field associated with Main Ethiopian Rift tectonic evolution; to date it seems that no dykes are intruded in the Conglomerate Formation.

The rock matrix is not altered by the interaction with a major hot fluid. Hand specimens show no visible open/sealed cracks, veins neither cavities. Ground-mass is made up of fine-grained crystals of plagioclase, pyroxene and Fe-oxides. Very thin secondary and late calcite veins are present. Rock cores have generally high RQD >80% and an estimated strength (ISRM, 1978) ranging from strong to very strong (50-150 MPa).

(A1) – Andesite Autobreccia Formation

abundant pores and cavities formed during the lava emplacement that can be filled by calcite albite and subordinate zeolites. The intensity of the interaction process between the magma body and/or magmatic heat and the external water supply has been variable. when the fluid-rock interaction is heavy and led to a brecciation of rock mass as consequence of the available water explosive

transition phase.

When the fluid-rock interaction level is lower, the brecciation did not occur but the interaction produced pores and cavities in the rock filled mainly by calcite up to 40% of the rock volume.

Rock cores generally have a high RQD (mean 80%) and an estimated strength (ISRM, 1978) ranging from strong to weak (5-100 MPa) according to the grade of the alteration.

Dykes, that outcrop as a swarm of tabular sub-vertical bodies NW-SE oriented (orthogonal respect the river) and has a very low occurrence. They are basaltic bodies <1 up to 3 meters thick crosscutting both the A1 and A2 Units. The dykes emplaced along tardive tectonic alignments.

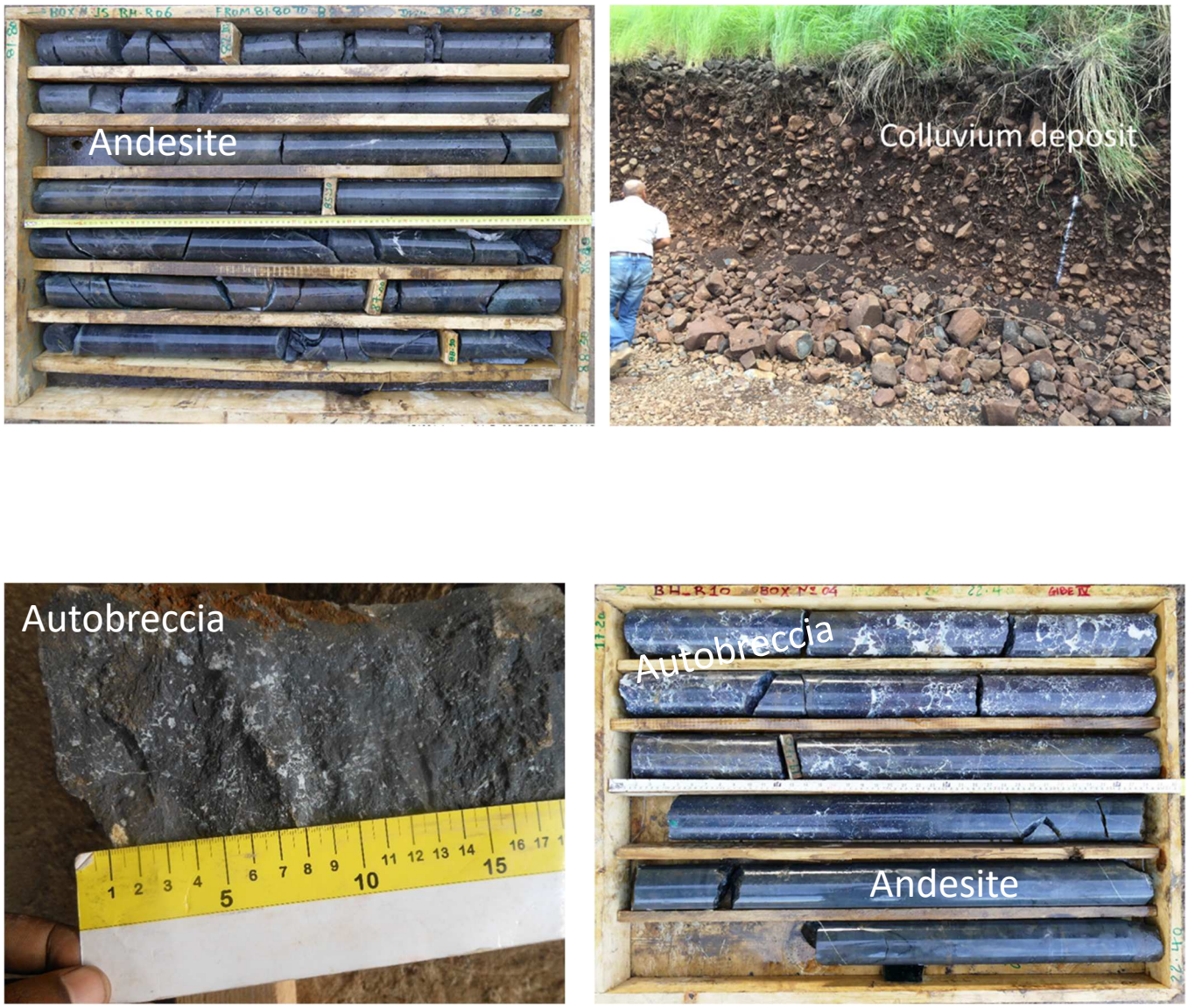

Figure 3.9. the geological units in the area

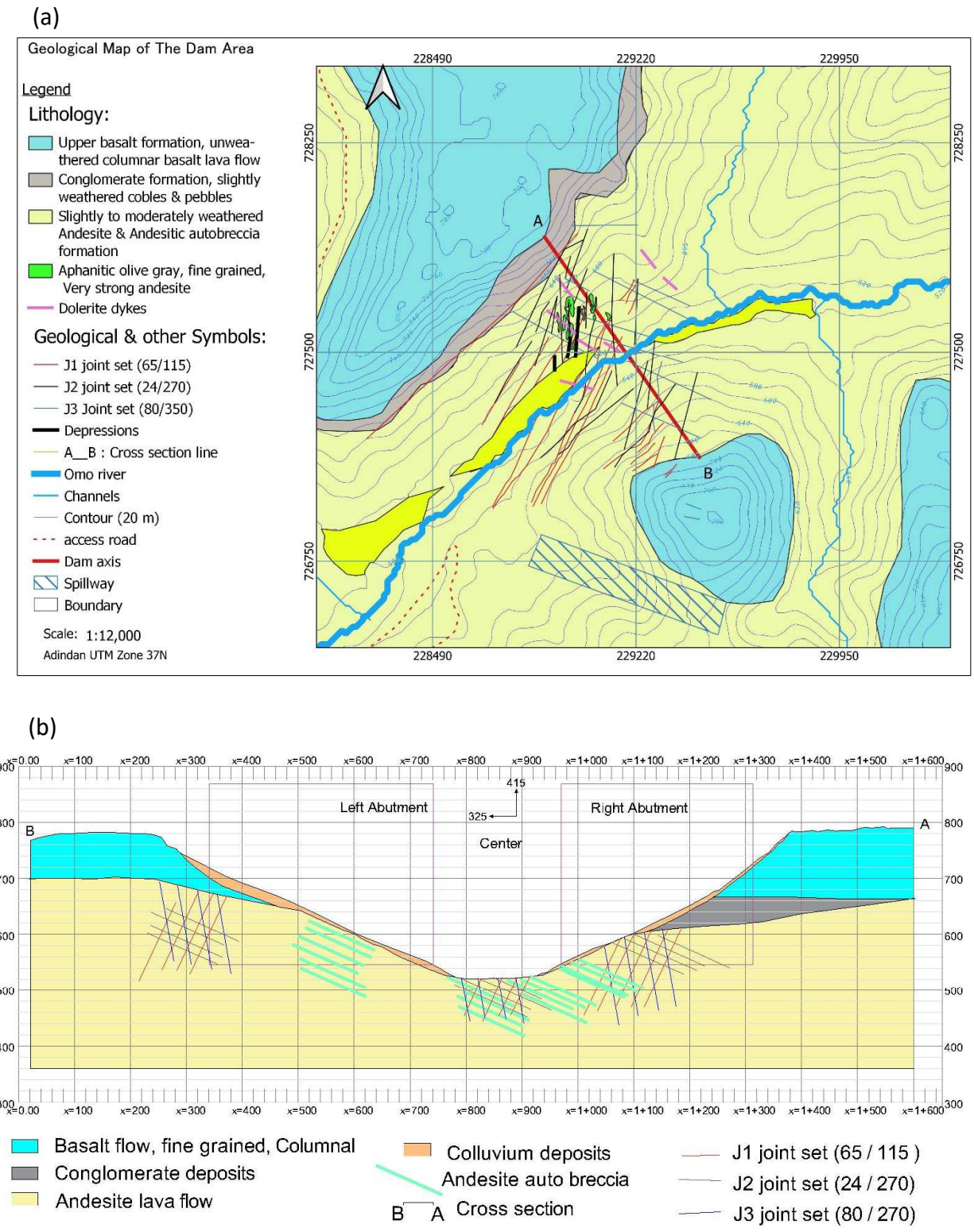

Figure 3.10. Geological map of the study area (a), and vertical cross section of the dam site (not scaled) (b) (modified from Koysha hydroelectric project, investigation report, 2016)

3.6.2. Geostructural Survey of the dam area

Three major discontinuity sets have been identified and defined according to the results of the geostructural surveys performed on surface. These joint sets are affecting the dam foundation. The following table summarizes the joint properties. Figure 15 illustrates the major joint sets block setups.

Table 3-5. Summary the major joint sets properties

	J1	**J2**	**J3**
Dip	65°	25°	79°
Dip Direction	115°	275°	350°
Persistent (m)	3 – 10	>20	1 - 3
Aperture (mm)	0.1 - 400		
Filling	Cemented	Clay matrix + weathered materials	Cemented
Roughness	Rough to Smooth		
Shape	Planar	Undulating	
Spacing (mm)	60 - 200	200 - 600	60 - 200

The J1 set orientation is related to the main faults of the Main Ethiopian Rift. The dipping 24/290 of the J2 set is consistent with the reported tilting direction (Davidson A. 1983).

CHAPTER 4: MATERIALS AND METHODS

4.1. INTRODUCTION

This chapter concerned with the general procedure and methodology followed during desk work, model generations and analysis. As it has been discussed so far, Koysha dam is designed to be placed on heterogeneous foundation of jointed rock mass. The natural in-situ conditions of the rock foundation structures need the right representation in numerical modeling. Now days, Discrete Element Methods, in particular, have proved a suitable tool to assess failure mechanisms in jointed rock (Lemos, 2021), if it is implemented properly with good understanding of numerical

assumptions in complex computer code and boundary conditions which may include discontinuities (distinct boundary interactions between blocks), stress boundary, applied force (load) boundary. Therefore, for the research purpose, one of the discrete element methods (DEM), which is 3DEC has been adopted.

The numerical modeling approach known as the distinct element method (DEM) is the basis for the numerical formulation. It allows the modeling of in-situ discontinuity conditions, zoning of the geological units, significant movements and deformations, and automatic investigation of blocky and jointed rock structures.

The essential issues involved in the utilization of discrete element modelling on stability analysis of jointed rock foundation of Koysha hydropower RCC gravity dam are the model generation, the representation of discontinuities, simulations of various loads which may include static, and hydrostatic loads analysis.

4.1. RESEARCH METHOD

This section concerned with the general procedures and methodology followed during desk work, detailed field survey, laboratory test, data processing and analysis to achieve the general and specific objective of the study.

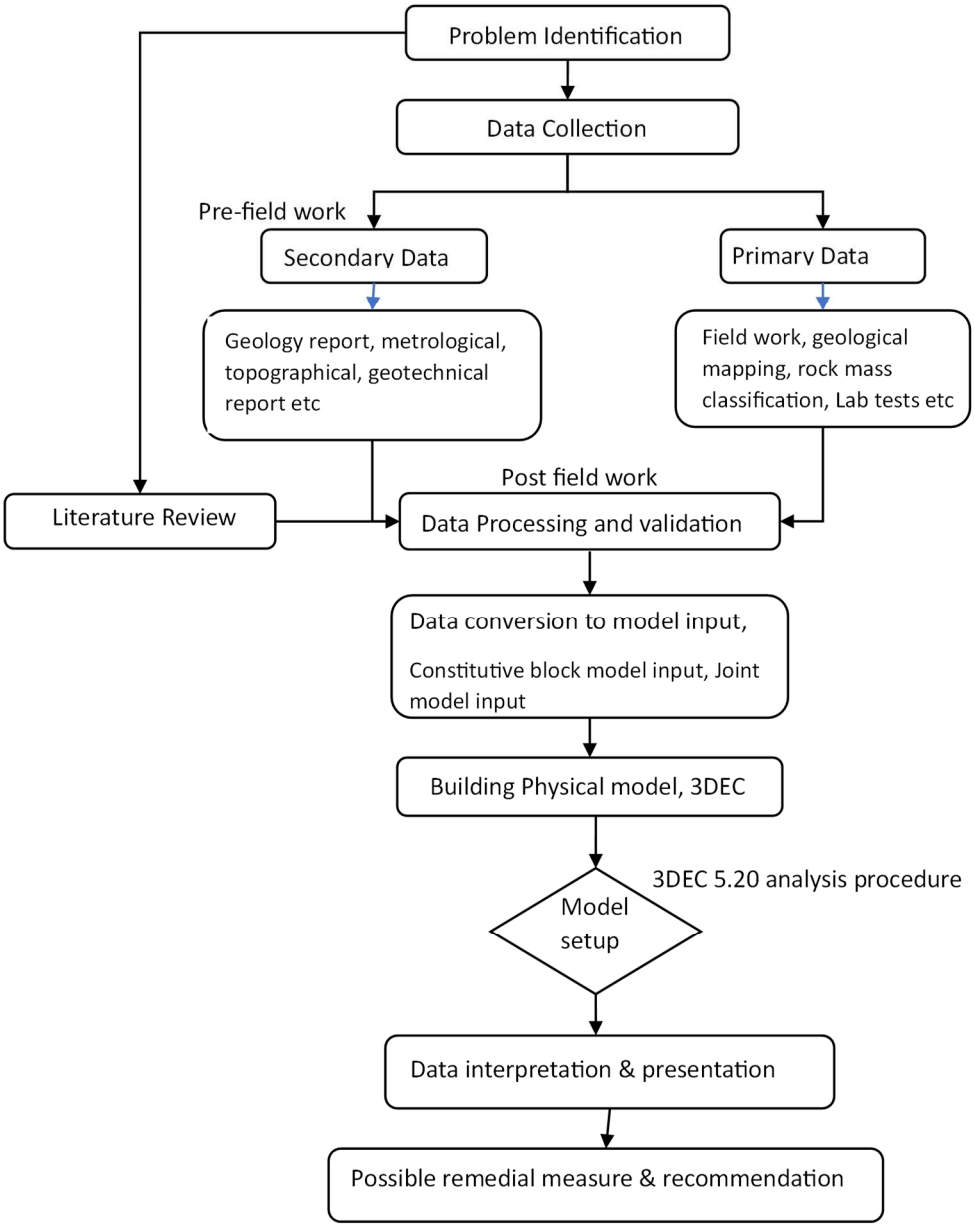

Figure 4.1. Detail method flow chart of the research

After conversion of the data to model input, building of the 3DEC model took place and then the analysis was carried out according to the procedure formulated by Itasca. The general solution procedure for an explicit static analysis with 3DEC is illustrated in Figure 4.2. This procedure is suggested by the Itasca Consulting Group Inc. (Itasca, 2016), is convenient since it represents the sequence of processes that occurs in the physical environment.

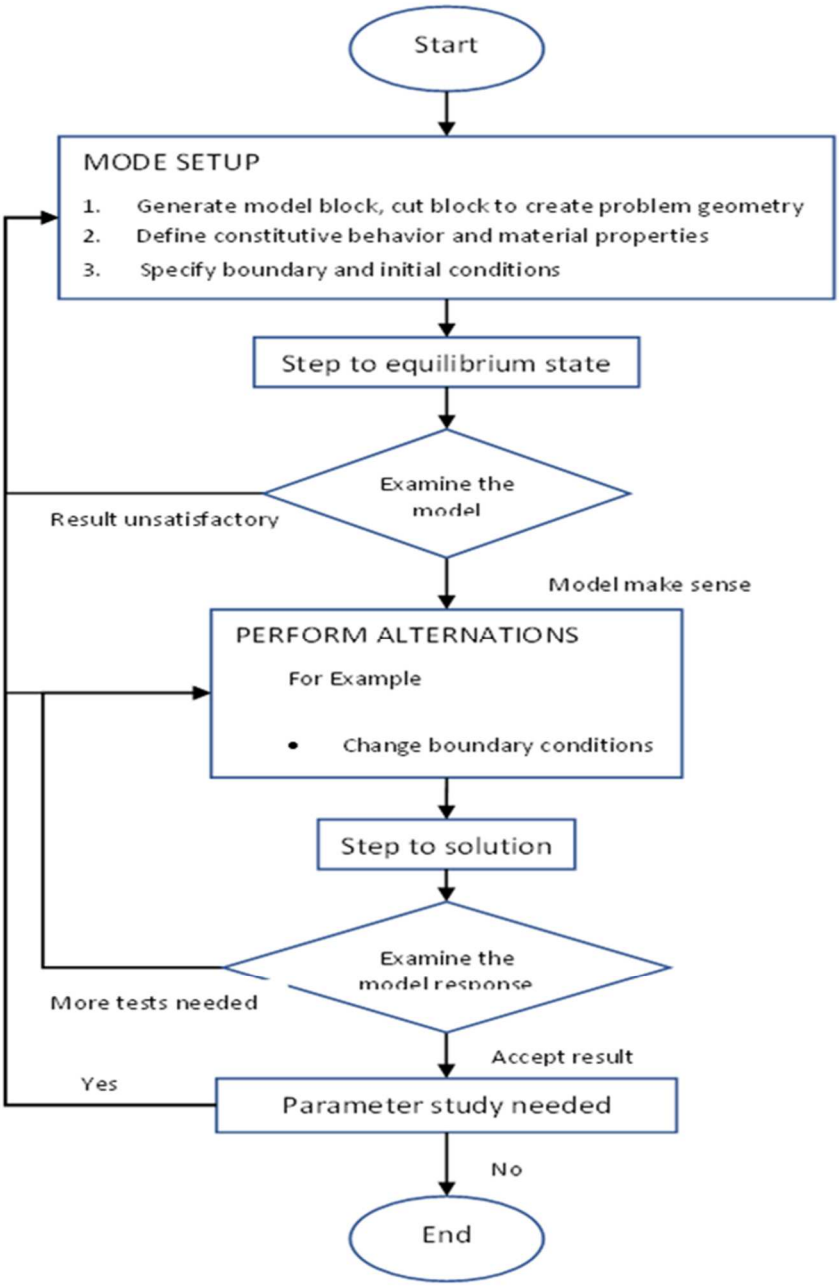

Figure 4.2. General solution procedure for static analysis (Modified from Itasca 2016)

4.2. DATA COLLECTION

Before conducting of any research, it is imperative to make a tough search for the data therefore, required data were collected from Head office of Ethiopian Electric Power (EEP) and from the

project site offices. Since the project was commenced six years before, and still undergoing and in progress, the relevant data will be obtained dominantly by secondary data collection method. The secondary data will include the deign documents, technical specification, investigation reports, laboratory test reports, section drawings, regional geological map from geological survey, geological data from site offices including boreholes and engineering geological mappings, metrological weather data, and so on. The primary data will be obtained by measuring at in situ.

4.2.1. Secondary Data

Searching for potential sources of articles, books, journals, proceedings, scholars, any relevant publishers, records, published and unpublished materials related with the research. Article review on the subject matter is one of the primary jobs in order to build conceptual framework, to design and modify the methodology and instruments effectively. Secondary data have been collected for the pre-field works from Addis Ababa offices and site project office. These data include,

- Relevant information has been collected from various sectors, this information may include
  - Regional geological and hydrogeological maps of the study area from geological survey of Ethiopia and Ethiopian Mapping Agency.
- General information of the project may include most important features of the dam and location from Ethiopian Electric Power, Addis Ababa project office, these included,
  - Dam cross section profile,
  - Required Information for Modeling like geological information, geometrical and propriety of the dam foundation.
  - Metrological weather data of the study area. This information has been presented so far in chapter 3.4.
- Relevant secondary data has been collected from site project offices, such as the employer representative (Stantec consulting), the contractor (webuild group S.p.A.) and the designer (studio petrangeli S.p.A.). The secondary data will include:
  - Geometrical profile of the dam and the dam foundation which are important for modelling,
  - Geological data, including lithological and geo-structural mapping, reports of dam foundation mapping and abutments mappings (described and presented in chapter 3.6),
  - Laboratory tests reports for the intact rock specimens and joint and infilling properties, these reports include strength data, unit weight, cohesion, internal friction angle, core

logging of the lithological units,

- Stability analysis design report,
- As built drawings,
- Construction materials investigation reports,
- Basic investigation report of geology and hydrogeology,
- Method statements and specification documents,

Intact Rock Data:

During investigation and construction period detailed geotechnical and laboratory works has been carried out. As it is mentioned so far, the project area is covered with three geological / lithological units, such as basalt, conglomerate and andesite/autobrecia. Physical and deformational properties of these rock have been examined. The bulk and shear modulus are determined based on empirical formula adopted from (Barton, 1972). Some of secondary reports which are relevant for this study are described here after. Uniaxial compressive and bulk density test reports of core samples no. 184 representing different depths from various boreholes located at different parts of the foundation has been analyzed and summarized in the table 4-3. below. These core samples are assumed to represent the lithological units in the right and left abutment as well as the central part. 48% of the core samples are to represent the andesite unit, 36% representing the autobreccia and the remaining 16% are represents the basalt unit. It is difficult to treat the andesite and the autobrecia separately as their mode of appearance is mixed and from the same lava flow. The geotechnical laboratory report shows that the weighted average density of the andesite/autobreccia, conglomerate and basalt are 2690 kg/m^3, 2437 kg/m^3 and 2912 kg/m^3 respectively. The young's modulus and poisson's ratio of the intact rock specimens are taken from laboratory test results (secondary data). The average density of the RCC dam from actual report is taken as 2563 kg/m^3. The bulk modulus and shear modulus of the intact rock can be calculated using the following empirical formula:

$$K = \frac{E}{3(1-2\upsilon)} \qquad \textit{Equation 4.1}$$

$$G = \frac{E}{2(1+\upsilon)} \qquad \textit{Equation 4.2}$$

Where K is bulk modulus, G is shear modulus and υ is poisson' ratio

Table 4-1 Material properties of the intact rocks (geological units)

Parameters	Basalt	Conglomerate	Andesite/Autobreccia
Bulk density (kg/m^3)	2912	2437	2690
Uniaxial Comp. strength, MPa	139	9.8	76.7
Cohesion (kPa), C	0.59	0	0.5
Friction angle	55.25	23.95	51
Young's modulus, E (Gpa)	57.5	5.3	37.7
Poisson's ratio, υ	0.24	0.17	0.18
Bulk modulus, K	36.9	2.7	15.4
Shear modulus, G	23.2	2.3	12.3

The bearing capacity of the intact rock is strong enough to carry safely the total load exerted on it by self-weight of the dam and the reservoir pressure. The presence of discontinuities reduces the physical and mechanical properties of the foundation. The discontinuities and thick infills exist in the rock mass will result in shear failure and the shear failure intern will result in bearing capacity failure. The mechanical properties in the rock mass may govern the mode of failure of bearing capacity.

Geostructural Data:

The bottom valley foundation of the dam was about 300 meter wide. The dam was seated on the andesite rock mass unit with complex geological structures. From the information of the rock foundation collected, two regions are selected to the study. The first one is weak zone highly jointed, fractured, infills with thick compressible soft clayey materials and weathered rock fragments, situated on the andesite unit on the right abutment of the dam. This zone is dominantly affected by the J2 joint set (25/275) and infill with alternating maximum thickness of 400mm. The second region of interest is highly jointed zone at the central foundation where the foundation is subjected to maximum pressure at probable maximum operating flood level (according to the basic design data).

A simple geological mapping has been modified and prepared at selected region from the general geological mapping report to observe the geostructural data, to cross check the intact rock properties of the core from boreholes and to represent in the numerical modeling, Figure 4.5). A

total 241 joints are collected from the two interest regions and out of which 135 are filtered and found to be categorized into 3 joint sets using stereograph projection (Rocscience Dips 7.0) (Figure 4.4). All of the three joint sets are highly persistent and locally infilled with materials. The joint set J1 is sub vertical and orthogonal to the river flow direction, the second joint J2 is sub horizontal nearly parallel to the river and the last joint J3 is nearly vertical. The orientations of the joint sets are presented in the table 4.3 below.

Table 4-2. Orientation of the joint sets in the studied regions

Joint sets	dip	dd	Number of joints		
			Region 1	Region 2	Total
J1	65	115	18	19	37
J2	25	275	22	16	38
J3	79	350	18	42	60
Total			58	77	135

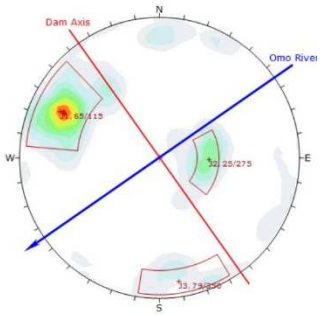

Figure 4.3. Stereographic projection of the joints

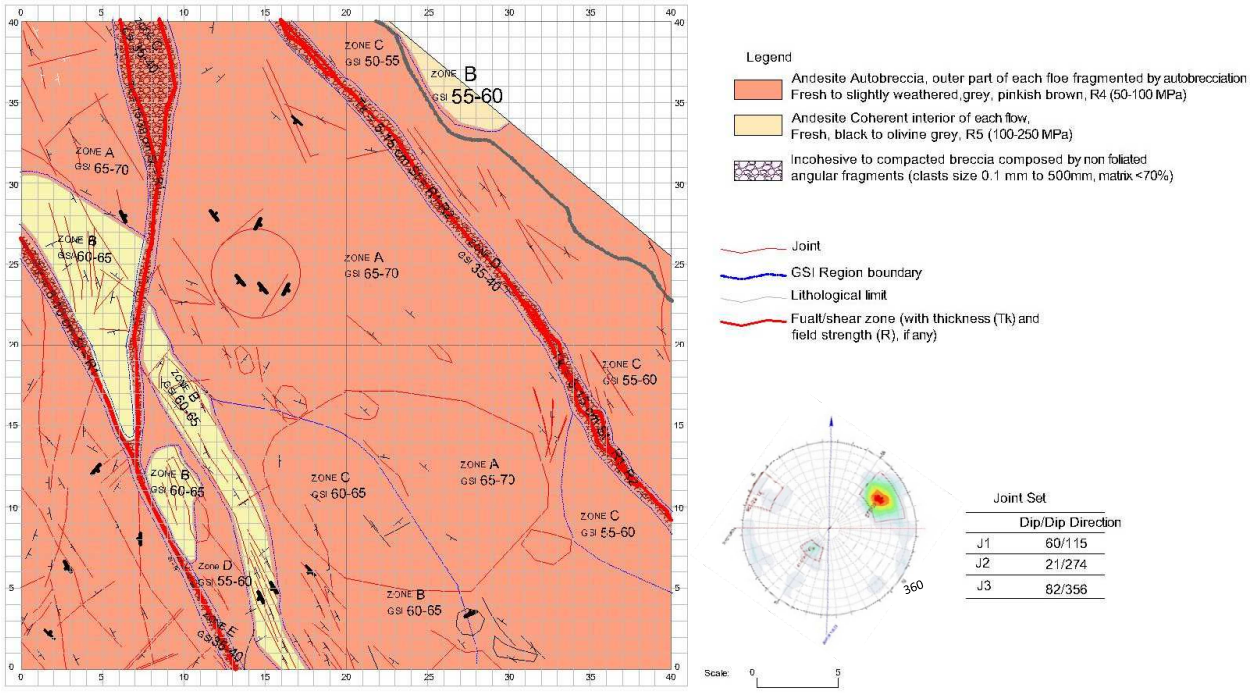

Figure 4.4 Simple mapping of region 1 in the central foundation (4 grids, each 20 x 20 meter gridding) (modified from general geological foundation mapping report, 2017, for modeling purpose)

Mapping of the interest region 2 on the right abutment has been modified and prepared in order to survey the joint sets as shown in the figure 4.6. below.

After relevant information about the intact rock has been obtained and a part of the foundation has been classified from the mapping of the region of interest, the material properties of the rock mass can be defined using the Roclab software, which is presented in Table 4.4. below.

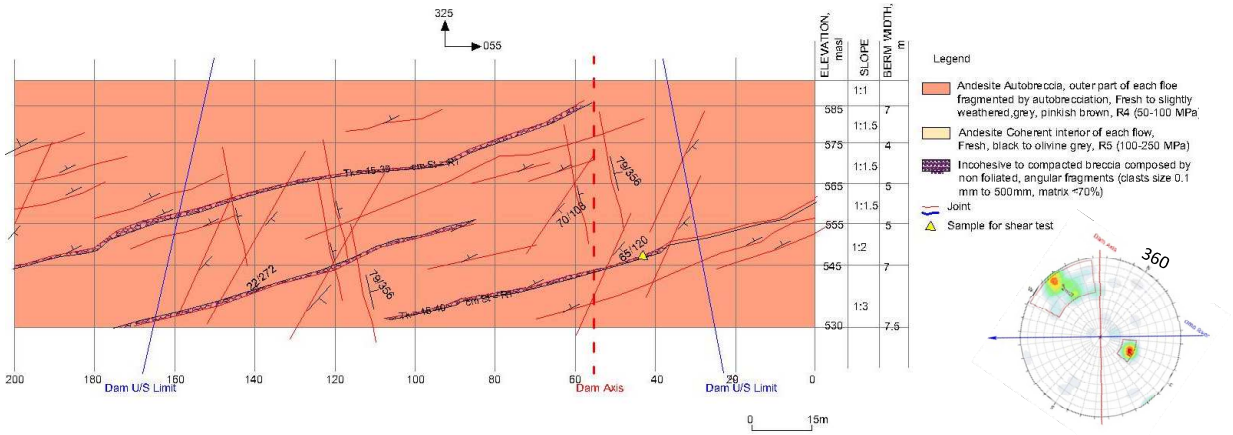

Figure 4.5. Simple mapping of interest region 2 on the right abutment slope, (modified from J2 joint investigation report 2016)

Table 4-3. Material properties of the rock mass

Lithology	Intact Rock			Rock Mass										
	m_i	UCS, Mpa	E_i, GPa	GSI	D	E_{rm}, Gpa	m_b	s	a	σ_{cm}, Mpa	σ_t, Mpa	σ_c, Mpa	Cohsn, C	fricn, φ
Autobreccia	20	50.4	19.9	50	0.6	5.0	1.56	0.001	0.506	8.28	0.03	1.50	2.4	30
Andesite	25	102.9	55.5	60	0.6	12.4	3.25	0.004	0.503	24.91	0.12	6.30	6.3	36
Andesite/Autobreccia (wted aver.)	22	76.65	37.7	55	0.6	8.2	2.22	0.002	0.504	15.17	0.07	3.28	4.1	33

The following figures 4.7. illustrates Hoek-Brown criterion in the Mohr plane, together with Mohr Coulomb criterion in Roclab software.

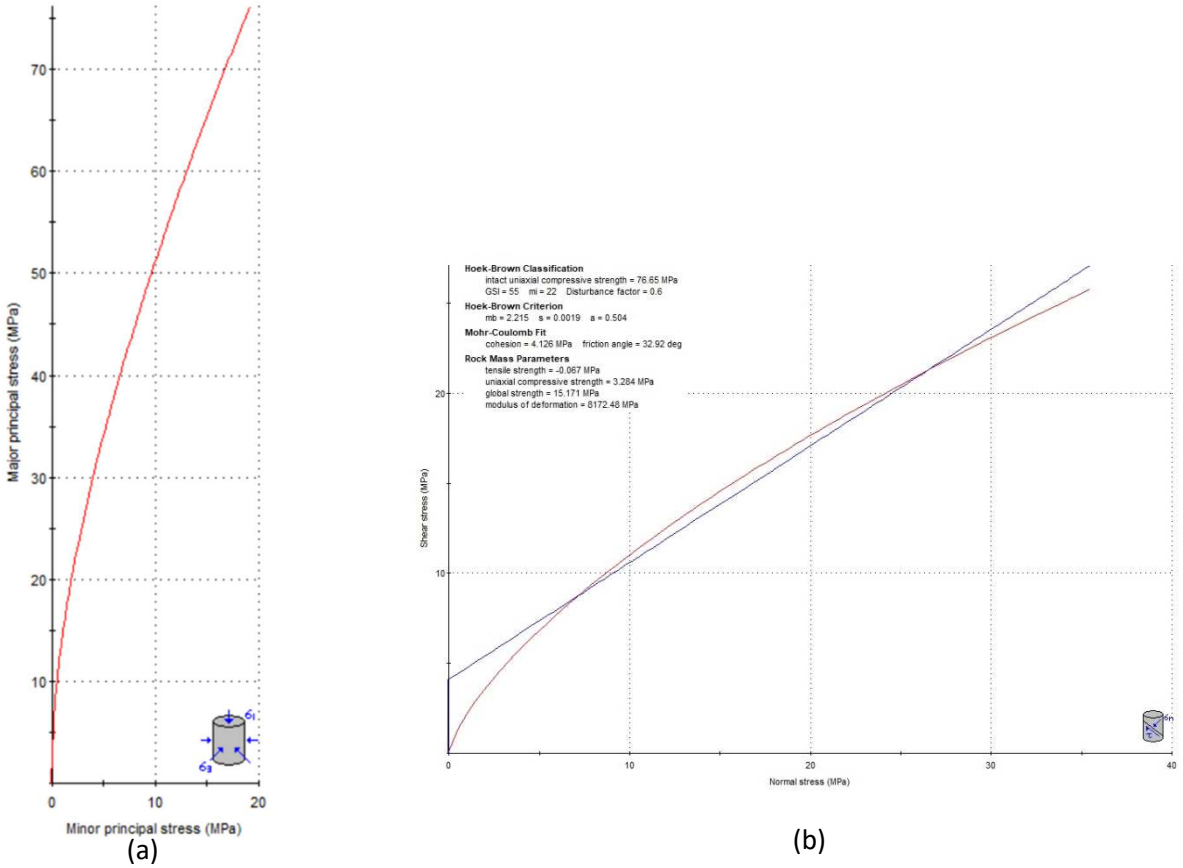

Figure 4.6. Hoek Brown Criteria for the Andesite/breccia (a) principal stresses, (b) Hoek brown criteria in Mohr Coulomb plane

J2 joint Infilling Material data:

Infilling samples were collected (with minimum disturbance) from the abutment slope of region 2 which represented the joint infillings of joint set J2. The samples were collected using 150 mm diameter steel cylinder with sharpened cutting tip with coupled plastic PVC cylinder inside and to evaluate infilling shear strength. sampling methodology has been carried out only where the thickness and stiffness of the infilling were such as to allow the hammering of the steel pipe into the joint. Therefore, these tests may be considered representative of the lower boundary of the infilling shear strength. Number 6 direct shear tests under drained conditions have been carried out in external laboratory according to ASTM-D3080. The average friction angle and cohesion are reported as 27° and 16 kPa respectively.

Additionally, repeated various laboratory tests have been carried out on additional infilling samples in order to identify and characterize the physical properties, these tests are including bulk density, moisture content, grading and Atterberg limit. The main observations from the lab test are summarized hereafter:

- The average bulk density and moisture content of the J2 joint infillings are 18 kN/m3 and 19% respectively.
- Infilling is mainly constituted of highly to moderately weathered autobreccia (weathered rocky fragments in clayey matrix),
- From the grading test, the fine content (minus 75μm) ranges between 20 and 80 % and it is mainly constituted by CL / CH, and the coarse fraction (coarse sand / gravel ranges between 5 – 30 %.
- Upper layer of clay is observed in the upper portion of the infillings.

4.2.2. Primary Data

The primary data collection includes visiting, visual inspection, assessing the current condition of the project related with foundation, measuring and recording the current geological information, dam foundation monitoring instrumentations to cross check with the secondary data.

These data may include:

- Physical observation of current foundation condition,
- Taking measurements and records of current geology and geological structures of the foundation and abutments, the instruments for this purpose will be mobile GPS, clinometer compass, the geostructural data collection carried out from abutment which is above concreting of dam were reached. During geostructural data collection, attention was given to the three dominant joint sets. Since the purpose of collecting these data were to cross check the consistency of the secondary data, hence, it is found to be consistence.
- Core samples were prepared from nearby boreholes which are representing the two regions of the study (Figure 4.7). Three core samples were tested in site laboratory for each region of interest. The results of the uniaxial compressive strength tests and density of the six cores are presented in table 4-4 below. These test results were found to be consistent with the secondary data.

Table 4-4. Results of core samples

Region of intererest	BH ID	Depth (m)	Rock Description	Diameter (mm)	Height (mm)	Area (mmq)	Max. Load (kN)	UCS (MPa)	Spec. Gravity (kg/dmc)	Mode of Failure
Region 2	BHR_23	64.58 - 64.75	Andesite	63.5	127.0	3,167	312.1	98.5	2.91	
	BHR_23	66.30 - 66.50	Andesite	63.5	127.0	3,167	364.9	115.2	2.91	
	BHR_24	40.10 - 40.34	Autobreccia	85.0	170.0	5,675	353.2	62.2	2.62	
Region 1	BHR_13	77.36 - 77.50	Andesite	63.5	127.0	3,167	341.4	107.8	2.94	
	BHR_13	77.50 - 77.65	Andesite	63.5	126.0	3,167	329.7	104.1	2.96	
	BHR_13	19.35 - 20.21	Autobreccia	85.0	170.0	5,675	314.2	55.4	2.63	

Figure 4.7. Core samples laboratory tests, weighing tha core sample (left), UCS test of core sample (right)

– Taking pictures of the current conditions using digital camera.

4.3. MATERIALS MODELS

There are number of various rigid/deformable material models to represent rock discontinuities, joints, and faults in simulation and to execute detailed 3D rock discontinuum analysis in 3DEC. Some of the material models available are presented hereunder:

1. Null (EXCAVTE command): is assigned to represent material which is removed from the model,
2. Linear elastic model: is valid for homogeneous, isotropic, continuous materials which exhibit linear stress-strain behavior. Used to describe uni-axial, triaxial compression, and extension tests.
3. Elastic, anisotropic: is appropriate for elastic materials that exhibit a well-defined elastic anisotropy,
4. Mohr-Coulomb plasticity: utilized to define the strength of a rock mass using Mohr-Coulomb criteria and applied for materials that give when subjected to shear loading.
5. Bilinear strain-hardening/softening, ubiquitous joint, and

   Jointed rock model, uses the blocky approach, and represent rocks with discrete and planar structural features, including jointed rock mass. Fluid flow model which requires the rock mass to exhibit both mechanical and hydraulic non-linearities.

As discussed so far, the geology of the dam site is mainly composed of three lithological units that are the Andesite/autobreccia, Conglomerate and the columnar basalt flows. The bottom central foundation of the dam has an approximated dimensions of 299 x 160 meter and covered by the andesite /autobreccia lithological unit. The properties of the intact andesite rock and the presence of defined joint sets (J1, J2, J3) with unique properties particularly thick joint infills and random joints are combined together and represent as rock mass properties. Hence, in this paper the elastic, Mohr-Coulomb and Jointed rock model reasonably used to represent the rock mass properties. The geological mapping of the foundations has been carried out and classified using Geological Strength Index (GSI). The GSI values at the foundation show a wide range variation. In this paper, the average GSI value of the foundation assumed to be 50. The existence of discontinuities reduces the mechanical parameters of a rock mass and differs from the intact rock parameters (Brown 2008; Mostyn et al. 1997).

There are several methods to scale down the rock mass parameters. The empirical formula proposes by Hoek et al. (2002) and Hoek and Diederichs (2006) are utilized to estimate the equivalent continuum strength and deformability parameter values for the rock mass. The deformation modulus (E_{rm}) of the rock mass was determined by the following empirical equation:

$$Erm = Ei\left(0.02 + \frac{1-\frac{D}{2}}{1+e^{\frac{60+15D-GSI}{11}}}\right) \quad \textit{Equation 4.3}$$

Where E_i is the youg's modulus of the intact rock; D is a factor describing the disturbance degree of the rock mass subjected by blast damage and stress relaxation.

The equation to equivalent Mohr-Coulomb parameters, friction angle (ϕ) and cohesion C, are given by:

$$\emptyset = \sin^{-1}\left[\frac{6am_b(s+m_b\sigma_{3n})^{a-1}}{2(1+a)(2+a)+6am_b(s+m_b\sigma_{3n})^{a-1}}\right] \quad \textit{Equation 4.4}$$

$$c = \frac{\sigma_{ci}\left[(1+2a)s+(1-a)m_b\sigma_{3n}\right](s+m_b\sigma_{3n})^{a-1}}{(1+a)(1+2a)\sqrt{1+\left(6am_b(s+m_b\sigma_{3n})^{a-1}\right)/(1+a)(1+2a)}} \quad \textit{Equation 4.5}$$

Similarly, the rock mass constants m_b, s and a can be calculated the corresponding Hoek-Brown equation or using the software Roclab.

The material constant and physical and mechanical parameters to represent the rock mass in the numerical model presented in the tables below.

Table 4-5. Hoek Brown constant for the rock mass

Rock Mass	GSI	m_i	D	m_b	s	a	σ_{cm}, Mpa	σ_t, Mpa	σ_c, Mpa
Basalt	60	25	0.6	3.248	0.0039	0.503	33.65	-0.17	8.81
Conglomerate	35	21	0.7	0.59	0.0001	0.516	0.08	0.00	0.93
Andesite/ Autobreccia	50	22	0.6	1.716	0.001	0.506	2.29	-0.04	13.20

Table 4-6. Physical and mechanical values to represent the rock masses in the numerical model

Rock Mass	Density (kg/m^3)	E_{rm} (GPa)	Bulk modulus (GPa)	Shear modulus (GPa)	C (Kpa)	ϕ (deg)	σ_{cm}, Mpa	σ_t, Mpa	σ_c, Mpa
Basalt	2912	13.47	8.64	0.86	8.5	36.18	33.65	-0.17	8.81
Conglomerate	2437	0.24	0.12	0.01	0.16	30.09	0.08	0.00	0.93
Andesite/ Autobreccia	2690	4.74	2.50	0.25	3.8	30.777	2.29	-0.04	13.20

The mechanical characteristics of the discontinuities are described by the elastic-perfectly plastic (Coulomb slip model). Normal stiffness, shear stiffness, friction angle, cohesion, dilation angle, and tensile strength are necessary parameters for the Coulomb slip mode. The friction angle and cohesion of the infilling of J2 joint set are given to the joint property of J2 joint set since it may be governed by the infill material.

Joint sets / interface	Normal stiffness (Gpa/m)	Shear stiffness (Gpa/m)	Cohesion (Kpa)	Friction angle (ϕ)
J1	$1.04x10^9$	$1.04x10^8$	0	33
J2	$4.88x10^8$	$4.88x10^7$	16	27
J3	$1.04x10^9$	$1.04x10^8$	0	33
Basalt-conglomerate	$4x10^9$	$4x10^8$	0	24
Basalt-andesite	$1x10^{10}$	$1x10^9$	0.5	53
Andesite-conglomerate	$1x10^9$	$1x10^8$	0	24
Rock-concrete	$7.62x10^{10}$	$7.62x10^9$	$3x10^5$	50

The normal stiffness and shear stiffness of the discontinuities are calculated using the proposed formula (Barton 1972) shown below:

$$kn = \frac{EmEr}{s(Er-Em)} \qquad \textit{Equation 4.6}$$

Where: Em is rock mass Young's modulus, Er is intact rock Young;s modulus, kn is joint normal stiffness; and s is joint spacing.

$$ks = \frac{GmGr}{s(Gr-Gm)} \qquad \textit{Equation 4.7}$$

Where: Gm is rock mass shear modulus, Gr is intact rock mass modulus, and ks is joint shear stiffness.

If the joint has infill materials with known elastic properties, then the stifness can be calculated using the following formula:

$$Kn = E_0/h \qquad \text{Equation 4.8}$$

$$Ks = G_0/h \qquad \text{Equation 4.9}$$

Where: E_0 is Young's modulus of infill materials, G_0 is shear modulus of infill materials and h is thickness or aperture of the joint.

4.4. BOUNDARY CONDITIONS

Boundary conditions are critical for any numerical modeling exercise, including rock dam foundations in 3DEC. Specifying the boundary conditions determine the behavior and response of the material under different loading conditions and provide information on the interaction between the foundation and the surrounding soil and rock mass. There are two kinds of boundaries: natural and artificial. The physical thing being modeled (for instance the ground surface) has real limits. Artificial boundaries must be set up in order to confine the required number of items (such as the dam), even though they don't exist in nature. For the rock foundation some of the boundary conditions that need to be considered include the type of loading applied, the placement of the boundary elements, and the level of deformation or displacement allowed at the boundaries. Boundary and initial conditions must be applied until after all block cutting is complete and the mesh for deformable blocks is generated. Mechanical boundary conditions command is used to specify force, stress and velocity (displacement) boundary conditions. In comparison to stress boundary conditions, the application of displacement boundary conditions speeds up computation times and decreases the possibility of faulty Model bending (Andrew, 2020). In this study, displacement (velocity) and stress, two mixed-type boundary conditions, are utilized. A zero-velocity horizontal boundary was used at bottom depth of the model in order to prevents the model from moving due to gravity. A zero vertical velocity boundary also used at ends of the model in the x and y direction to fix the model from any movement.

4.5. MODELLING APPROACH AND BUILDING THE MODEL

In *3DEC,* model is usually created by cutting the original *3DEC* block into smaller blocks that

represent boundaries of physical features in the problem. Some of the commands to create blocks with different shapes includes the poly brick, tunnel, poly prism, poly cube and poly face. Poly prick and poly prism are used to create and represent the physical features of the ground geology and the geometry of the dam. Initially, the dam geometry and the ground geology and its surroundings are prepared in Autocad 2018 and converted to blocks by cutting poly brick and poly prism. The actual dam dimension assumed to be represented in the model by a height of 180-meter, base length 299 meter, and crest length of 1000 meter (figure 4.6). The dam consists of 50 vertical blocks with 20 meter length each, each block should stand safely by itself, so that the whole 50 blocks stands as a monolithic dam to create a reservoir with holding capacity of nine billion cubic meter (bcm) of water. Within the dam structural design, there are five temperature zonings with specified materials properties. In the model, the ground geology model size assumed large enough to withstand the effect of the boundary conditions (Shang, Y., 1999 & Sun, G. et al., 2018). The block size extends to the downstream direction by three times the height of the dam from the toe and three times the height of the dam in the direction of upstream from the heel. The bottom extension of the model extends by three times the dam height from the base of the dam. Eventually, the total ground geology block designed to be estimated by 1229m x 500m x400m size. The block is divided into two regions for discontinuum model and equivalent continuum model (Lemos, 2012). The discontinuum model is situated at the center of the model where the dam foundation is located with dimension of 1179m x 590m x 360m. the second region is the outer block which is assumed to be treated by equivalent continuum model.

In this paper, the blocks are created to be rigid and then converted to deformable blocks. The main difference between rigid and deformable blocks in the DEM is their ability to deform under an external force. Rigid blocks are non-deformable (Cundall et al., 1978), while deformable blocks can change their shape, size, or orientation due to the external forces applied to them (figure 4.7. b).

In 3DEC, there are five main materials models for deformable blocks built in. The behavior of the dam is represented applying an elastic model. Several properties are required for this model: density (d), bulk modulus (k), and shear modulus (G). The shear failure in the deformable blocks of the soil and rocks is represented by the Mohr Coulomb elastic entirely plastic model. Dry density (d), bulk modulus (k), shear modulus (G), friction angle ($\emptyset$), cohesion (c), dilation angle (ψ), and

tensile strength (t) are the parameters required to run this model. Any of these properties' default values are 0 in the event they are not assigned.

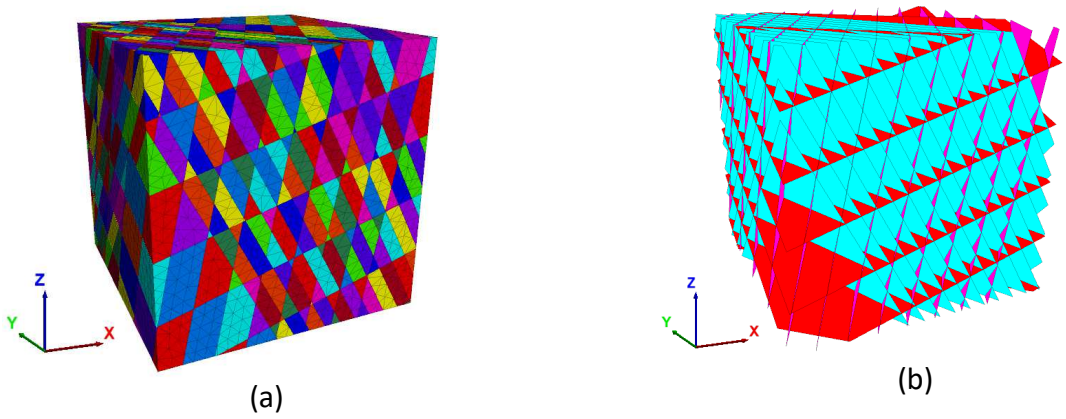

Figure 4.8. (a) Generation of Poly brick block (50m X 50m), the three joint sets, and deformable blocks (meshing) and (b) representation of the discontinuities constitute in the block model

The normal and shear interaction between blocks at their contact (sub-contact) sites is illustrated by the joint constitutive model. A normal and shear elastic stiffness component in addition to a limiting shear and tensile strength component have been included in the joint model. The Coulomb-slip model is the basic joint model. This model uses the assumption that the Mohr-Coulomb failure criterion governs the behavior of the discontinuity. The model can be used to simulate the behavior of rock masses under both low and high stress conditions and is appropriate for rocks with clearly defined shear strength parameters. The model mimics the joint weakening due to displacement caused by the loss of cohesive and tensile strength at the point of shear or tensile failure. There are two built-in models available to represent the material behavior of discontinuities:

1. Joint area contact — Coulomb slip (elastic-perfectly plastic)
2. continuously yielding.

The physical reaction of rock joints is intended to be represented by the joint constitutive models. The joint area contact model is intended for closely packed blocks with area contact. A contact plane between a bin or chute and the material it contains, a contact between two colliding objects, joints, faults, or bedding planes in geological medium are just a few examples of interfaces found in rock mass foundation in geotechnical engineering. The conventional Mohr-Coulomb joint area

contact model has been selected for this study. The model, which is based on elastic stiffness, frictional, cohesive, and tensile strength characteristics as well as dilation features typical to rock joints, provides a linear representation of joint stiffness and yield limit. The normal stiffness, shear stiffness, friction angle, cohesion, dilation angle, and tensile strength are the required parameters for the coulomb slip model. In the study area, J1, J2, and J3 are the three identified joint sets. These joint sets can be identified by the particular mean projected orientations, dips, and spacings that they exhibit. The joint set spacings are extended to 5 meters in order to simplify things and speed up computation.

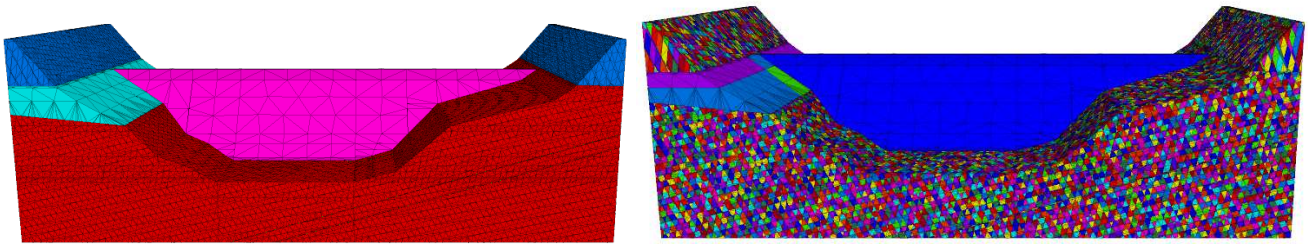

Figure 4.9. Model geometry, (a) rigid blocks, constitutive model of the geological lithologies (blue - basalt, green - conglomerate, red (lower part) - andesite), joints generation, (b) deformable blocks (meshing)

Figure 4.10. constitutive deformable blocks of the dam and section side view

There are several forces acting on a dam, including: the self - weight of the dam body, hydrostatic pressure force, generated by the weight and pressure of the water stored behind the dam, earth pressure force exerted on the dam by the surrounding earth and rock that the dam is built upon; wind force create pressure on the upstream face of the dam which can cause forces acting horizontally on it; dynamic seismic force; buoyancy force; ice force; silt pressure; temperature force and so on. For simplicity purpose only the self-weight and the hydrostatic forces are taken

into considerations (Figure 4.9). Water pressures along the discontinuity interfaces and rock concrete interface are critical in stability analysis however they are not considered in this study.

Self-load weight is represented by elastic model defining the density, bulk modulus, Poisson's ratio, cohesion, friction angle and shear and geometry of the dam materials such as the concrete in the numerical model. The hydrostatic forces acting on the dam can be calculated using the fluid pressure distribution along the vertical and horizontal direction at different levels of the dam. This can be determined by taking into account the fluid properties such as the water density and its distribution behind the dam, as well as the geometry of the submerged area.

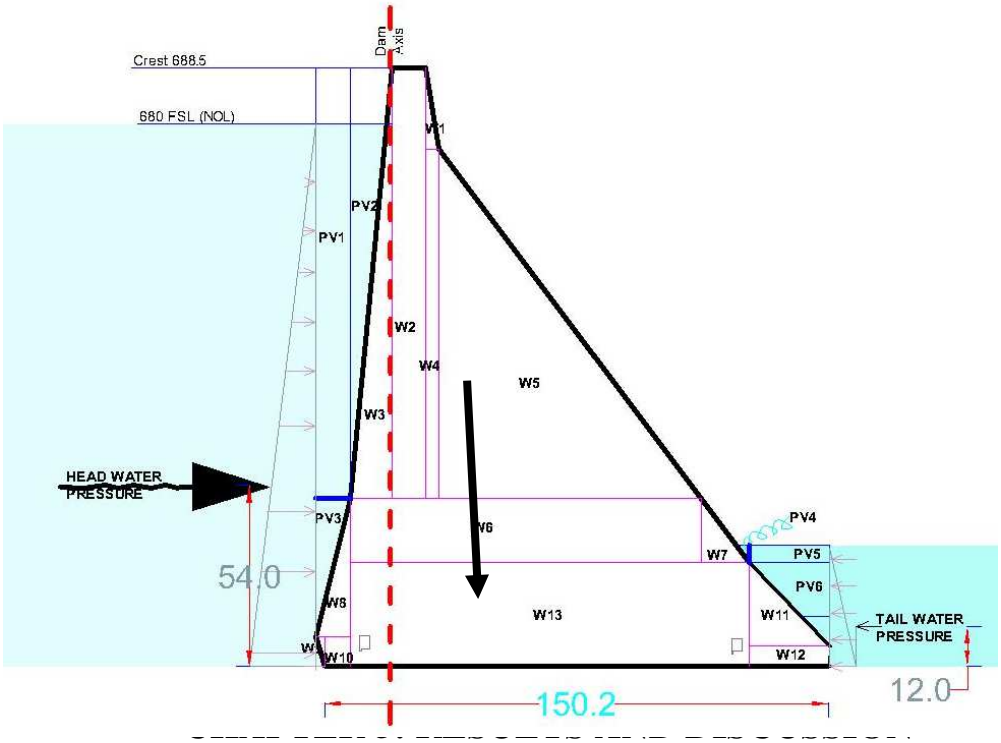

Figure 4.11. Vertical self-load and horizontal water pressure distributions at central section of the dam

The analysis started after constructing the finite element block of the dam and the foundation blocks. The generated rock block has been zoned to their lithological units to represent the actual geology based on the orientation (dip/dip direction) and elevation (figure 4.7. a. above). After the lithological unit, discontinuities are generated on the andesite unit. The polyhedron foundation blocks are changed to deformable blocks and followed by assigning the proper material and joint properties including the interfaces between the concrete and the foundation rocks. It has been found that difficult to run the analysis as a single holistic model due to its size and number of

discontinuities found. For example, to initiate a single first stage of the in-situ stress, it required more than 660 Hrs. Prolonged time to complete a single stage coupled with frequent interruption of power made it impossible. Hence, it is recommended to perform the analysis by trying multiple models at different rock foundation sections separately (Lemos, 2012).

The model has been prepared into two trial foundation zones that are the left abutment where the potential wedge and left reservoir rim where sliding plane are possible and the central foundation of the dam where maximum load is applied. When the analysis is performed for the left abutment and reservoir rim, the foundation of the left abutment where the dam load laid and the downstream stretch of the same abutment treated as discontinuum medium and all the discontinuities are initiated, joint properties are assigned and joint stresses are set. The remaining parts of the model has been treated as equivalent continuum. Likewise, in the latter case, running the model for the central part of the foundation, the central part of the foundation and the downstream stretches are treated as discontinuum medium and the remaining part of the foundation are treated as equivalent continuum.

The first stage of the analysis is assigning the in-situ stresses to initialize the valley stresses and defining the gravity. Unlike stresses of equally leveled rock mass or stresses at deep locations in underground mass, stresses at topographic places or valleys varies based on their density and depths. Figure 5.2 presents the stress differences that follows the contour of the topography. The stresses at the surfaces of the topography and valley are zero. The vertical stresses at the bottom corners of the figure are the maximum vertical stress that is as a result of the maximum abutment height and the overburden materials. the stress at the bottom of the abutments is about 8.5 MPa and at the bottom of the central valley is about 3.2 MPa. These results are consistent with theoretically calculated stresses using the depth of overburden material and density.

In this stage boundary conditions are applied and monitoring histories are assigned for the maximum unbalanced forces, followed by sequential loading of dam self-weight and reservoir hydrostatic pressure. In calculation of the self-weight, material density and gravity acceleration are the input for the self-weight. When loading of the dam real material property is assigned to the dam and interface contacts are assumed to be elastic. The third stage is loading of water on the upstream face of the dam and upstream walls of the abutments and the floor. The tail water pressure

in the downstream area and in the plunge pool area are not used for simplicity purpose. Assuming that the effectiveness of the curtain grouting and drainage systems, and to avid the complexity, uplift pressure is not applied in the analysis. In this stage fixing the base boundary for the fluid is important. The fourth stage is putting the joints to the real values. Each sequential loading took place after equilibrium reached. A loading change must cause unbalanced forces to develop in order to effect a change in model response. The plot of the loading stages and the unbalanced forces for the left abutment is presented in figure 5.1.

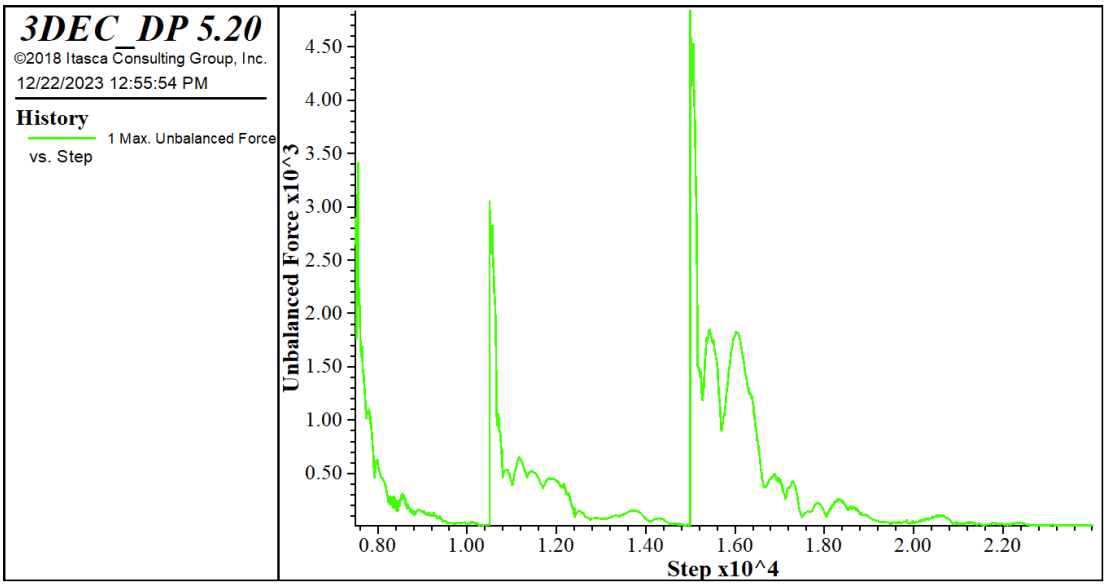

Figure 5.1. Analysis steps and the unbalanced forces for the left abutment trial model

The results of the analysis presented will consist of minor and major principal stresses, shear stresses and vertical and horizontal deformations. Here and under the negative sign of stress will be utilized to represent compression and positive represents tension. Negative sign will be utilized to represent compression and positive will represent extension for displacement.

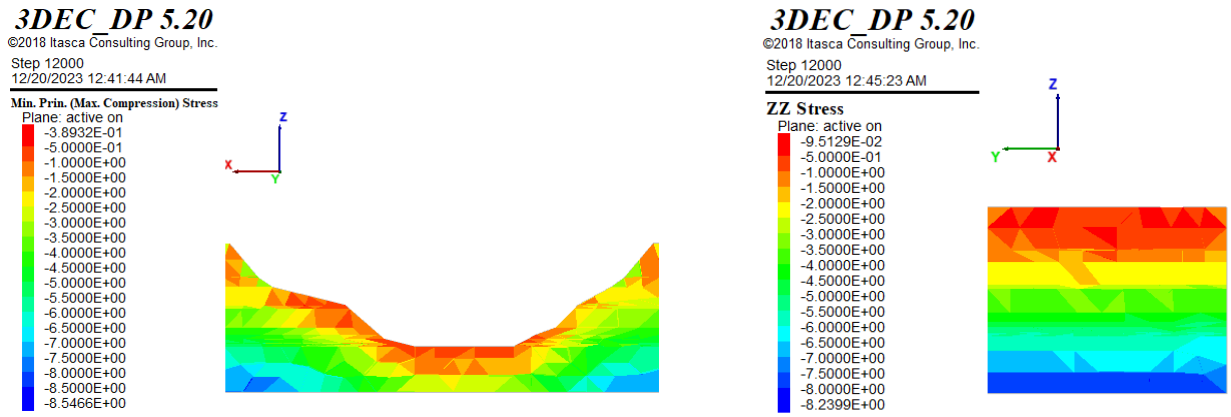

Figure 5.2. Topographic stresses after initialization of in-situ stress, xx cut plane & yy cut plane at max abutment height.

5.1. DISPLACEMENT

Displacement response of the model was recorded after the dam was placed on the foundation and after loading the reservoir water. In 3DEC 5.20, negative strain or displacement indicates compression and positive strain and displacement indicates extension. The displacement history recorded for the two region of interest that is the central foundation and the abutment slope. The Y-axis parallel to river flow, indicates the upstream direction, the X-axis represents the dam axis and indicates towards the left abutment direction and the Z-axis indicates the upward direction.

The Central Foundation

The first region of interest is the central foundation that is the first model trial. It is important to simulate the model at the central foundation of the dam since it is the place where maximum load experienced due to the dam self - weight and the reservoir pressure. As discussed, the reason so far, the region of interest is treated as discontinuum medium by applying the three joint sets and two of the infilled J2 joint with infilled material properties and representing them by corresponding joint models. The rest of the block model treated following equivalent discontinuum concept.

The second stage after the unbalanced force was reached in equilibrium was placing the dam body and recording the history of the model. The maximum resultant displacement of the model after placing the dam on the foundation was 36 cm of which the dominant displacement took place in the z-direction with maximum compressional displacement of 32 cm concentrated in the central foundation along the infilled J2 joint. The dam displacement occurred at the central crest with 1.2 cm and displacement vector indicated toward upstream direction.

The next stage was impounding the reservoir with water. The analysis carried out under two loading conditions, the middle level outlet (95 meters of water) and the normal operation water level (150 m water level) following the steps described so far for initiation of the in-situ stress and for dam self-weight.

Analysis Result of Central foundation at Middle level outlet (95 meter of water)

Middle level outlet serves as temporary discharge outlet during the first phase of impounding and for emergency outlet, situated below the minimum operating level. The maximum displacement during middle level outlet analysis was 67 cm in the foundation of the dam along the infilled J2 joint. Figure 5.4 (C) shows the dominant displacement that is the compressional z-displacement with max 62 cm. Figure 5.3. shows the displacement of the foundation at downstream area.

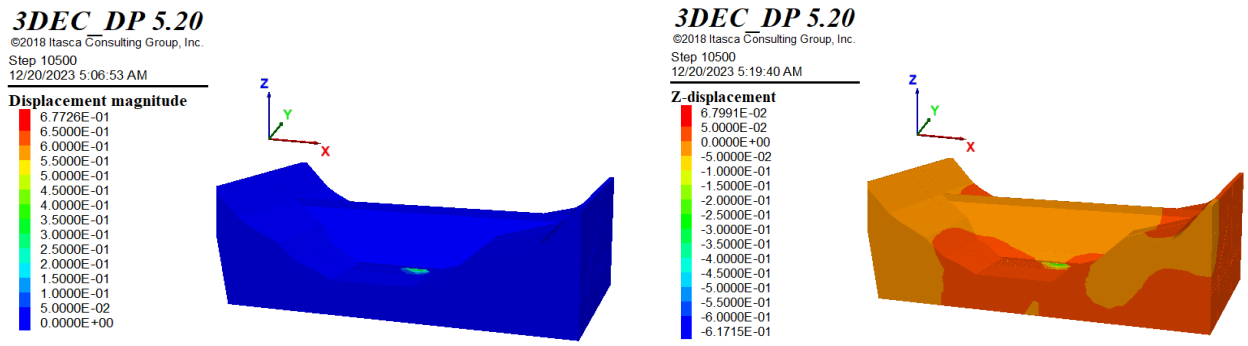

Figure 5.3. Displacement of foundation for middle level outlet, left: Resultant displacement magnitude, right: the dominant compressional z-displacement

Plane cut sections are prepared to see the displacement of the foundation in detail. The maximum displacement was located 19.5 meter from center toward left, 75 meters from the dam axis toward downstream and at a depth of 14 meter (Figure 5.4). The displacement has increasing pattern from upstream to downstream and from right to left within the extent of the joint. Generally, the displacement stretches from right upstream center towards left downstream following the pattern of the infill J2 joint.

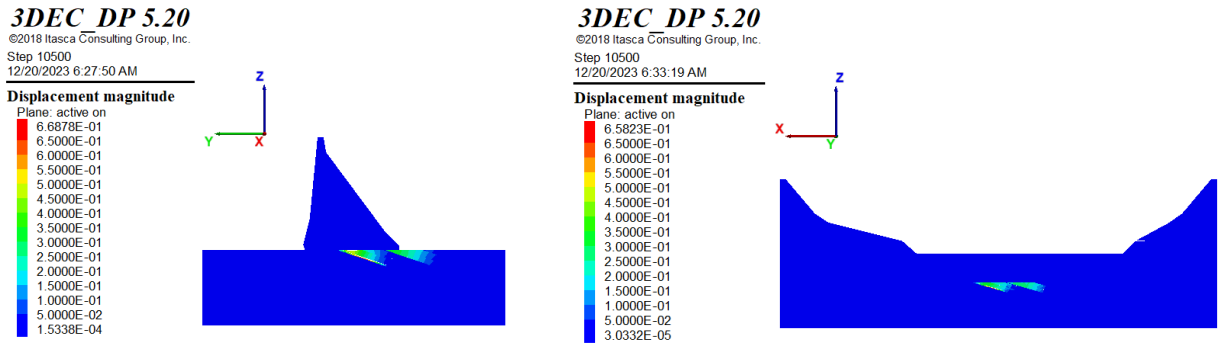

Figure 5.5. Displacement cut plane section at x=19.5, y=-75, z=-14, left: y-y section, right: x-x section

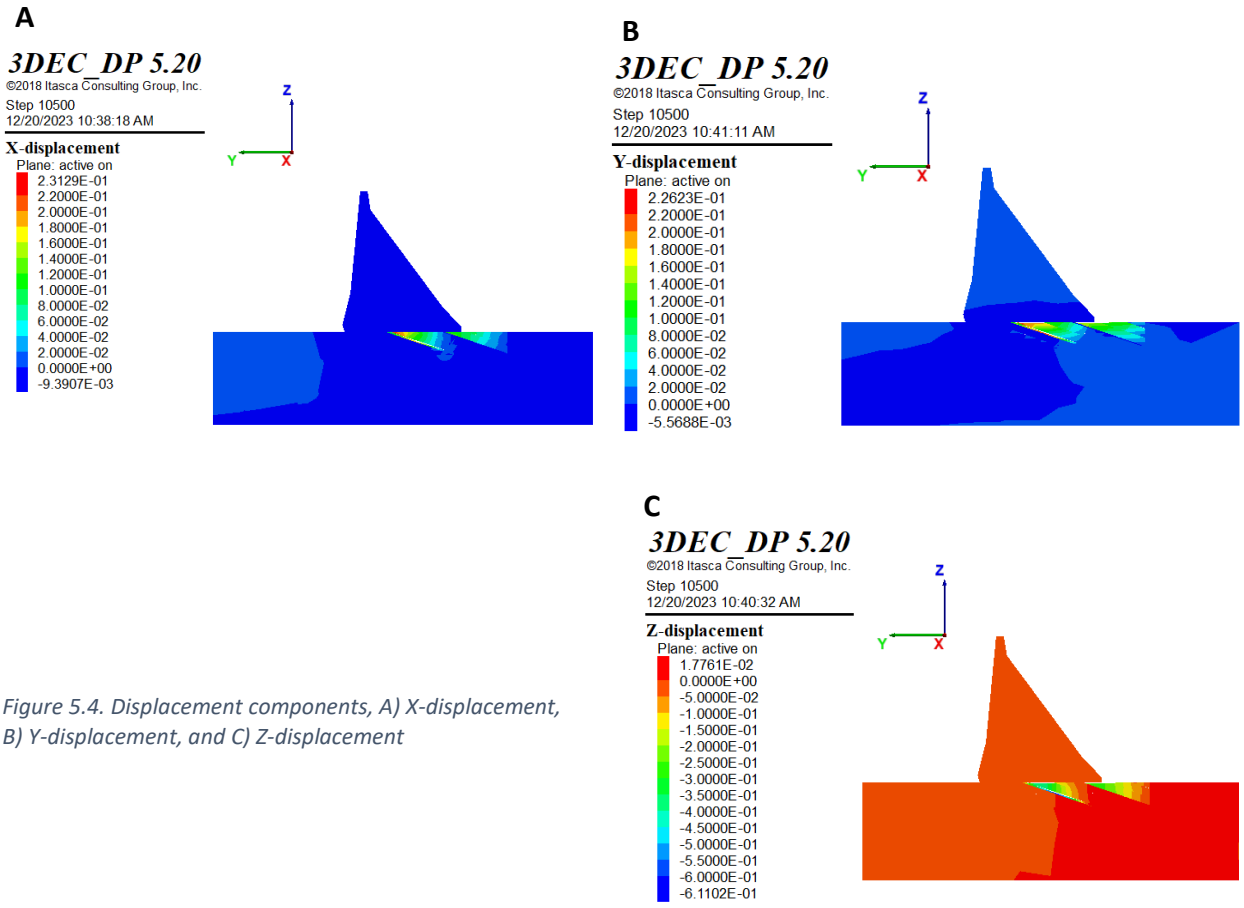

Figure 5.4. Displacement components, A) X-displacement, B) Y-displacement, and C) Z-displacement

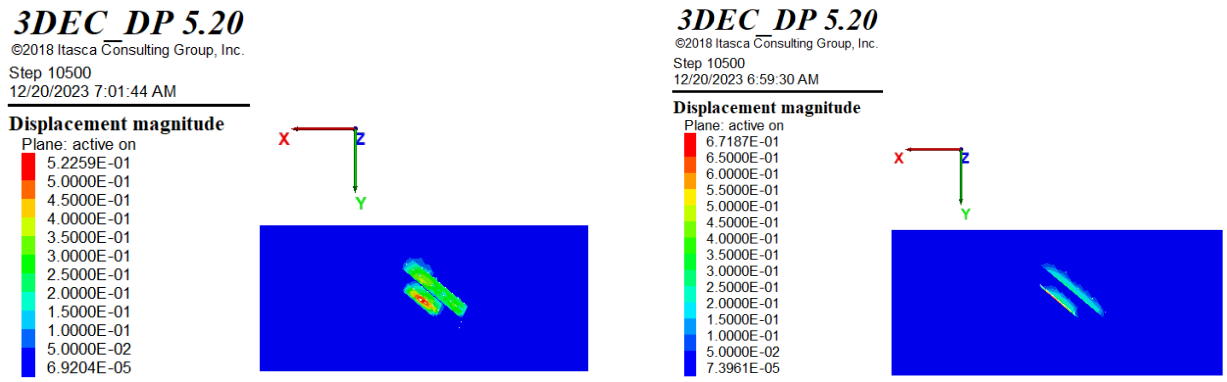

Figure 5.6. bird view plane cut section of foundation at depth of, left: 0.4 m and right: 14 m, displacement follows the joint pattern

Analysis Result of Central foundation Under Normal Operating Level

Analysis was carried out for the model under normal operating level. Figure 5.7. shows the general displacement of the foundation that occurred after full reservoir was loaded. As it is shown in the figure the maximum displacement recorded was 1.08 m. Figure 5.8. indicates the dominant displacement which is responsible for the resultant displacement was the Z-displacement with magnitude of compression 98 cm.

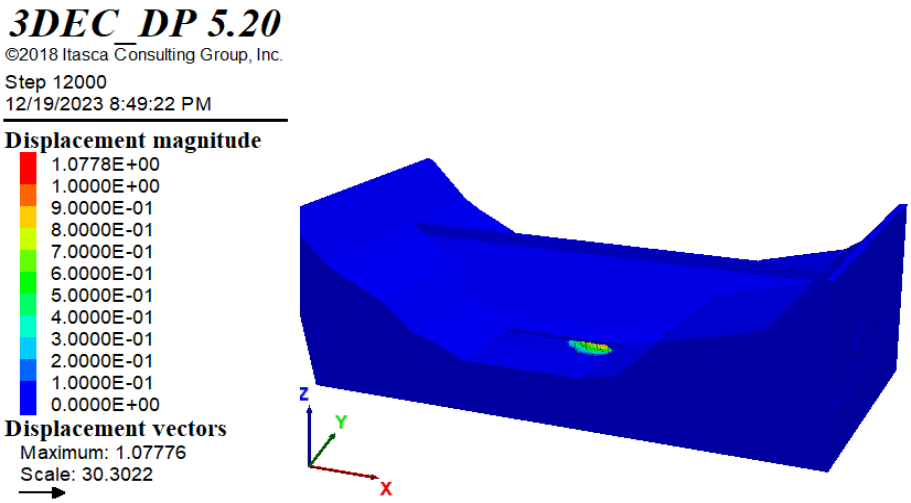

Figure 5.7. Displacement of the foundation

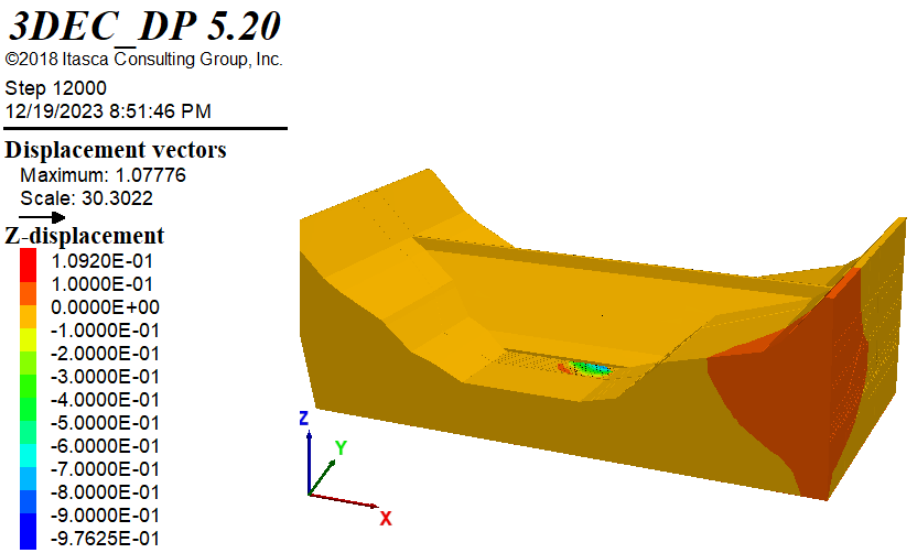

Figure 5.8. Z-displacement which is the dominant one

Plane cut section is prepared to observe the deformation of the foundation in detail. The maximum displacement occurred with an offset of 18 meter from the center towards the right, 26 meters from the axis of dam in downstream and at depth of 5 meter (x=-18, y=-26, z=-5). As shown in Figure 5.10., the magnitude is 1.1 meter with the Z-displacement dominancy.

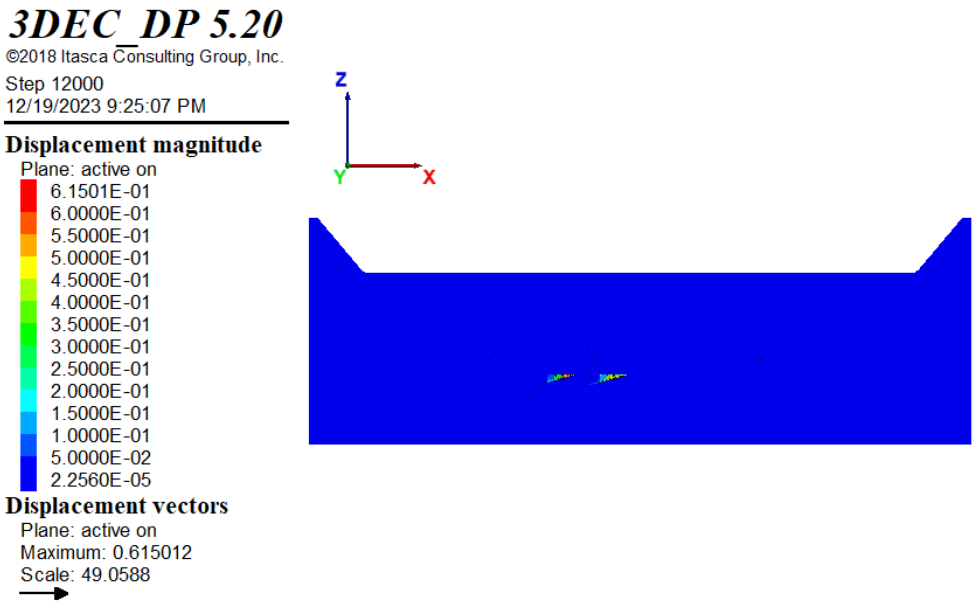

Figure 5.9. plane cut section along the dam axis (x=0, y=0 and z=0)

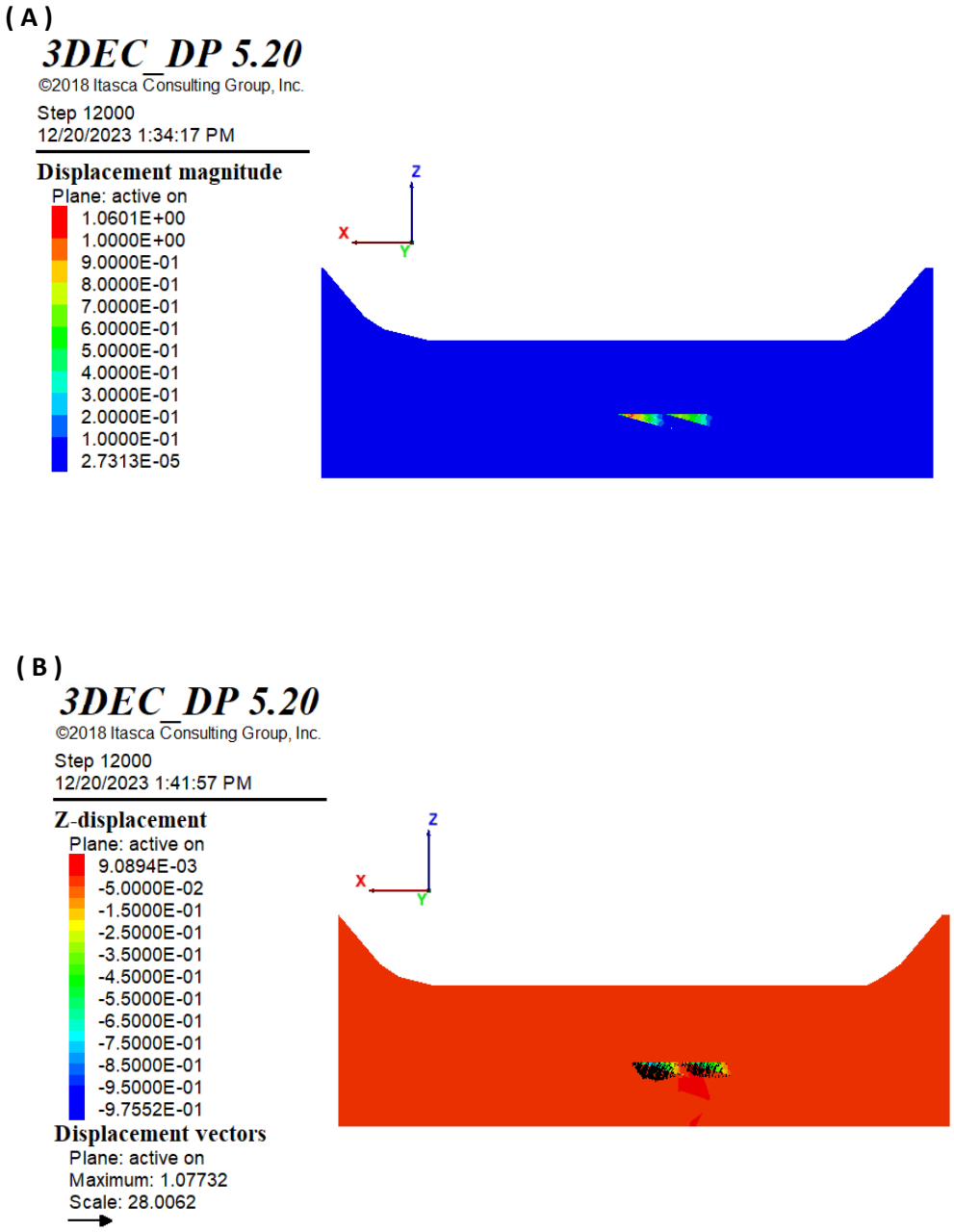

Figure 5.10. Plane cut section of the model at, y=-26 (downstream), (A) Resultant displacement, (B) The dominant displacement

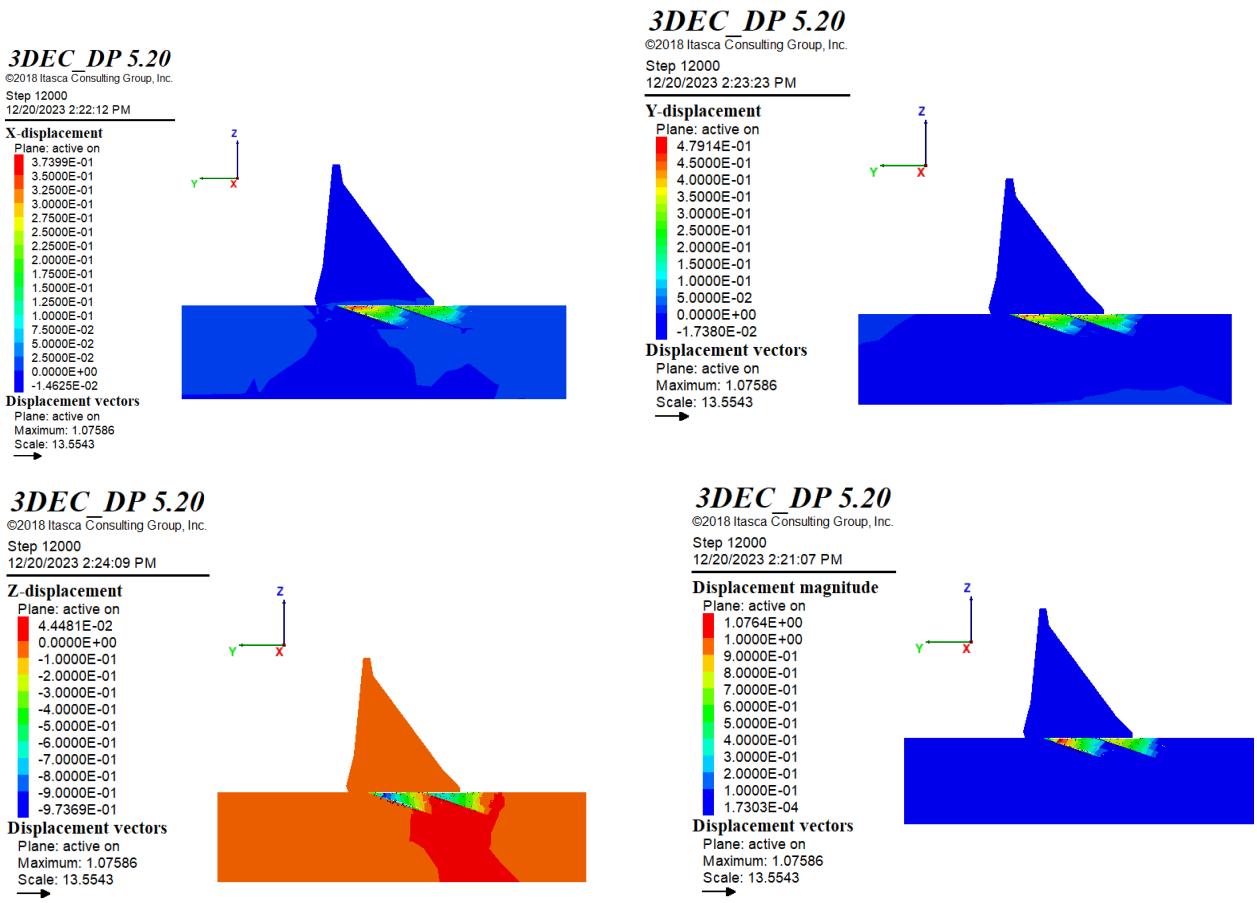

Figure 5.12. Displacement components of the maximum displacement at x=-13, y=-26, z=-5

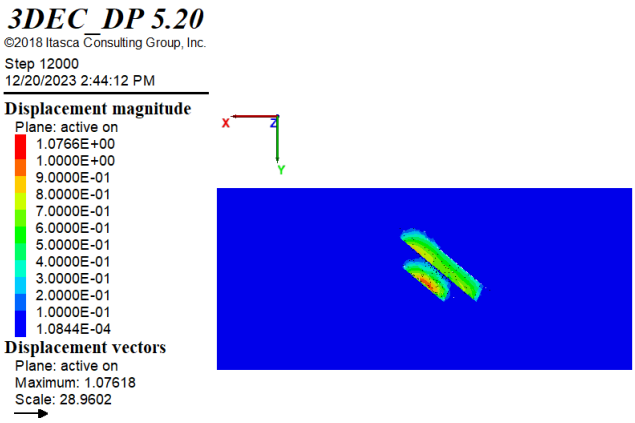

Figure 5.11. bird view the displacement pattern, that follows the J2 joint set, horizontal plane cut at depth of 5 meters

Like the pattern of displacement in the middle level outlet analysis, here it also follows the same orientation pattern of the infilled J2 joint set (Figure 5.11).

The above discussions of the result indicates that the foundation rock mass is undergoing in the state of deformation through all loading conditions, the two loading conditions that are the middle level outlet and normal operating analyses. Significant deformations were limited merely along the weak zone in the infilled J2 joints. The results of the analysis of the during two loading conditions are presented in Figure 5.13. The displacement along the infilled J2 joint set increases from 67cm to 1.1 meters when the loading of reservoir water increases by 55 meters. The compressional Z-displacement was responsible for the general displacement. The patterns of the deformation were parallel and particularly along the strike of the infilled J2 joint set. There was compression under the dam and some places along the failure area, opening and lose of contact between the dam body and the foundation rock was observed. The state of deformation was not observed along the other J2 joint set members without infills and the other joint sets (J1 & J3). From these results, the property of the infill material within the J2 joint set may be governing the phenomenon and responsible to the failure. The result of the study looks consistent with the findings concluded as the mechanical behavior of infilled rock joint depends on the mechanical characteristics of infilled materials (Borko Miladinovic, 2021).

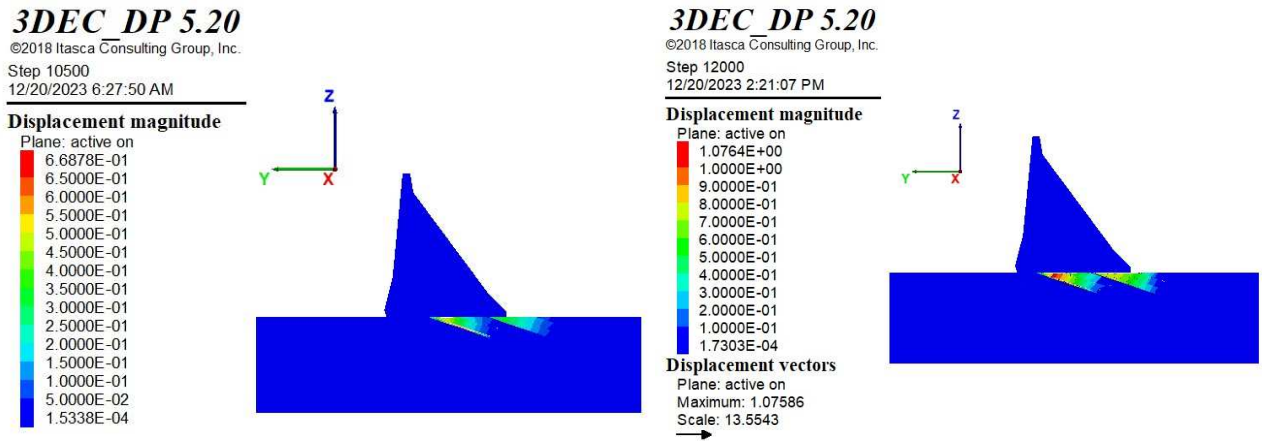

Figure 5.13. Plastic deformation in the profile cut through the center of the dam under different loading conditions; at middle level (left), at normal operation level condition (right)

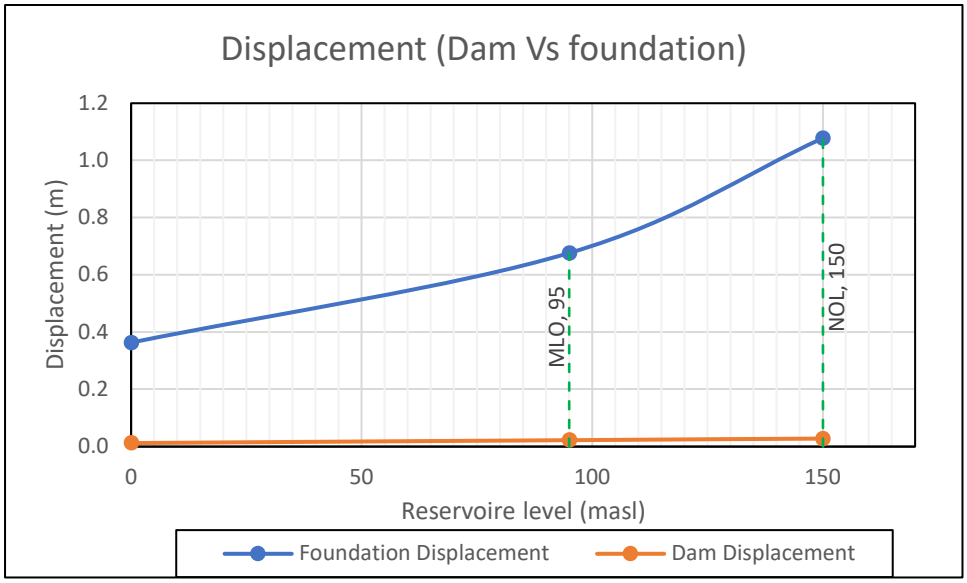

Figure 5.14. Displacement of the dam and foundation under middle level outlet (95 masl) and normal operating level (150 masl) conditions

Left Abutment Analysis

The left abutment of the foundation is taken as one of the interest regions for slope analysis, this is due to the J2 joint set is coming out of the slope. Analysis Result at Middle level outlet (95 meter of water)

Analysis Result of Left abutment at Middle level outlet (95 meter of water):

The abutment analysis has carried out at reservoir water level of 95 meter that is the Middle level outlet. Figure 5.15 & 5.16. presents the result of the analysis at middle level outlet. As it can be seen in the figure, the maximum displacement magnitude of the left abutment is 32cm. this deformation of the left abutment rock causes displacement of the left dam body. The displacement of the dam block increases from the right dam body (1.5cm) to left dam body (6.4cm). Figure 5.21 shows the maximum displacement occurred at left crest foundation of the abutment.

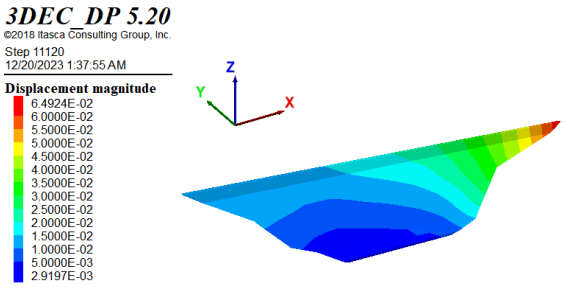

Figure 5.16. displacement of the dam body at middle level outlet

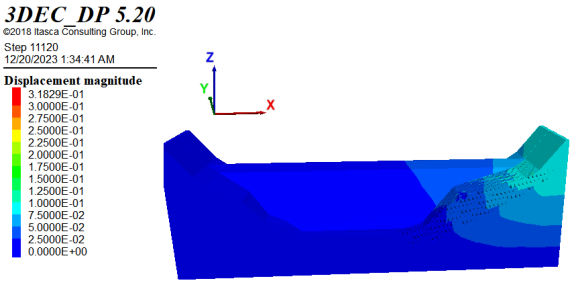

Figure 5.15. displacement magnitude at middle level outlet

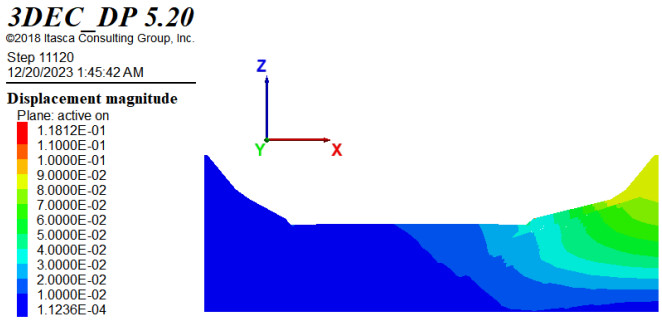

Figure 5.18 plane cut at y=-30m d/s from the dam axis

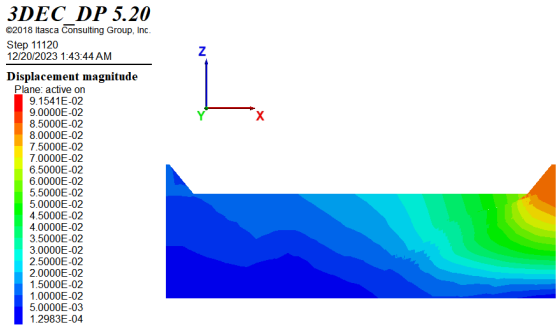

Figure 5.17. plane cut section along the dam axis @ y=0

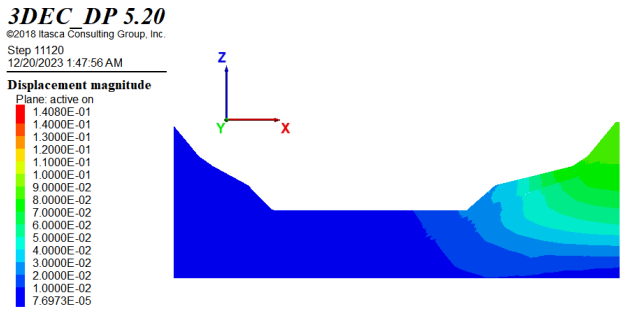

Figure 5.20 plane cut @y=-90m from dam axis

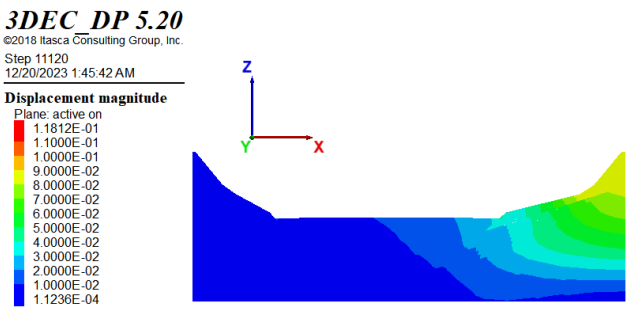

Figure 5.19 plane cut @y=-60m from dam axis

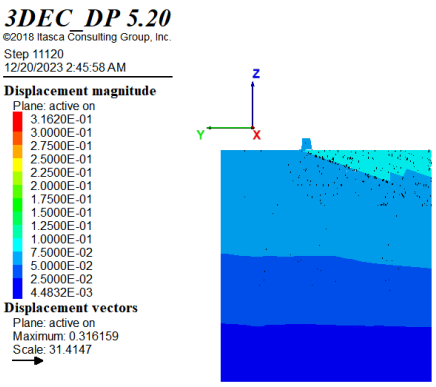

Figure 5.22 plane cut @x=452m

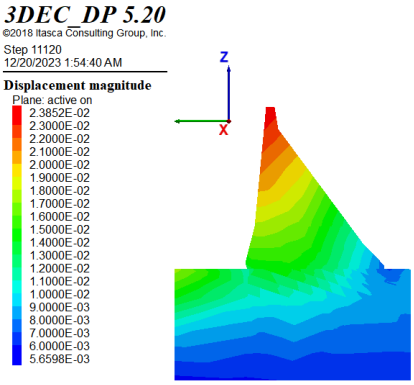

Figure 5.21 plane cut @x=80m from the center to left abutment

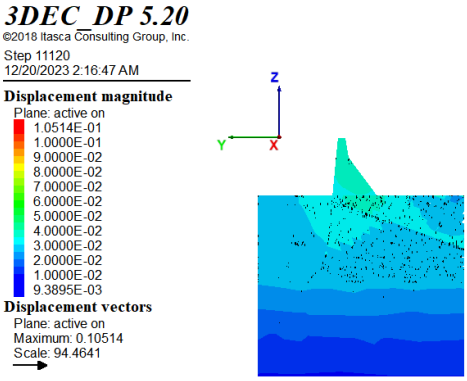

Figure 5.23plane cut along flow direction @x=252m to the left

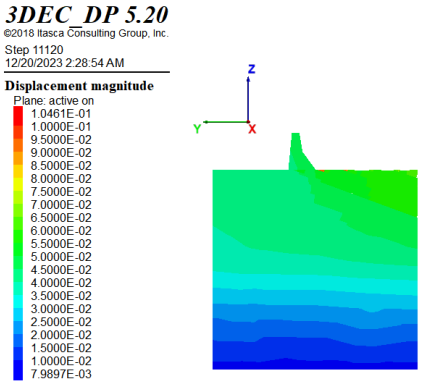

Figure 5.23 plane cut along the flow @x=350m to left

Analysis Result of Left Abutment Under Normal Operating Level (150 meter):

After completing the analysis at middle level outlet, the pressure of the reservoir increased to represent full or normal operating level reservoir. This pressure applied on the upstream reservoir area and upstream face of the dam. History of displacement was recorded during the analysis, figure 5.34. Figure 5.24. shows the general displacement of the left abutment foundation that occurred after full reservoir was loaded. As it is shown in the figure the maximum displacement recorded was 45.7 cm. the maximum displacement occurred at left crest foundation of the

abutment. Figure 5.24. indicates the dominant displacement which is responsible for the resultant displacement was the Z-displacement with magnitude 44.4 cm which is compressional displacement.

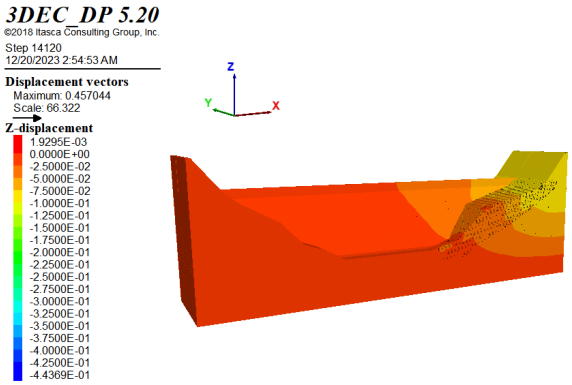

Figure 5.25 Z-displacement of the model

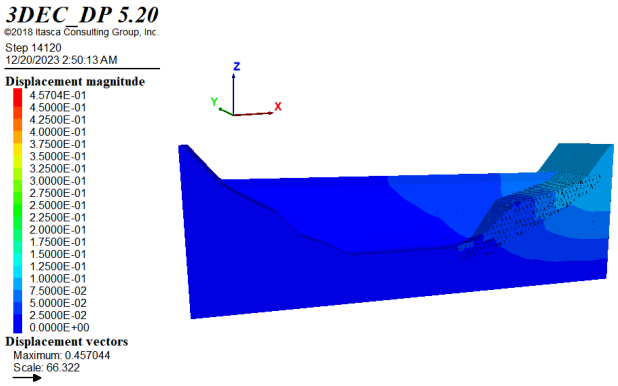

Figure 5.24 Displacement magnitude of left abutment

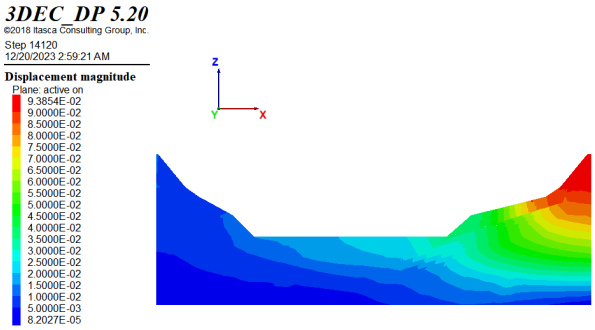

Figure 5.27 plane cut @y=-90m d/s, from dam axis

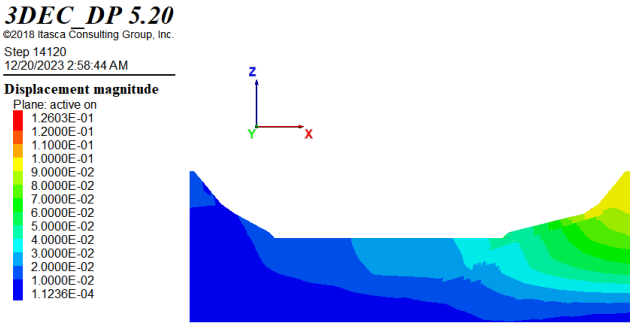

Figure 5.26 plane cut @y=-60 d/s, from dam axis

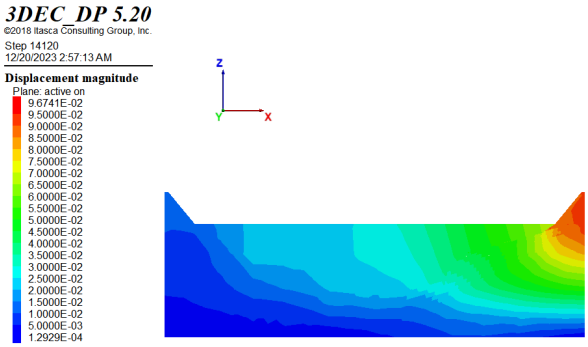

Figure 5.29 Plane cut along dam axis @y=0m

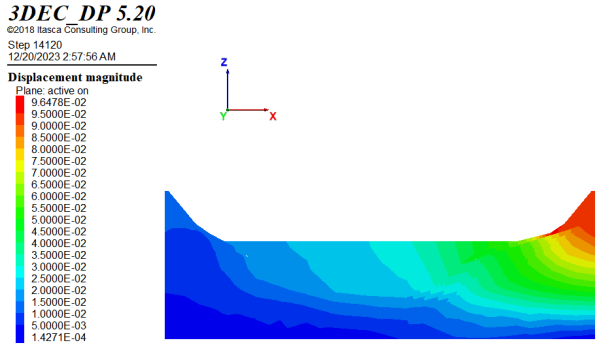

Figure 5.28 plane cut @y=-30m d/s, from dam axis

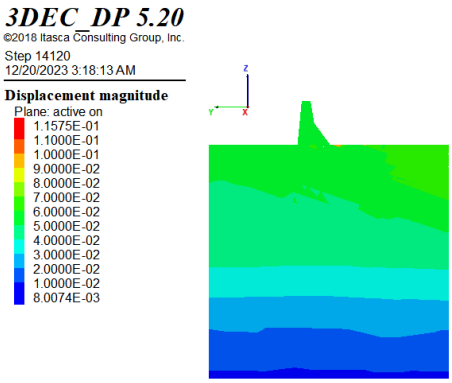

Figure 5.31 plane cut @x=350m from dam center

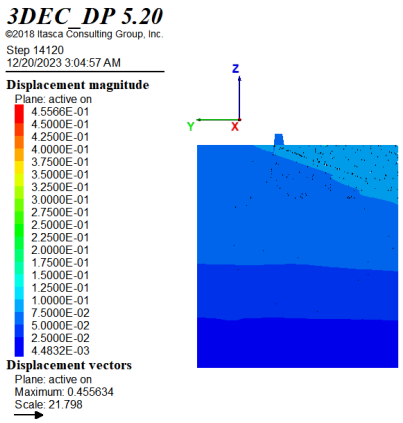

Figure 5.30 plane cut @x=452m from center dam

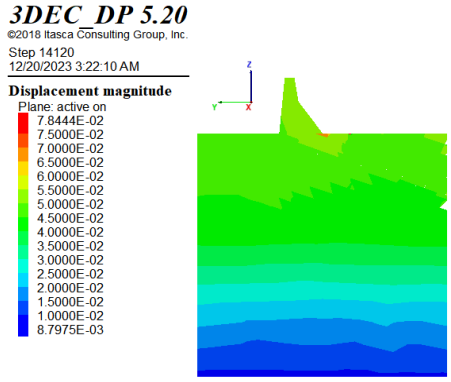

Figure 5.33 plane cut @x=315m from the center of dam

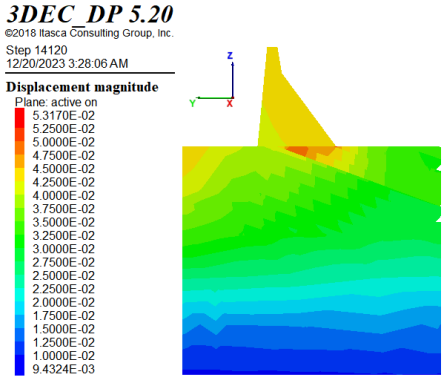

Figure 5.32 plane cut along the flow @x=230m from center

The result of the response of the analysis is summarized in table 5-1. Figure 5.36 and displacement plot history show that the compressional z-displacement is the dominant and may be responsible for the total displacement of the model.

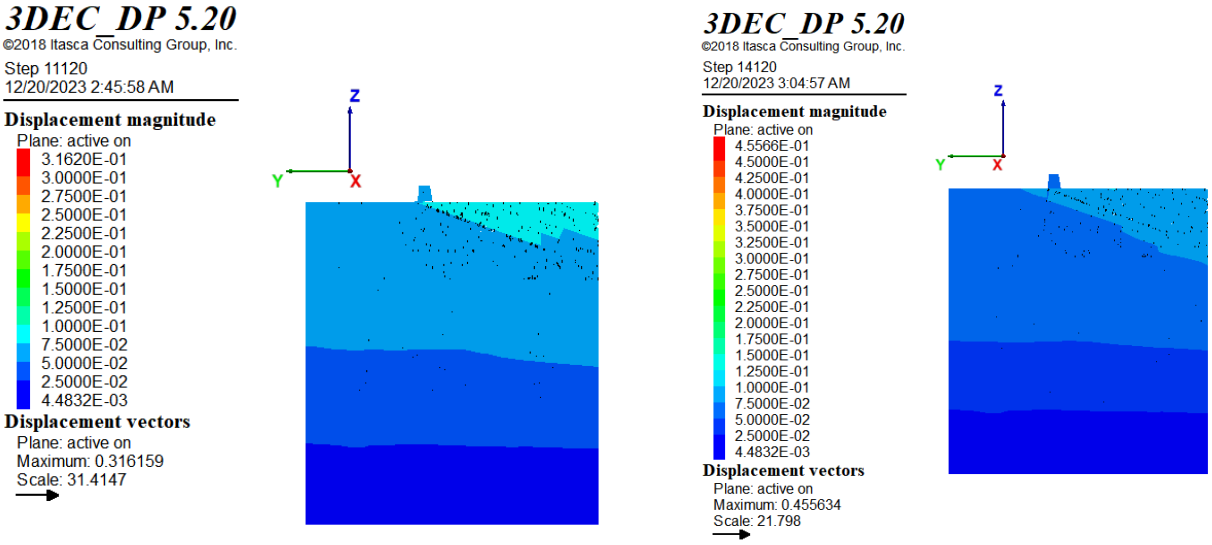

Figure 5.34. Plastic deformation in the profile cut through the abutment of the dam under different loading conditions; at middle level loading condition (left), at normal opering level condition (right)

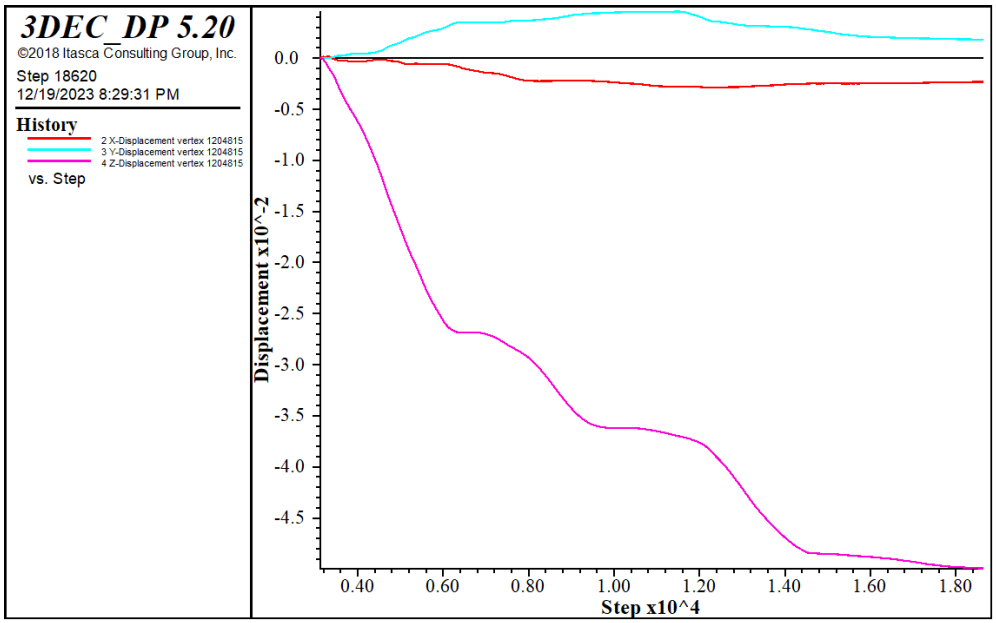

Figure 5.35. History of displacement components of the left abutment analysis

Table 5-1. Summary of displacement result of left abutment analysis under different loading conditions

	Loading condition	prior to loading	middle level outlet (MLO)	nor. operating level (NOL)	after discharge (MLO)
Reservoir water level (m)		0	95	150	95
dam displacement		4.09E-02	6.49E-02	7.11E-02	7.54E-02
foundation disp.		1.62E-01	3.18E-01	4.57E-01	5.95E-01
x-displacement	extension	1.91E-02	4.34E-02	6.23E-02	8.12E-02
	compression	-1.02E-01	-1.06E-01	-1.05E-01	-1.05E-01
y-displacement	extension	1.44E-02	6.04E-02	9.03E-02	1.19E-01
	compression	-8.42E-03	-1.09E-02	-1.50E-02	-1.62E-02
z-displacement	extension	1.84E-02	8.83E-03	1.93E-03	0.00E+00
	compression	-1.33E-01	-3.09E-01	-4.44E-01	-5.78E-01

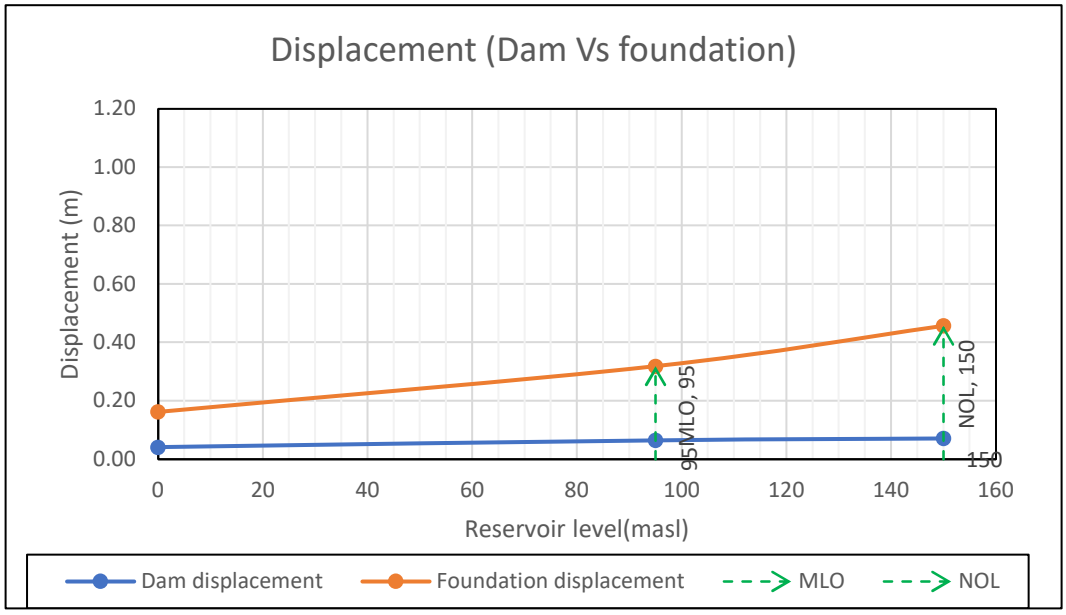

Figure 5.36. Displacement results of left crest under different loading conditions

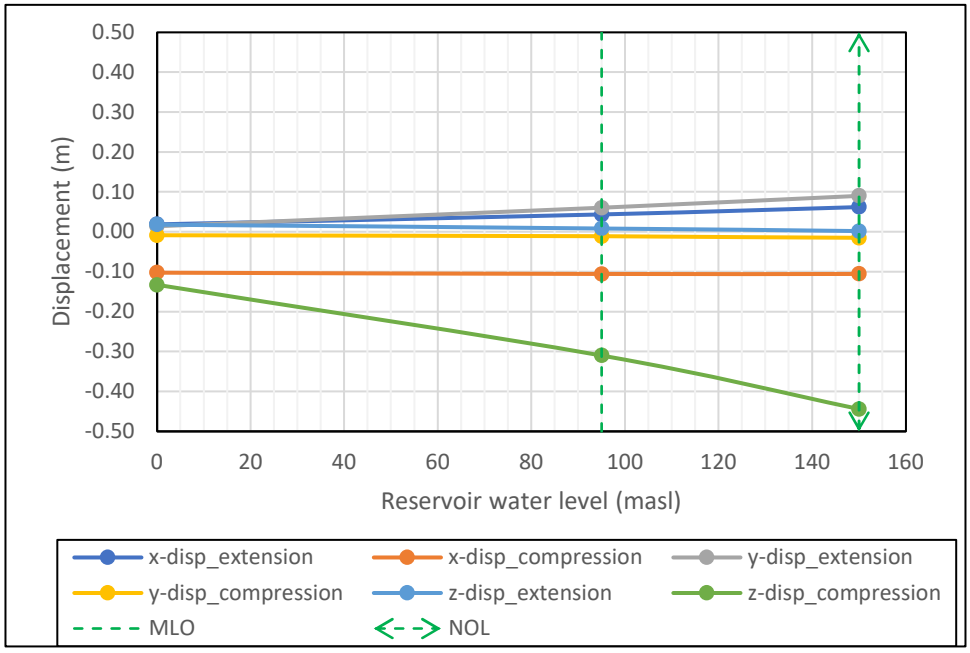

Figure 5.37. Displacement components of left abutment analysis under different loading condition

Foundation Improvement:

Grouting of dam foundation is one of foundation improving techniques in civil engineering structures. It has been developed through time and become a good practice in order to treat weak fissured rock, reduce deformation, enhance bearing capacity and control settlement of dam foundations. The selection of types of the grout method and types of the grout solution depends on the findings of the geology, construction techniques, availability of materials.

As the result of this study so far, displacement of foundation along the infilled J2 joints was observed on both the central and the left abutment model analysis. Hence additional analysis was required in order to see the response of the model by considering injection of cement grout mix along the two J2 joint set with weak infilled materials in the central foundation. previously, the maximum displacement was occurred along these infilled J2 joints on central dam foundation analysis. The primary purpose the cement grout is to replace the infilled weak material in the J2

joint. For this purpose, the properties of grout material were assumed to be similar to the grout result of J2 joint grout test Pannel carried out by site geotechnical laboratory. The average fresh density of PPC cement grout and mixture of bentonite slurry is 1.67 g/cm2, viscosity is 33, bleeding 3% and 28 days of hardened compressive strength is 27 MPa. The spacings of grout injection holes were 6 meters along the weak zones. The following assumptions of grout properties were adopted from the Itasca manual for simplicity. Shear modulus of grout is 9GPa, friction angle is 30°, cohesion strength is 1.5 Kpa. The grout mix injection took place prior to loading in order to fill fissure and to replace the weak infill material.

The response of the analysis is summarized in the table 5.3. From the table, the result shows that there is a reduction of displacement by 62% after completion of the full reservoir load (normal operating level (NOL). The history of displacements components is presented in figure 5.40.

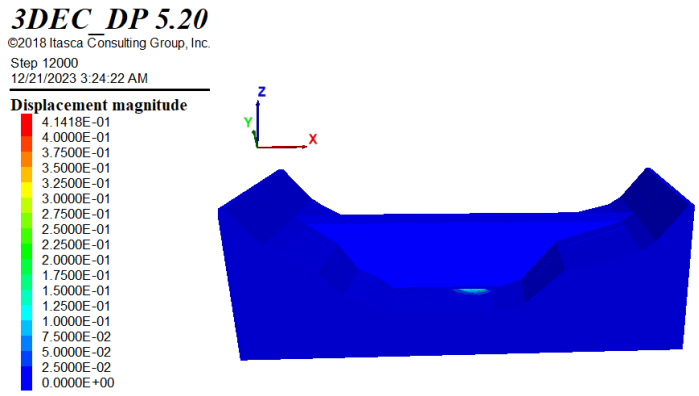

Figure 5.38. Displacement magnitude of central foundation after injection of cement grout.

Table 5-2. comparison of displacement of central foundation before and after improvement

	Loading conditions		
	prior to improvement	Middle level outlet (MLO)	Normal operating level (NOL)
Reservoir water level (m)	0	95	150
dam displacement	1.23E-02	1.70E-02	2.15E-02
before improvement	3.63E-01	6.76E-01	1.08E+00
after improvement	3.63E-01	4.05E-01	4.14E-01
% improvement	0.00E+00		-62%

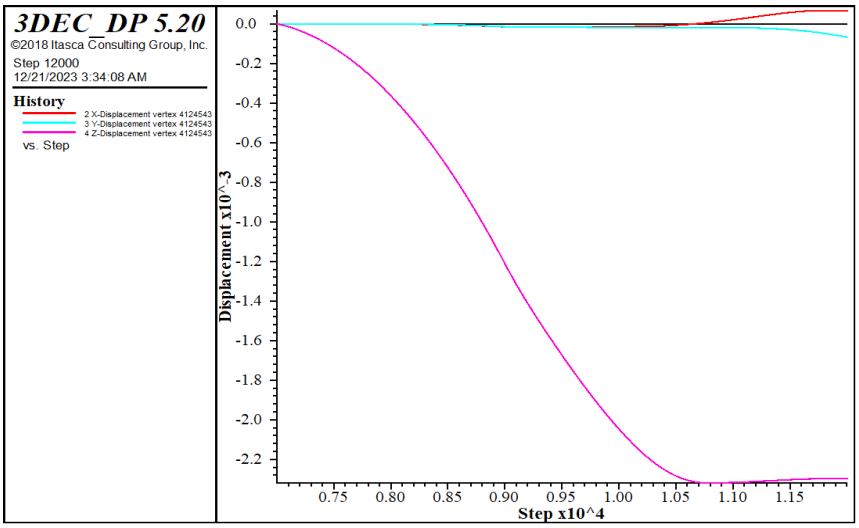

Figure 5.39. History plot of displacement components after improving the weak material in the joint by cement grout

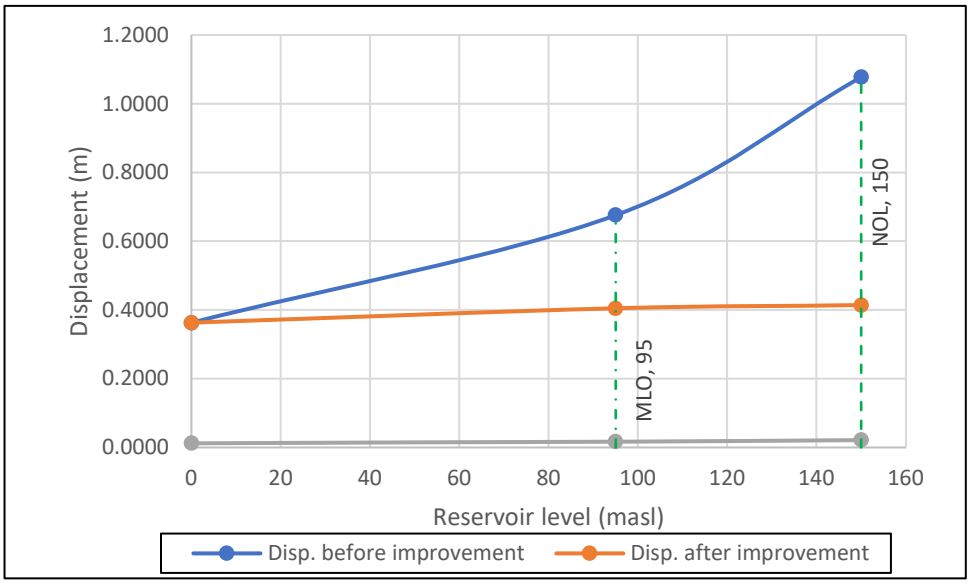

Figure 5.40. Comparison of foundation displacement along the infilled J2 joint after improvement of the weak material along the joint by cement grout

CHAPTER 6: CONCLUSION AND RECOMMENDATIONS

6.1. CONCLUSION

The Omo River, which divides Ethiopia's southern and southwest regions, is home to the Koysha hydropower dam. At present, it is the nation's second largest project, with a planned capacity of 2160 MW. When completed, a 180-meter-tall roller compacted concrete (RCC) dam will produce a reservoir with a capacity of nine billion cubic meters of water. A deeper comprehension of the failure modes of the foundations supporting the dam structures is crucial for the safe operation of these structures. The Koysha hydroelectric dam is being built on a complex geological structure with thick joint infills of soft material that include faults/seams and discontinuities. With regard to their alignment and distinctive features, the three main discontinuities in the project area are designated as J1, J2, and J3.

The quality of the rock mass was decreased and the foundation's stability has been adversely affected by the existence of discontinuities, their orientations or directions, forms, and soft and weak infillings. The shear characteristics of the rock mass may be impacted by the extensive soft clay infilling. Due to the type and thickness of the infillings in the J2 joint, and design teams have conducted detailed site investigation and analytical assessments and characterizations of this joint, which is crucial to the stability of the Koysha hydropower dam. The engineering and rock mechanical properties of the three joint sets were characterized and generated to input parameters for the model so that the properties of joint model can be represented.

The present research aimed to carry out stability analysis for the jointed rock mass foundation and left abutment. Mainly secondary data were collected from site and project branch offices. The collected information was converted to the model parameters to represent the material properties and joint properties in the model.

In order to achieve the goals of this study, the jointed rock mass foundation of the dam and abutment were analyzed using 3DEC 5.20 software. Due to the size of the model, the research carried out two model separately, one for the central foundation and the second one was for the abutment. The research also employed the techniques of discontinuum concept for the joints in the region of interest and equivalent continuum concept for the rest of outer parts of the foundation

which are not significant due to their distance. In order to observe the responses of the shear failure, the Mohr Coulomb elastic completely plastic model was used to represent the deformable blocks in the model, while an elastic model represents the dam block.

The conceptual model is divided into two categories, each category is then subjected to a separate analysis due to the conceptual model's size and the number of discontinuities that must be included in the study.

(i) the central foundation, where the largest load is applied, the result of this model indicated the deformation of the foundation along the joints, particularly the J2 joint set with infillings. The displacement magnitude, displacement vector, and velocity show that it is compressional displacement. Even though the dam displacement is relatively low, the deformation in the foundation along the infilled J2 joint keeps propagating laterally and vertically in depth with respect to time and under sequential increments of loading conditions. This infilled material and the J2 joint set with infill are found to be critical for the stability of the dam foundation rather than the joint itself. It is found to be that; the soft thick infill material may govern the deformation in the foundation along the joint. Hence it may be the thickness and shear properties of the infill materials responsible for the results. and

(ii) the left abutment. The result of the left abutment analysis experienced significant displacement on left crest foundation of the dam. This is because of the infilled joint is appear to be close to the surface. The maximum total displacement occurred on the left crest abutment is found to be 45.7cm. The deformation on the abutment caused displacement variability on the dam body.

(iii) Eventually, additional model analysis carried out to investigate the response of the central model if the weak material is replaced by cement grout mix. The analysis was conducted to determine if the improvement technique using cement grout is effective. The result of the analysis of the cement grout improvement technique revealed a 62% improvement in the foundation along the weak infilled J2 joint.

As outcome, the search produced the following findings. As a result, the investigation produced the following conclusions:

1. There was dominantly compressional displacement along the J2 joint set infilled with weak compressible materials, the result indicated that the infill material within the joint is responsible for the failure of the foundation rather than the joint itself.
2. The ongoing cracks and opening of the foundation along the weak infilled joint set may resulted the existence of the weak compressible material and hence may poses differential settlement on the foundation.
3. The maximum displacement occurred at central part of foundation 26m offset from the axis toward downstream along the joint, may runs deep upto 14 m.
4. From the response of the left abutment model: the maximum deformation of occurred on left abutment crest foundation that was probably the appearance of the infilled weak and compressible material closer to the surface.
5. The dam body experienced displacement variability at right and left as a result of displacement of left crest foundation.
6. Generally, it can be possible to conclude that the whole rock foundation of the dam was found to be stable except part of the foundation along the weak compressible infilled J2 joint.
7. From the central foundation evaluation, it can be concluded that the joint stiffness using proposed estimation method in equations 4.8 & 4.9 were not strong enough and efficient means to represent the infillings properties of the J2 joint set.
8. It is observed that the replacement of the weak compressible materials along the J2 joint set with cement grout may effectively improve the foundation with some extent.

6.2. RECOMMENDATIONS

Based on the results of this research, the following recommendations are proposed:

1. Application of high-pressure wash and appropriate cement grout injection (jet grouting) may improve the foundation at depth. Appropriate safety care should be employed during

this time for the high-pressure wash that reach up to 400bar. (methodologies may be available from previous experiences example Gibe III project).

2. Appropriate suitable material may be replaced at shallow depth along the weak zones. For example, dental work. Standard procedures and specifications shall be considered during the application of dental work to determine the extent (depth & width) of the work.
3. Application of appropriate dam monitoring instrument may provide timely information of the safety of the critical dam foundation areas where deformation was observed.
4. Appropriate drainage systems should be employed particularly along the J2 join to reduce the effect of water presence. The lubrication effect of water may reduce the shear properties of the joint.
5. Infilling may govern the shear strength of the rock mass if the thickness to amplitude ratio is above the threshold according to (Papaliangas (1993), in this case the technique of representation of infilling required rather using equations 4.8 & 4.9. This should be addressed by future study.
6. The limitations of representing the shape of joints and roughness of joint wall surfaces in the model will be addressed in the future study.

*****

7. REFERENCES

A. Bottrill1, J. Herwanger1, P. Popov1 2020. Boundary Conditions for Geomechanical Simulations, Eagle Annual 82nd Conference Paper, Amsterdam the Netherlands.

Barton, N., Lien, R. & Lunde, J. 1974. Engineering classification of rock masses for the design of tunnel support. Rock mechanics, 6(4): 189-236.

Bieniawski, Z. 1973. Engineering classification of jointed rock masses. Trans. S. Afr. inst. civ. eng., 15(12): 335-344.

Bieniawski, Z. 1978. Determining rock mass deformability: experience from case histories. International Journal of Rock Mechanics and Mining Sciences & Geomechanics Abstracts, 15(5): 237-247.

Bieniawski, Z. T. 1989. Engineering rock mass classifications. NewYork, John Wiley & Sons.

Bieniawski, Z. T. & Orr, C. M. 1976. Rapid site appraisal for dam foundations by the geomechanics classification. Proc. 12th Congr. Large Dams, ICOLD, Mexico City. ICOLD, 483-501.

Borko Miladinovic, 2021. The shear strength of infilled rock joints, Scientific Journal of Civil Engineering. Volume 10. Issue 1.

Boyer, D. D. 2006. Geological factors influencing dam foundation failure modes. The Role of Dams in the 21st Century, 26th Annual USSD Conference. San Antonio, Texas, USA: U.S. Society on Dams.

Davidson A., 1983. The Omo River project. Reconnaissance geology and geochemistry of parts of Illababor. Kefa. Gamu Gofa and Sidamo. Ethiopia. Ethiopian Ins!. Geological Surveys Bull., 2: 89.

Deere, D. U. & Deere, D. W. 1989. Rock Quality Designation (RQD) after Twenty Years. DTIC Document.

Douglas, K. J. 2002. The shear strength of rock masses. PhD Thesis.The University of New South Wales, Sydney, Australia.

Eduardo M. Bretas, 2013, Hydromechanical analysis of masonry gravity dams and their foundations, Rock Mechanics and Rock Engineering volume 46, pages327–339 (2013), Lisbon, Portugal.

Fell, Robin 2014, Geotechnical engineering of dams, second edition,

Hoek, E. & Brown, E. T. 1997. Practical estimates of rock mass strength. International Journal of Rock Mechanics and Mining Sciences, 34(8): 1165-1186.

ISRM, 1978. International Society of Rock Mechanics – Suggested methods for the quantitative description of discontinuities in rock masses, International Journal of Rock Mechanics & Mining Sciences 41 (2004) 3–19, Sudbury, Ont., Canada.

Lemos J V 2012 Modelling the failure modes of dams' rock foundations MIR 2012 ed G Barla (Torino, Italy: Politecnico di Torino) pp 259-278.

Lemos J V, 2012. Discontinuum models for dam foundation failure analysis. Harmonising Rock Engineering and the Environment – Qian & Zhou (eds). Lisbon, Portugal.

Lemos J V, 2021, Arch dam static and dynamic modelling with discrete elements, IOP Conf. Ser. 1700-066 Lisbon, Portugal.

M. Cai, 2003, Estimation of rock mass deformation modulus and strength of jointed hard rock masses using the GSI system.

Robert B. Jansen, (2003) Dams, Dikes, and Levees, Encyclopedia of Physical Science and Technology (Third Edition), (Volume 18, Pages 171-190), Tarzana, California, USA, Academic Press

Schnitter, Nicholas J., A History of Dams, The Useful Pyramids. A.A. Balkema: Rotterdam, Netherlands, 1994.

Shang, Y. The ways of determining boundary conditions in geomechanical numerical simulation. Chin. J. Rock Mech. Eng. 1999, 18, 201–204.

Sun, G.; Lin, S.; Cheng, S.; Sui, T.; Li, C.; Zheng, H. Mechanisms of Interaction between an Arch Dam and Abutment Slope Using Physical Model Tests. Rock Mech. Rock Eng. 2018, 51, 2483–2504. [CrossRef]

Tarekegn D. (2018, Geology, geochemistry and gravity survey of dime, Geological survey of Ethiopia, Addis Ababa, Ethiopia.

Tefera M., Chernet T. and Haro W., (1996). Explanation of geological map of Ethiopia at 1:2.000.000 published by the Ethiopian Mapping Authority (EMA)

7. APPENDIX

APPENDIX A: Modeling Pictures

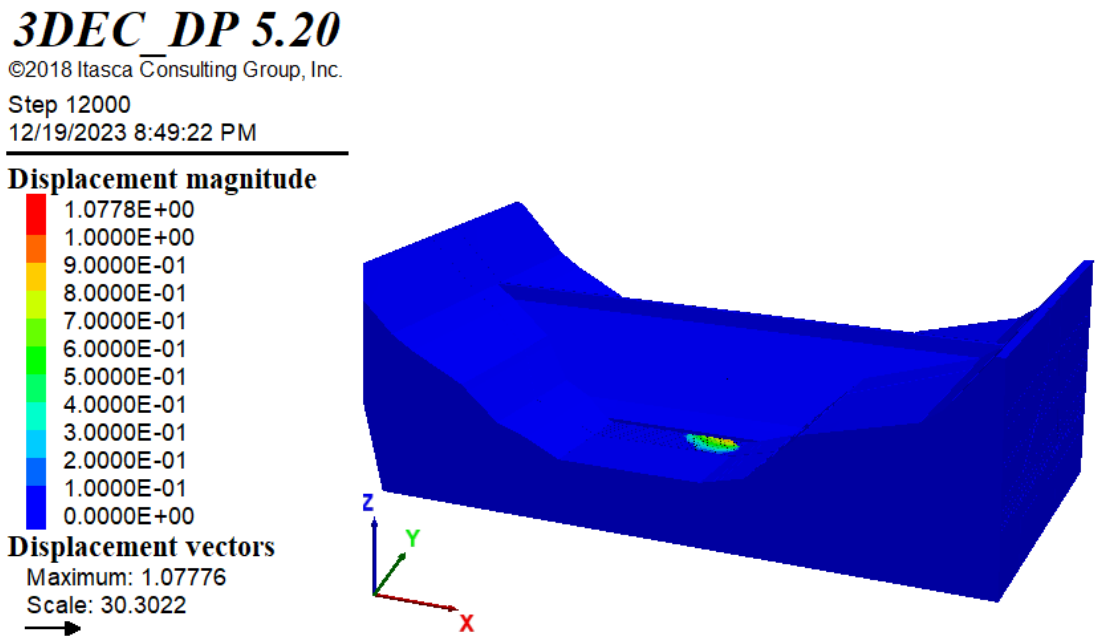

Figure 7.1. Displacement of central foundation

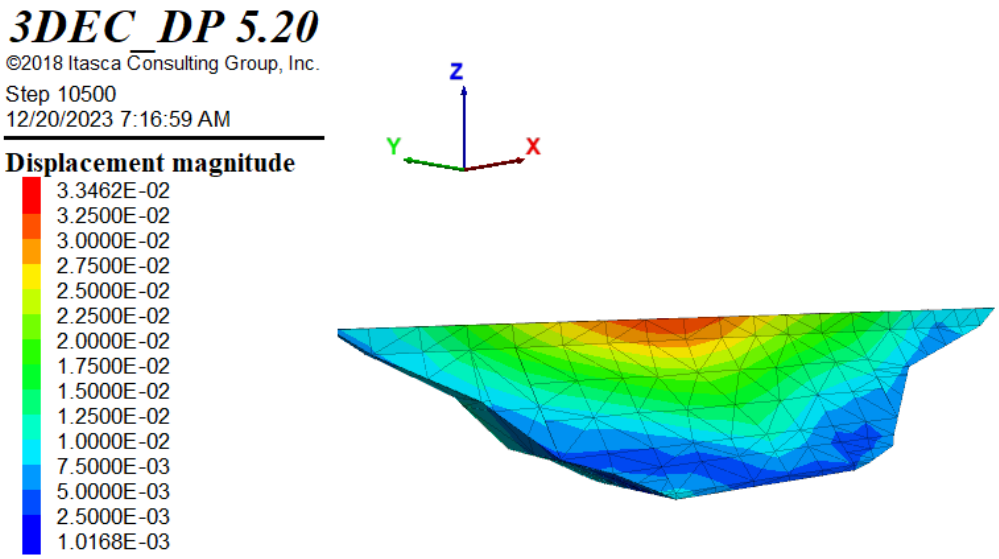

Figure 7.2. Displacement magnitude of dam body after loading at middle level outlet (95m)

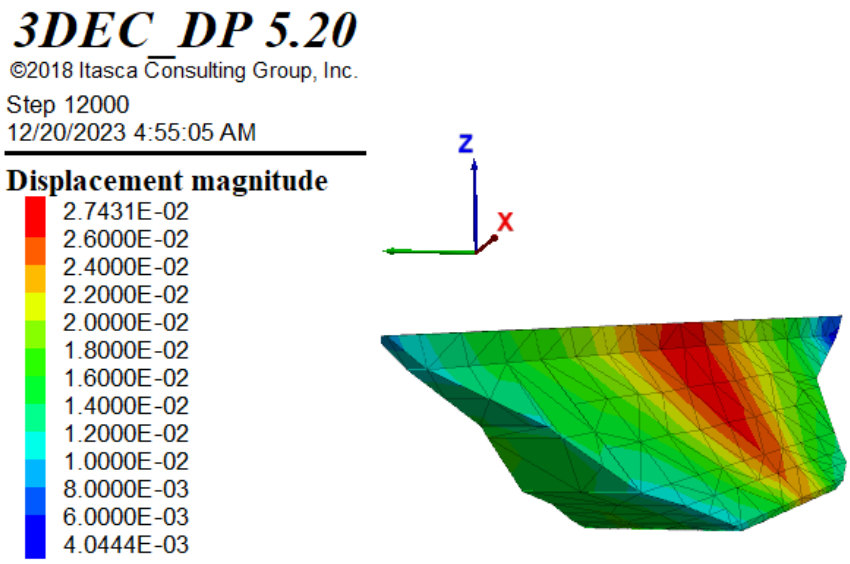

Figure 7.4. Displacement magnitude of dam body after loading at normal operating level (150m)

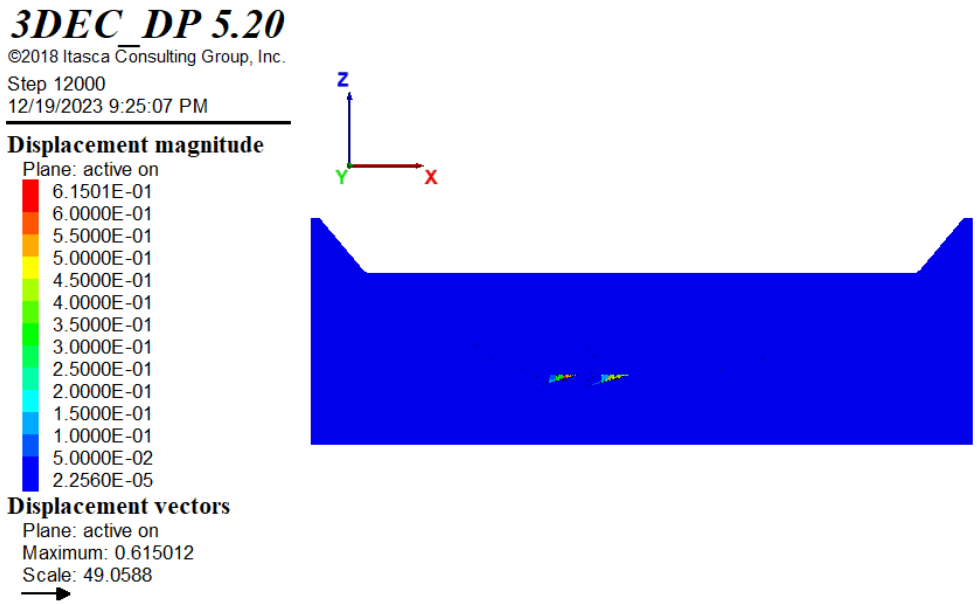

Figure 7.3. Displacement of foundation shown on plane cut on the dam axis

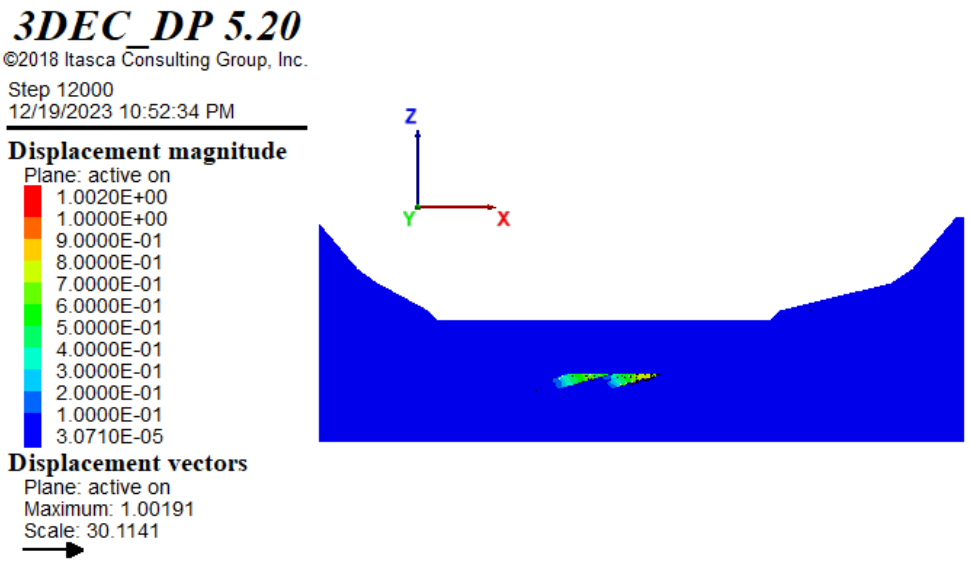

Figure 7.5. Plane cut at 60 meter offset from dam axis ,displacement of central foundation

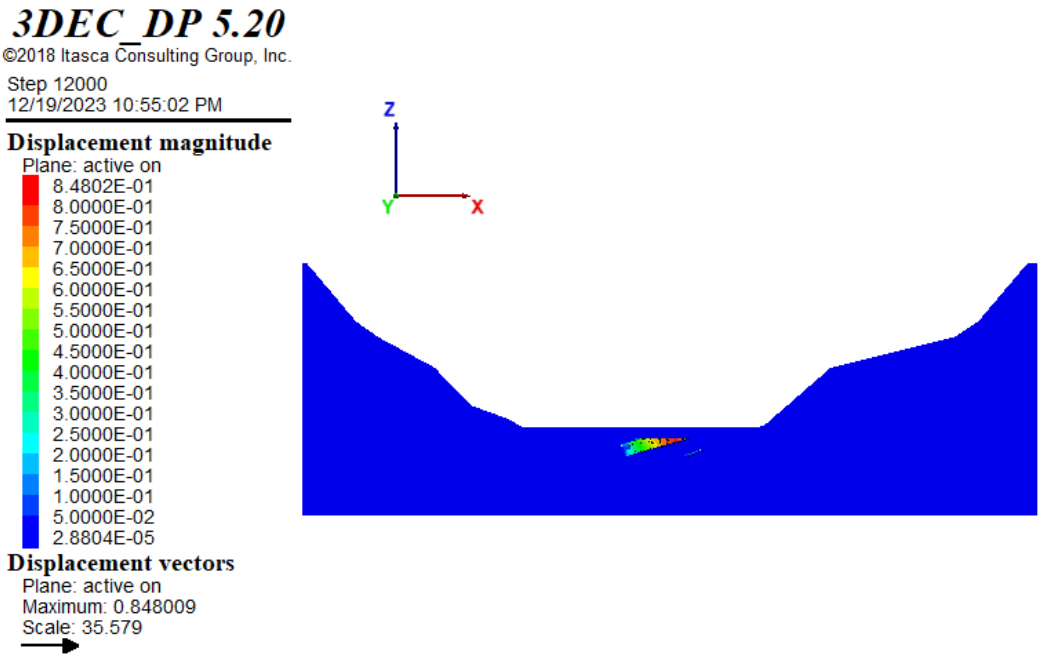

Figure 7.6. plane cut around the toe of the dam body,

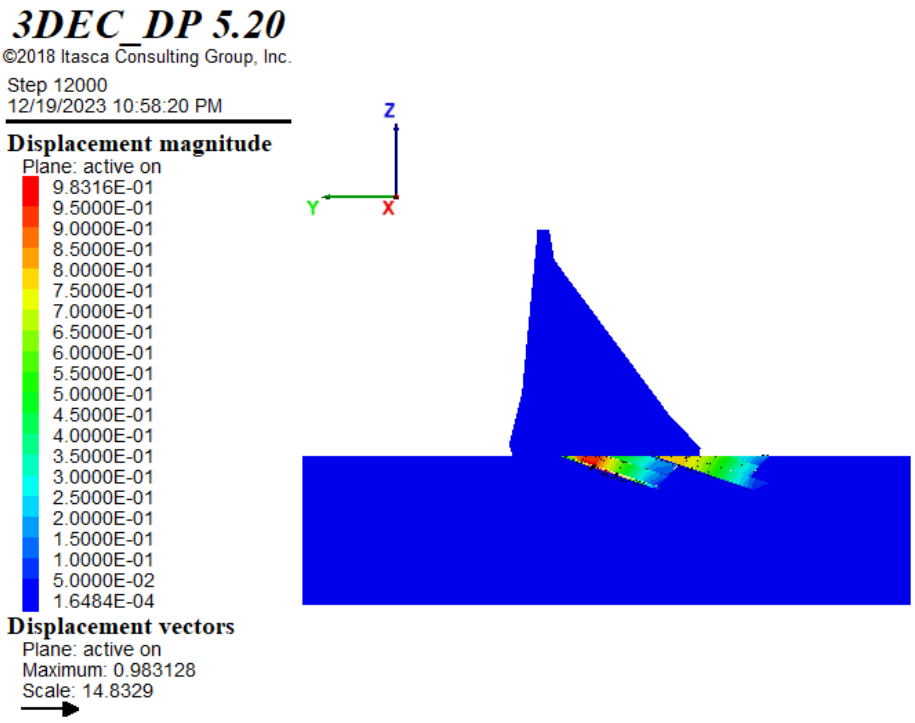

Figure 7.8. Plane cut along river flow; maximum displacement observed at 60 meter offset from dam axis

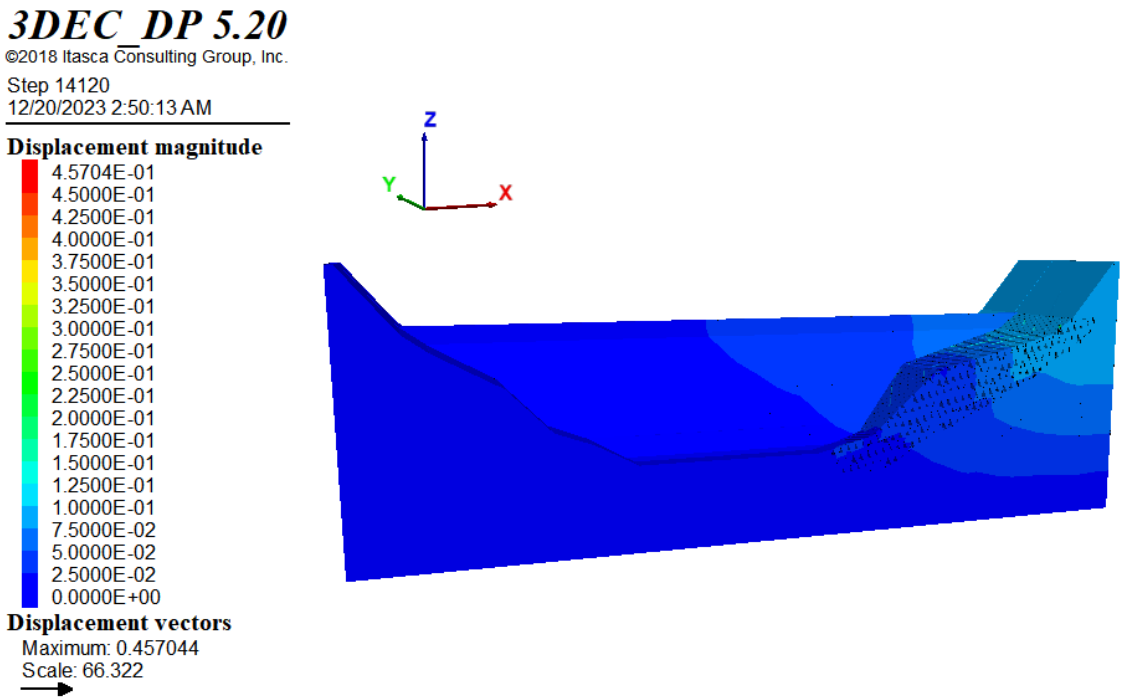

Figure 7.7. Displacement of the left abutment

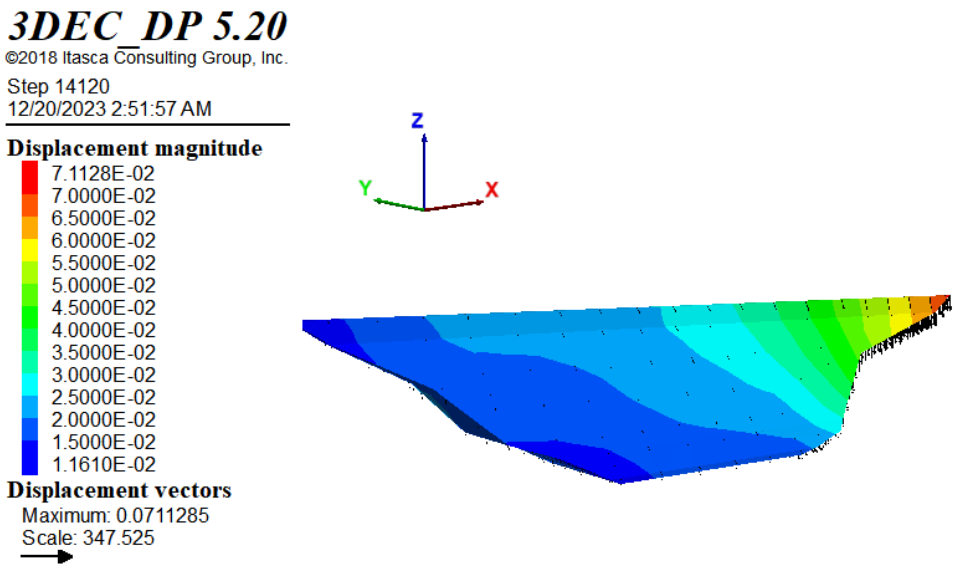

Figure 7.9. Displacement of left crest dam body

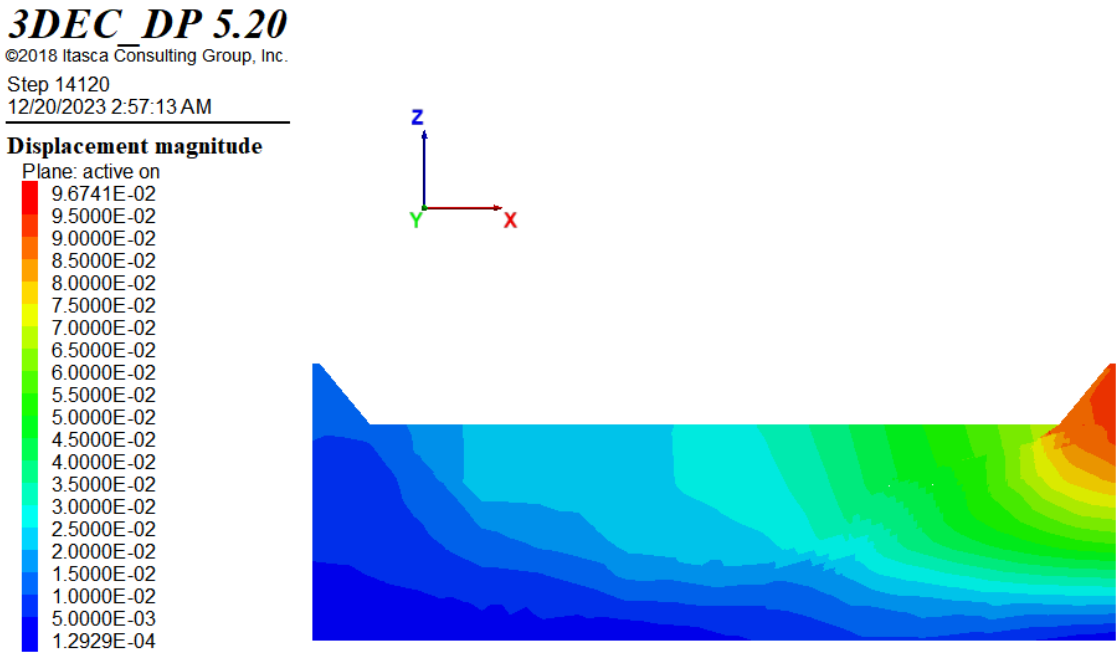

Figure 7.10. plane cut along the dam axis

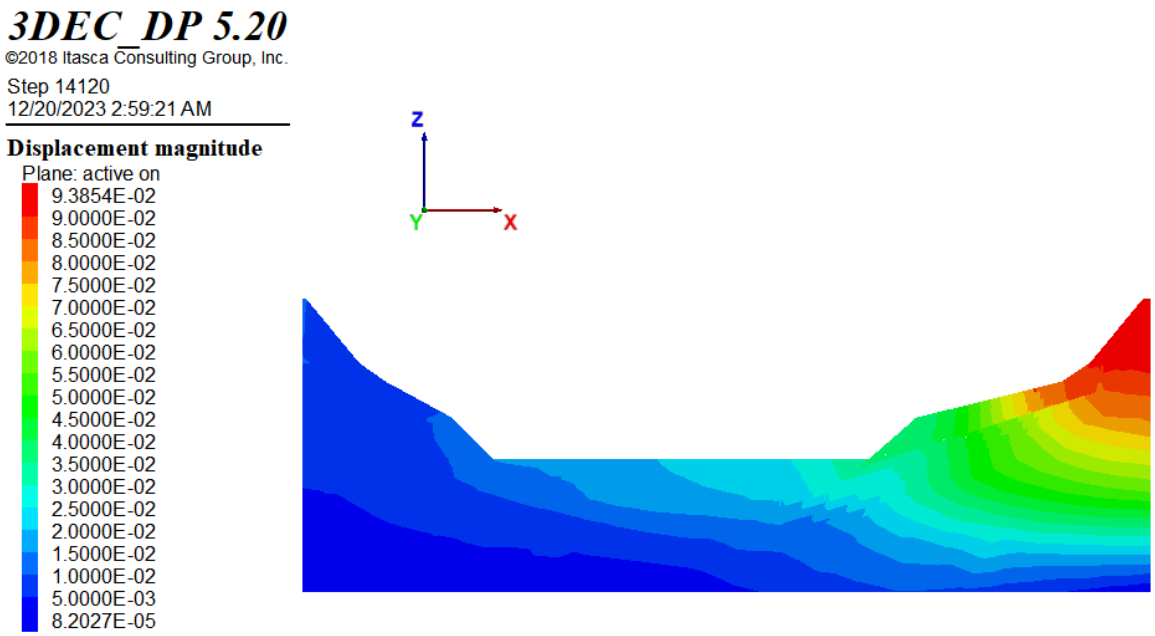

Figure 7.11. plane cut in downstream 90 meter from dam axis,

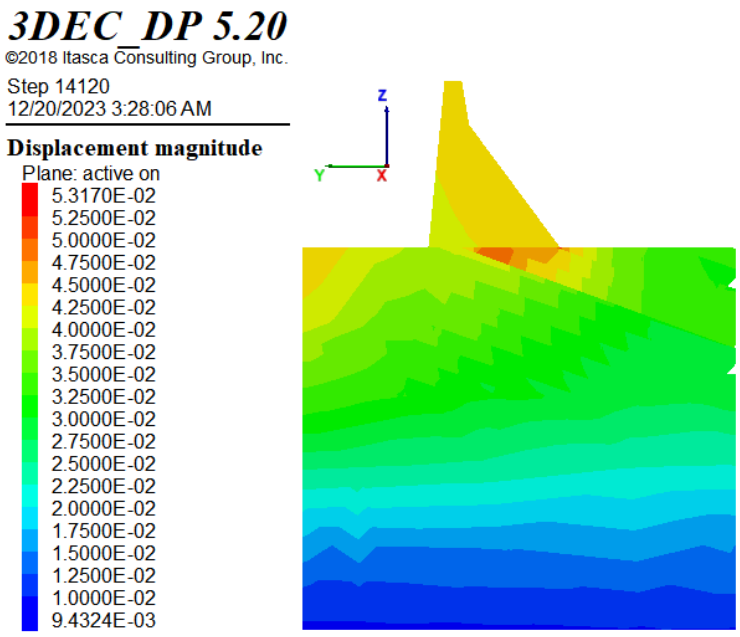

Figure 7.12. plane cut on the left abutment along the river direction

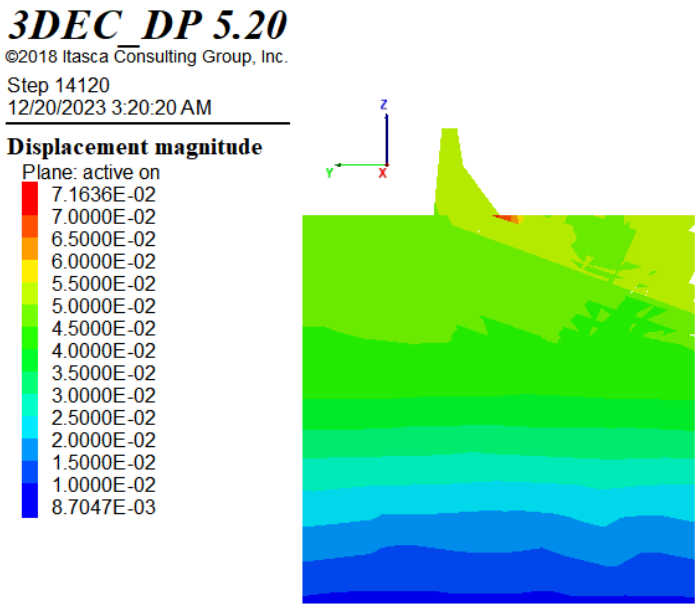

Figure 7.13. plane cut on left abutment along the river direction

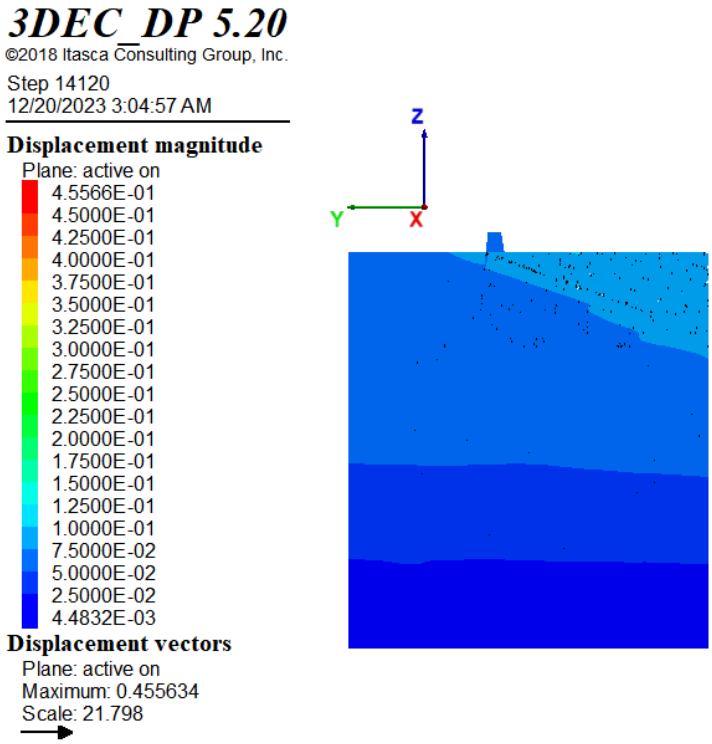

Figure 7.14. Plane cut on left abutment along river direction

APPENDIX B: Soil sampling and test results

Figure 7.15. Sampling of infilling material from J2 joint set

Figure 7.16 Recovery of PVC pipe

salini impregilo GEOTECHNICAL LABORATORY	Particle-Size Analysis of Soils ASTM D-422	KOYSHA H.E.P.P. E.E.P.

Site : Koysha	Sampling Date : 28/10/2016
Sample Location : River Div. - el. 545-555 - ch. 0+490	Testing Date : 30/10/2016
Sample Description: Joint K2 Infiling	Lab. Ref. No.: PS 62/16

Soil Sample Initial Weight (gr) : 681

Particle Description & Percentage (Retained)		Sieve Opening (mm)	Retained (gr)	Retained (%)	Passing (%)
Boulders	0.0	400	0	0.0	100.0
		300	0	0.0	100.0
Cobbles	0.0	200	0	0.0	100.0
		100	0	0.0	100.0
		75	0	0.0	100.0
Gravel 0.9	Coarse	50	0	0.0	100.0
		37.5	0	0.0	100.0
		25	0	0.0	100.0
		19	0	0.0	100.0
	Fine	12.5	0	0.0	100.0
		9.5	0	0.0	100.0
		4.75	6	0.9	99.1
Sand 24.8	Coarse	2.00	16	2.4	97.6
	Medium	1.18	28	4.1	95.9
		0.600	51	7.5	92.5
		0.425	65	9.6	90.4
	Fine	0.300	81	11.9	88.1
		0.150	121	17.8	82.2
		0.075	175	25.7	74.3
Silt or Clay	74.3	<0.075			

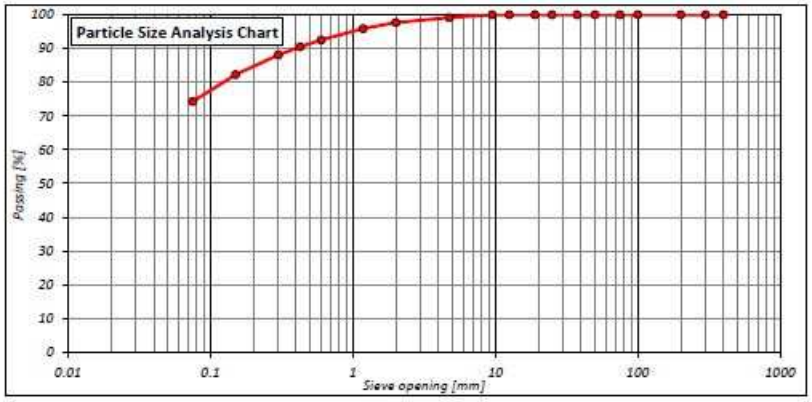

Performed by:

Checked by:

Figure 7.17. Grading result of one of the infilling material

salini impregilo GEOTECHNICAL LABORATORY	Atterberg Limits ASTM D-4318	KOYSHA H.E.P.P. E.E.P.

Site : Koysha	Sampling Date : 28/10/2016
Sample Location : River Div. - el. 545-555 - ch. 0+490	Testing Date : 30/10/2016
Sample Description Joint K2 Infiling	Lab. Ref. No.: PI 53/16

Test		LIQUID LIMIT			
N° of blows	n°	18	25	30	34
Can	n°	A4	88	26	20
Weight of can + wet soil	gr	36.50	32.00	33.00	35.90
Weight of can + dry soil	gr	28.60	26.00	26.80	28.60
Weight. of water	gr	7.90	6.00	6.20	7.30
Weight. of can	gr	17.10	17.00	17.20	17.10
Weight. dry soil	gr	11.50	9.00	9.60	11.50
Moisture content	%	68.7	66.7	64.6	63.5

Test		PLASTIC LIMIT			
Can	n°	24	AA		
Weight of can + wet soil	gr	28.60	30.20		
Weight of can + dry soil	gr	26.40	27.70		
Weight. of water	gr	2.20	2.50		
Weight. of can	gr	17.30	17.20		
Weight. dry soil	gr	9.10	10.50		
Moisture content	%	24.2	23.8		

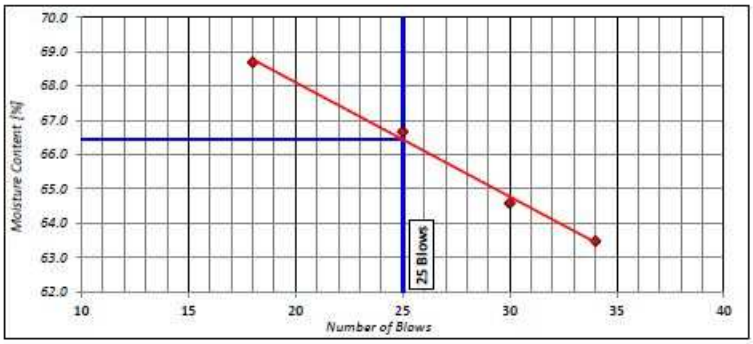

Limit Liquid WL :	66
Plastic Limit WP :	24
Plastic Index PI :	42

Performed by:	Checked by:

Figure 7.18. Atterberg test result of one of infilling material at site lab

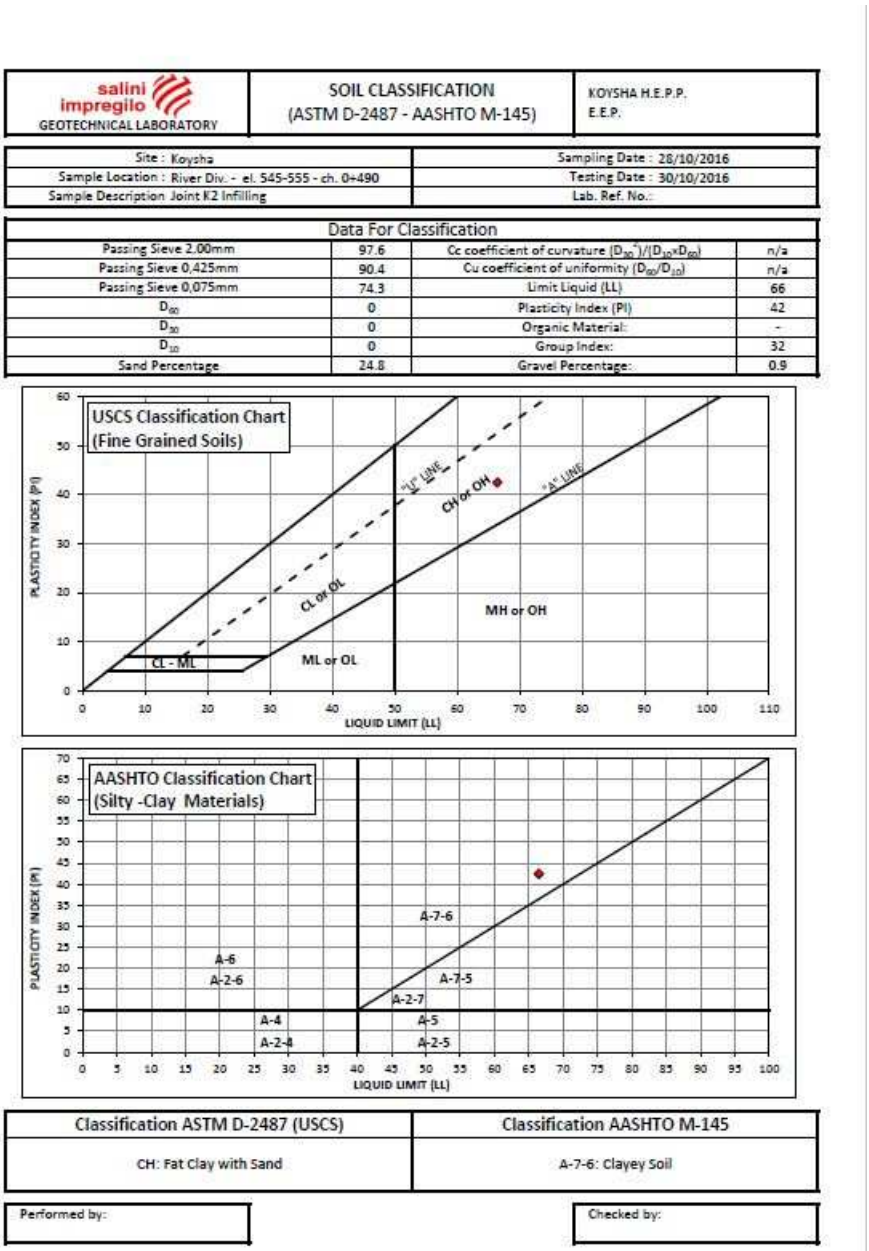

Figure 7.19. Soil classification

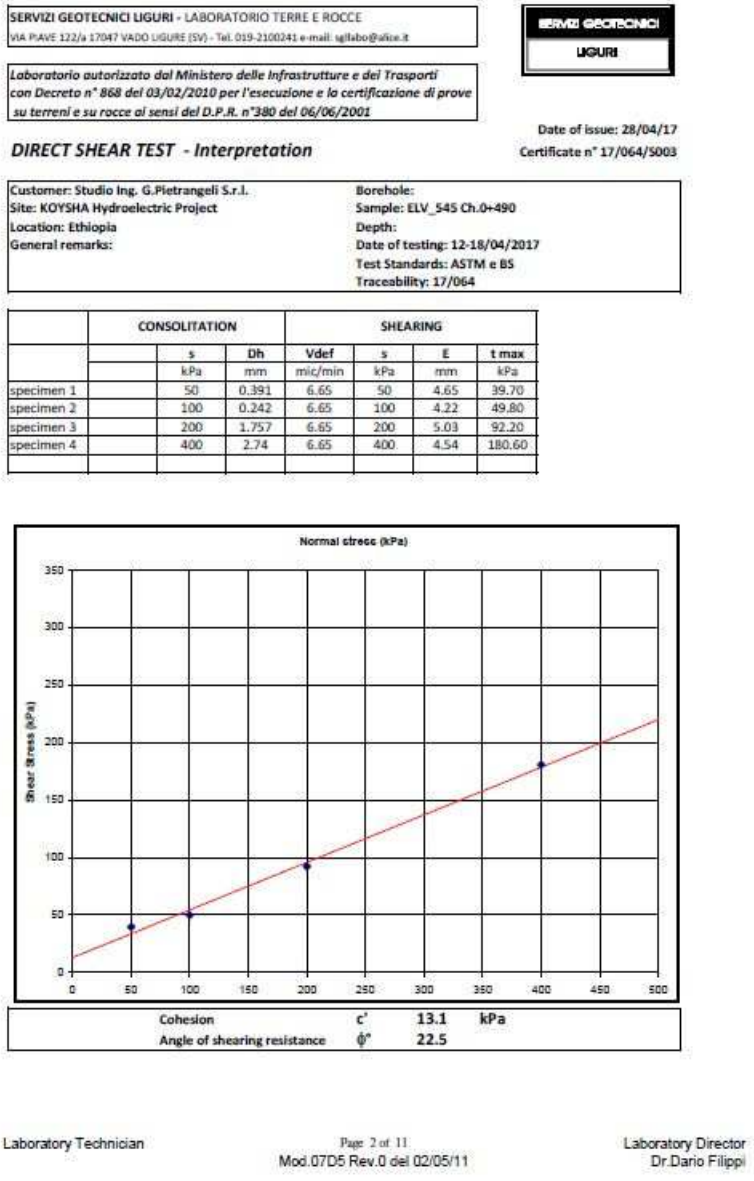

SERVIZI GEOTECNICI LIGURI - LABORATORIO TERRE E ROCCE
VIA PIAVE 122/a 17047 VADO LIGURE (SV) - Tel. 019-2100241 e-mail: sgllabo@alice.it

Laboratorio autorizzato dal Ministero delle Infrastrutture e dei Trasporti con Decreto n° 868 del 03/02/2010 per l'esecuzione e la certificazione di prove su terreni e su rocce ai sensi del D.P.R. n°380 del 06/06/2001

SERVIZI GEOTECNICI LIGURI

Date of issue: 28/04/17
Certificate n° 17/064/S003

DIRECT SHEAR TEST - Interpretation

Customer: Studio Ing. G.Pietrangeli S.r.l.
Site: KOYSHA Hydroelectric Project
Location: Ethiopia
General remarks:

Borehole:
Sample: ELV_545 Ch.0+490
Depth:
Date of testing: 12-18/04/2017
Test Standards: ASTM e BS
Traceability: 17/064

	CONSOLITATION			SHEARING			
		s	Dh	Vdef	s	E	t max
		kPa	mm	mic/min	kPa	mm	kPa
specimen 1		50	0.391	6.65	50	4.65	39.70
specimen 2		100	0.242	6.65	100	4.22	49.80
specimen 3		200	1.757	6.65	200	5.03	92.20
specimen 4		400	2.74	6.65	400	4.54	180.60

Cohesion	c'	13.1	kPa
Angle of shearing resistance	ϕ°	22.5	

Laboratory Technician

Page 2 of 11
Mod.07D5 Rev.0 del 02/05/11

Laboratory Director
Dr.Dario Filippi

Figure 7.20. direct shear test result at external lab

APPENDIX C: Site photo

Figure 7.21. J2 joint with thick infilling on the abutment slope